Contents

Spatial distribution of groundwater quality in connection with the surrounding land use and anthropogenic activity in rural areas

Cristina L. Popa[1], Petre Bretcan[2], Cristiana Radulescu[3], Elfrida M. Carstea[1], Danut Tanislav[2], Simona I. Dontu[1] *and* ***Ioana-Daniela Dulama[4]***

Water quality is essential for ensuring humane living conditions for inhabitants around the world. In this context, an important aspect that must be taken into consideration is the water quality in rural areas. Special attention must be given in such cases due to a large number of possible pollution sources, from industrial or agricultural, to wastewater resulted from human use of water supplies. This paper provided valuable information on the status of a number of groundwater sources (60 wells) throughout Targoviste Plain, Romania. An extended study of the spatial distribution of groundwater quality in connection with the surrounding land uses was achieved. The results obtained using fluorescence spectroscopy have been completed by chemical studies in order to better establish the influence of nearby land use on well water quality. It was concluded that external influences, such as soil type or land use, had a significant effect on the chemical content of the shallow groundwater that supplied the wells. High concentrations of different pollutants found in shallow groundwater are determined by anthropogenic activities, industrial an agricultural, conducted in rural villages and their surrounding areas. High concentrations of humic-like organic matter (OM) were observed in a sparsely populated region, with a forest located nearby, thus evidencing a terrestrial input to the water system. On the other hand, in the region where the highest concentration of protein-like OM was registered, the land was used for agricultural purposes.

Keywords: *water quality; fluorescence spectroscopy; chemical analyses; rural area.*

Introduction

One of the world's pressing problems is referred to as the "global water crisis", which does not always imply the lack of water. The quality of water to which people have access is an emergent issue. The problem of poor water quality represents a daily concern, especially in developing countries, being considered a parameter for establishing the social and economic development of the countries (Draghici et al., 2017; Diaconu et al., 2017). In developing countries, inhabitants of urban and peri-rural areas rely on water wells as sources of drinking water and agricultural use (Lapworth et al., 2012; Cartwright et al., 2019). Therefore, innovative monitoring methods (Wittenberg et al., 2019; Yang et al., 2019) have to be developed and regulated for the microbiological, chemical and physical assessment of water (Jang 2013; Rotaru and Răileanu, 2008; Pavelescu et al., 2013; Zhou et al., 2016; Othman et al., 2018; Soler et al., 2018; Sakizadeh et al., 2019; D'Aniello et al., 2019). Contaminants produced by different anthropogenic activities (Ionus, 2011; Boengiu et al., 2016; Shaad & Burlando, 2019; Diaconu et al., 2019b) such as nitrates and pesticides caused by fertilization of agricultural fields as well as untreated human and animal wastes may leach into the groundwater, altering the quality of the water sources (Palmiotto et al., 2018; Thomas and Famiglietti, 2015). This increases the risk of contracting diseases associated with pathogens originating from faecal sources, such as cholera, dysenteric and enteric fevers (Bain et al., 2014; Sorensen at el., 2015).

During the last couple of decades, the attention of scientists has been directed towards the study and development of a rapid technique for investigating the composition and dynamics of organic matter (OM) present in every type of aquatic environment. Recent studies (Hudson et al., 2007; Sorensen at el., 2015, 2018; Nowicki at el., 2019) emphasized the importance of using fluorescence spectroscopy for testing water quality and its potential to be used as a tool for monitoring the microbial activity in aquatic media. The results of their research suggested that the study of peak T, according to Coble nomenclature (Coble, 1996), can be linked to the presence of pathogens, thus providing a tool for accurate assessment of the aquatic system water quality. Furthermore, fluorescence spectroscopy has proved to be able to offer valuable and reliable information on the type of OM content present in various water sources, either of proteic or humic origin. This method allows the

[1] *Cristina L. Popa, Elfrida M. Carstea, Simona I. Dontu*, National Institute of R&D for Optoelectronics, INOE 2000, Magurele, 077125 Romania, cristina.popa@inoe.ro, elfrida.carstea@inoe.ro, simona.dontu@inoe.ro
[2] *Petre Bretcan, Danut Tanislav,* Valahia University of Targoviste, Faculty of Humanities, Department of Geography, st. Lt. Stancu Ion, no.34-36, 130105, Romania, petrebretcan@yahoo.com, dtanislav@yahoo.com
[3] *Cristiana Radulescu,* Valahia University of Targoviste, Faculty of Science and Arts, 130082 Targoviste, Romania, radulescucristiana@yahoo.com
[4] *Ioana-Daniela Dulama,* Valahia University of Targoviste, Institute of Multidisciplinary Research for Science and Technology, 130004 Targoviste, Romania, dulama_id@yahoo.com

identification of different characteristic markers which suggest the presence of bacterial matter or the terrestrial influence on the studied water systems (Hudson et al., 2007).

This study aimed to provide scientific data for characterizing and evaluating the water quality of shallow groundwater from an extended rural area in Romania. To this purpose, 60 wells were chosen in order to cover an area of around 1,000 km2. The experimental results obtained using fluorescence spectroscopy have been correlated with chemical studies in order to better establish the influence of nearby land use on well water quality. The chemical tests performed on the samples targeted specific chemical compounds that pose a danger to human health. The novelty of this study consists of a large number of wells investigated spread throughout a large rural area in Romania. The information obtained upon analysing the water from wells spread on an extended area could provide insight on the characteristics of the groundwater in that region (Avram et al., 2018; Dontu et al., 2018). Thus, the premises for more extensive research regarding the water quality assessment in rural areas in Romania would be created.

Materials and methods

Site description

Targoviste Plain is situated in the South-central part of Romania (Dambovita County), with a surface of 1,061 km^2 and 200,000 inhabitants (60 % living in rural areas). In the rural side of Targoviste Plain wells are still being used as drinking water sources. The water quality provided by these wells must be monitored continuously due to contaminants resulted (Ionus 2011; Minea et al., 2016; Minea 2017) from domestic and agricultural activities (i.e., crops and livestock farming) and climatic factors (Official Report of the Ministry of Health, 2016; Marinică et al., 2016; Pravalie et al., 2016; Minea and Croitoru, 2017; Andronache et al., 2017; Romanescu et al., 2014; Dunca, 2018; van Engelenburg et al., 2018; Grigoraș & Urițescu, 2018 ; Gohar et al., 2019). Targoviste City is the only urban centre in the studied area with intensive industrial and commercial pollution. Targoviste Plain is defined mainly by meadows and broad terraces along the Ialomita and Dambovita Rivers, and by its gravels and sands content, covered by loess deposits. The altitude of the studied area decreases from north to south, from 400 m to 200 m. The phreatic layer is situated at depths of 1-3 m in the meadow, 4-6 m in the low terraces of Ialomita and Dambovita Rivers and 25-26 m in the high terraces of the Dambovita River. Anthropogenic involvement on both rivers (for example, dam reservoir, fish ponds, etc.) leads to modification of the hydrological regime with direct implications on the transit of alluvial deposits from the bedrock and on the supply of the aquifer (Sencovici, 2014). The predominant activity is agriculture (53% of the area is arable land, 9% grassland and meadow, and just 25% forest), the region is famous for vegetable crops (Sencovici & Costache, 2012; Costache et al., 2014; Costache&Sencovici, 2015; Dunea et al., 2018). The water samples originated from 60 wells located throughout the Targoviste Plain will be hereafter referred to as W0-W59 (Figure 1). Their association with the studied area is depicted in Table 1.

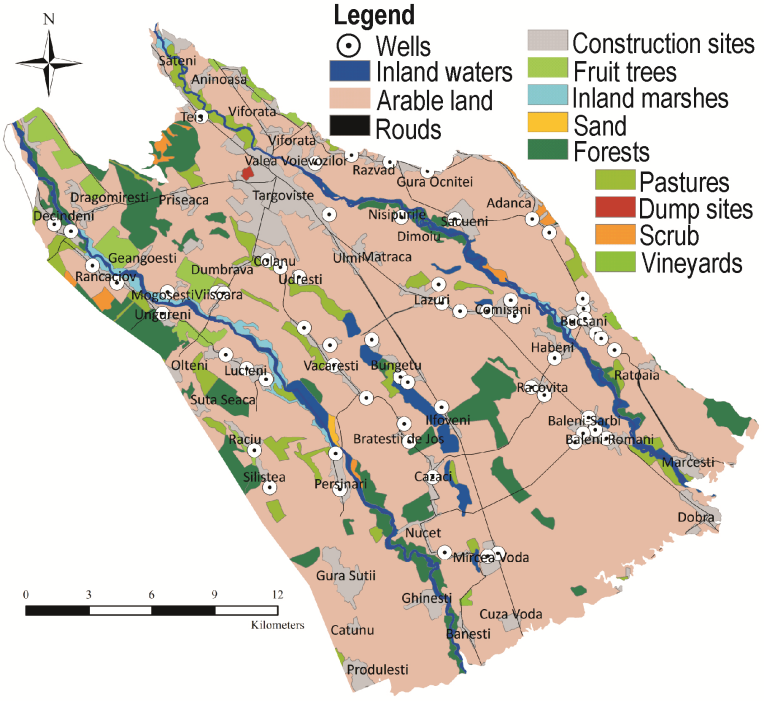

Figure 1. Map of samples location and the land use in the Targoviste plain

Table 1. Water supply status in Targoviste Plain

Investigated villages	Water Samples	Number of inhabitants	Total no. of dwellings	Dwellings with water supply		Dwellings without water supply	Dwellings with sewerage systems			Dwellings without sewerage systems
				Public network	Private supply systems		Public network	Private sewerage systems	Other situation	
Târgovişte city	W0	79,610	35,886	35,417	233	236	34,106	955	75	750
Baleni Sarbi	W1-W5	4,707	2,374	-	1,702	672	-	1,184	99	1,091
Bucsani	W6-W12	3,667	2,309	1,175	506	628	-	1,236	37	1,036
Habeni	W13	1,439								
Racovita	W14-W15	1,263								
Comisani,	W16-W19	3,480	1,835	743	717	375	-	1,068	3	764
Lazuri	W20-W21	1,920								
Decindeni	W22-W23	2,502	3,064	2,167	533	364	70	1,492	43	1,459
Mogosesti	W24	566								
Rancaciov	W25-W26	1,996								
Ungureni	W27	1,315								
Dragodana	W28	1,373	2,327	1,290	620	417	-	1,178	29	1,120
Gura Ocnitei	W29	3,160	2,748	1,546	611	591	148	1,522	38	1,040
Adanca	W30-W31	1,826								
Sacuieni	W32	1,830								
Lucieni,	W33	2,544	1,303	650	403	250	-	626	80	597
Nucet	W34	2,162	1,463	225	697	541	-	649	14	800
Cazaci	W35	1,396								
Ilfoveni	W36	499								
Persinari	W37-W38	2,750	934	-	483	451	-	252	12	670
Raciu	W39	1,566	1,505	1,018	233	254	-	609	102	794
Razvad	W40-W42	4,266	3,403	1,838	1,036	529	219	2,055	19	1,110
Valea Voievozilor	W43	3,023								
Teis	W44	2,489	2,247	1,498	405	344	174	1,129	130	814
Colanu	W45-W46	289	1,570	989	392	189	-	1,003	42	525
Nisipurile	W47	79								
Udresti	W48	216								
Viisoara	W49-W50	1,370								
Vacaresti	W51-W54	3,173	1,664	57	1,240	367	-	763	63	838
Bratestii de Jos	W55-W56	666								
Bungetu	W57-W59	1,407								

Sampling, sample preparation and analytical techniques

The water samples were collected in sterile plastic bottles and preserved in a cool box, at maximum 4°C, until analysis. All the samples were measured within 48 hours from the collection in order to minimise the risk of degradation. 60 wells (i.e. W0-W59) spread throughout Targoviste Plain were chosen for the study. The water analysis, including pH, electrical conductivity (EC), salinity and total dissolved solids (TDS), were performed by using pH/ISE meter inoLab® pH/ION 7320. Nitrate was determined using Dionex ICS-3000 Ion Chromatography system equipped with IonPac® AS9 analytical column with AG9 guard; the eluent was 1.8 mM Na_2CO_3/1.7 mM $NaHCO_3$; the flow rate was 2.0 mL/min, and the sample volume was 25µL. The analysis and quantification of elements (i.e. Cr, Fe, Co, Ni, Cu, Zn, Cd, and Pb) were performed by Inductively Coupled Plasma - Mass Spectrometry (ICP-MS) by using iCAP™ Qc device (Dulama et al., 2017). For ICP-MS analysis, the samples (about 15 mL) were digested with aqua reggia on a hot plate by using a TOPwave Microwave-assisted pressure system, according to the procedure proposed in previous studies (Radulescu et al. 2016; Radulescu et al., 2017). After the digestion process, the PTFE-TFM vessels with samples were cooled for 1 hour, and then the solutions were transferred with distilled water to 25 mL volumetric flasks. Finally, the clear solution samples were analysed by ICP-MS. The quantification of this technique was performed by a standard curve procedure. Metals calibration curves showed good linearity over the concentration range (0.1 to 10.0 mg L^{-1}), with R^2 correlation coefficients in the range of 0.996 to 0.999 (Chelarescu et al., 2017). Calibration was performed using standard aqueous solutions (Merck). The measurements were performed in triplicate mode. The relative standard deviation (RSD) was less than 5%.

Fluorescence spectroscopy was used in order to highlight the characteristics of OM. To this end, excitation-emission matrices (EEMs) were recorded using FLS-920 Edinburgh Instruments spectrofluorimeter which operates with a 450 W Xe lamp. Upon their recording, the spectra were analysed for distinct excitation/emission

wavelengths. Specific fluorescence maxima were identified, using the peak picking method and associated with different types of OM present in the tested water samples (Coble, 1996). The EEMs were registered using excitation wavelengths in the 230-400 nm range and emission wavelengths between 250 and 500 nm, with steps of 5 and 2 nm, slits of 4 nm and an integration time of 0.2 s. The water Raman peak was recorded before each set of measurements in order to establish the stability of the instrument. The spectra were recorded in triplicate, and average values were used in the analysis.

Topographic, hydrological, hydrogeological and statistical information were processed and digitized using ArcGIS 10.4.1, the resulted thematic maps is based on a spatial database. The spatial distribution of the values was determined using non-parametric and linear geostatistical methods for estimating the spatial variation of the variables (Joumel, 1983; Chica-Olmo et al., 2014; Secu et al., 2015; Diaconu et al., 2019a).

Results and discussion

Chemical analyses

For a proper understanding of the water quality in the studied area, a number of chemical investigations were performed (Table 2). A slight acidic tendency could be noticed, as most of the samples had pH values slightly lower than 7. The lowest pH value (6.53) was registered for water sample W2, while the highest value (7.39) was recorded for sample W55. Given the fact that the pH values were in the 5-7 interval, it should not be considered as an impact factor for the differences observed in the fluorescence intensities. Reynolds & Ahmad 1995; Patel-Sorrentino et al., 2002; and Spencer et al., 2007, evidenced that when at pH values comprised in the 5-7 interval there were no significant differences in the fluorescent intensity signals. With regard to the electric conductivity, elevated values were measured for three samples, W6, W8 and W12, originating from the same village - Bucsani. High conductivity values indicated high concentrations of TDS (Figure 2), which were charged minerals in most parts. International agencies such as World Health Organisation (WHO) and the United States Environmental Protection Agency (EPA) established a maximum TDS level that must not be exceeded in drinking waters of 500 mg/l (*www.epa.gov*, WHO Guidelines for Drinking-water Quality, 1996). It could be observed that almost all of the water samples presented TDS concentrations higher than the maximum accepted value, which suggested the presence of charged ions, including salts and metal ions. As could be expected, the highest salinity values were also registered for the same well samples W6, W8 and W12. Our results revealed that in the majority of cases, high concentrations of hydrogen carbonate were obtained, compared to the value used as a standard by global organizations such as EPA and WHO. The lowest concentrations were recorded for three out of five samples collected from Baleni village (W1, W2 and W3). Past studies (Rylander, 2008) suggested that waters with concentrations of hydrogen carbonate higher than 110 mg/l are more beneficial to human health.

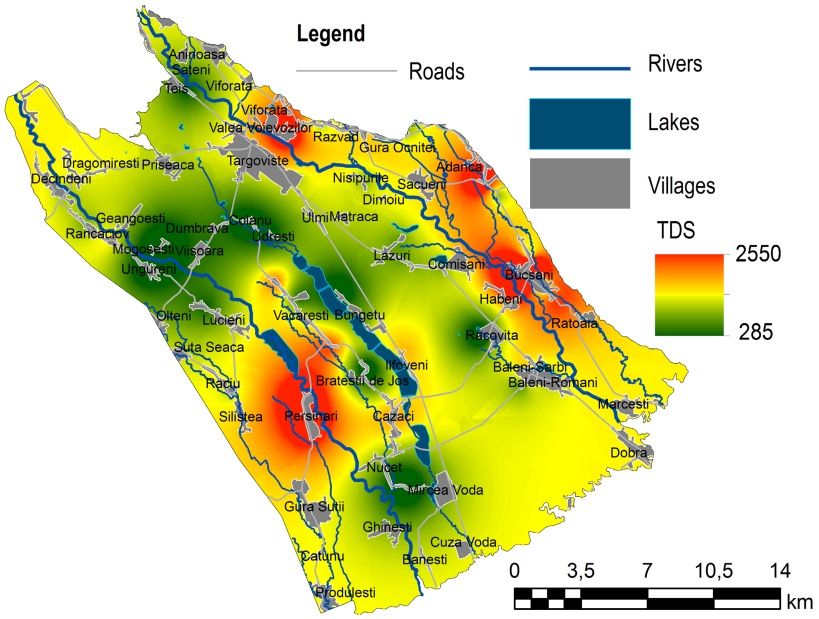

Figure 2. Spatial distribution of TDS in the study area

With regards to the concentrations of nitrates, sulphates, chlorides, calcium and magnesium from the water samples, the registered values were compared with the maximum allowed values, according to the Romanian and European Committee regulations (Romanian Law no. 311 from 28/06/2004; European Committee Directive 2006/118/CE). The results obtained indicated that well W18 registered the minimum Na, Ca, Mg, K, Sr and Ba

concentrations, while W38 had the maximum values for Mg, Ca and Sr concentrations out of all the recorded values. These areas are situated in the proximity of vineyards. Certain types of grapes used in the wine industry need soil with different concentrations of nutrients. This could explain our findings, the mass cultivation for obtaining wines being responsible for the alteration of soil composition and thus of the groundwater quality parameters. The greatest Ga, In and Tl concentrations were recorded for well W6. An explanation for these results was the exploitation practices in the surrounding area. Beside agricultural practices, the region surrounding Bucsani was known for oil and natural gas extractions. Therefore, the presence of heavy metals in the groundwaters was tightly linked to the human activities nearby, among which was the manufacturing of mechanical components.

The chemical analysis revealed that all the sulphate and chloride concentrations were much lower than the maximum allowed values, the highest being 31.25 mg/L (W15) and 98.75 mg/L (W6) respectively. In the case of nitrate concentrations, the majority of the registered values were below the maximum allowed by law. However, for sample W2 it was recorded a concentration of nitrates of 60.4 mg/L, this being the highest value. Such values could signify a potential of exposure of the population to the risk of developing methemoglobinaemia in new-borns and adults with deficiencies of glucose-phosphate dehydrogenase. Given the fact that W2, W15 and W6 were found in regions characterized by arable land and construction sites, it was assumed that the high values for the sulphate, chloride and nitrate compounds were determined by the agricultural uses of the land (mainly corn, wheat and sunflower crops).

The spatial distribution of nitrate concentrations was presented in Figure 3a. According to a study performed by the World Health Organization (WHO), the natural nitrate concentration in groundwater under aerobic conditions could reach a few milligrams per litre, but must not exceeding 10 mg/l, depending on the soil type and the geological background (WHO Guidelines for Drinking-water Quality 2011). However, as a consequence of different agricultural activities, the nitrate concentration may increase by 100%, an extreme example being an agricultural area from India, where the nitrate concentration from groundwater reached 1,500 mg/L (Jacks and Sharma 1983; Nitrate and nitrite in drinking-water WHO, 2011). Intensive agricultural practices in the area might explain the relatively high levels of nitrate represented in Figure 3a. Although nitrate content in water can have a significant influence on human consumers, there are other threats that can be found in the groundwater supplies. Among these dangerous substances, heavy metals must be mentioned due to their cumulative effect. Lead is a cumulative poison, which has a strong effect, especially on children as well as on pregnant women and their fetuses (Lead in Drinking-water – WHO 2011). It is considered that an intake of a maximum of 5 µg/l from drinking water should not pose immediate health issues. In this context, it could be observed in Figure 3b that some areas were more affected than others, especially the ones corresponding to samples W1-W5. Comparing the two maps presented in Figure 3a and Figure 3b, it could be noticed that the same approximate area had high levels of lead and nitrate, possibly coming from industrial chemical waste. We could suppose that previous anthropogenic activities caused high levels of lead and nitrate now found in the groundwater system.

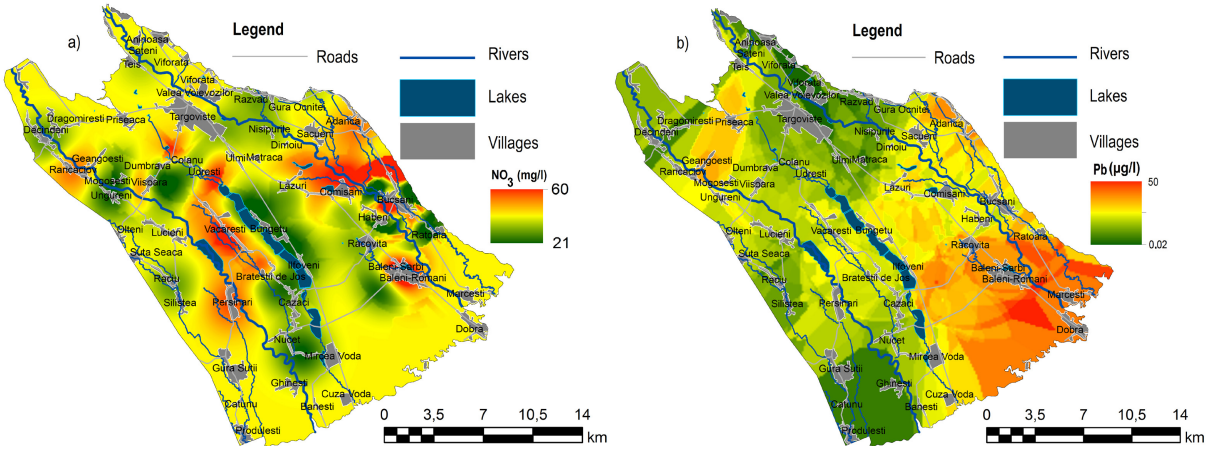

Figure 3. Accumulation of nitrates (a) and lead (b) in the water samples

Table 2. Information on sampling location and hydro chemical characteristics

n=60	Depth of hydrostatic level (m)	Sampling depth (m)	Temperature (°C)	pH	Conductivity (µS/cm)	Salinity (‰)	TDS (mg/L)	Cr (µg/L)	Fe (µg/L)	Co (µg/L)	Ni (µg/L)	Cu (µg/L)	Zn (µg/L)	Cd (µg/L)	Pb (µg/L)
Mean	6.02	9.04	13.58	6.88	1,397.98	0.69	680.00	49.93	341.04	0.93	37.40	13.44	44.06	0.21	18.86
Standard Error	0.65	0.72	0.15	0.02	99.36	0.05	51.31	1.69	19.06	0.05	2.62	1.09	4.41	0.07	1.99
Median	4.75	7.15	13.50	6.87	1,225.00	0.60	590.00	51.33	303.95	0.83	30.24	10.12	34.21	0.10	15.88
Mode	5.00	4.50	13.00	6.95	1,244.00	0.60	565.00	63.19	556.21	1.31	68.13	20.14	35.03	0.10	24.14
Standard Deviation	5.03	5.55	1.16	0.16	769.60	0.41	394.12	12.28	138.72	0.35	19.06	7.94	32.09	0.50	14.51
Sample Variance	25.32	30.78	1.35	0.03	592,286.15	0.16	155,327.14	150.72	19,244.46	0.12	363.35	63.00	1,029.61	0.25	210.61
Kurtosis	2.99	1.84	-0.34	1.05	10.50	10.58	10.88	4.08	-0.05	3.12	0.44	1.18	0.00	29.11	-0.42
Skewness	1.61	1.37	0.49	0.63	2.95	2.97	3.02	-1.42	0.56	0.90	1.00	1.32	1.07	5.07	0.76
Range	24.00	24.50	4.50	0.86	4,421.00	2.30	2,265.00	70.12	682.54	2.24	87.84	34.84	126.42	3.32	50.46
Minimum	1.00	3.00	12.00	6.53	599.00	0.30	285.00	0.12	14.32	0.04	0.10	0.17	2.94	0.00	0.02
Maximum	25.00	27.50	16.50	7.39	5,020.00	2.60	2,550.00	70.24	696.86	2.28	87.94	35.01	129.36	3.32	50.48

The accepted maximum concentrations of different metal ions, in groundwaters are regulated by national and international laws enforced by different agencies (Ministry Order 621/July 2014, Romanian Law no. 311 from 28/06/2004; European Committee Directive 2006/118/CE and U.S. Environmental Protection Agency). The spatial distribution of some heavy metals concentrations was shown in Figure 4. Our studies showed that the tested samples have Cr concentration close to the maximum accepted value, with the lowest concentration registered for sample W18. Co, Cu, Cd and Pb concentrations remained within the allowed range, while the iron concentrations were close to the maximum allowed limit. Also, 95% of the samples presented high concentrations of Ni, the highest value being registered for sample W37, over three times greater than the maximum allowed value. The high concentrations of Ni which were found in groundwater bodies could be a result of ore-bearing rocks found in the vicinity of the water sources, this supposition being also backed-up by research undertaken by WHO concerning the influence of ore-bearing rocks on the environment (WHO 2011). With regards to the Zn concentrations, in three cases, W26, W42 and W56, the registered values exceeded the maximum allowed limit. The high concentrations of this particular compound could have originated from the agricultural and industrial activities in the area, such as oil extraction and refineries.

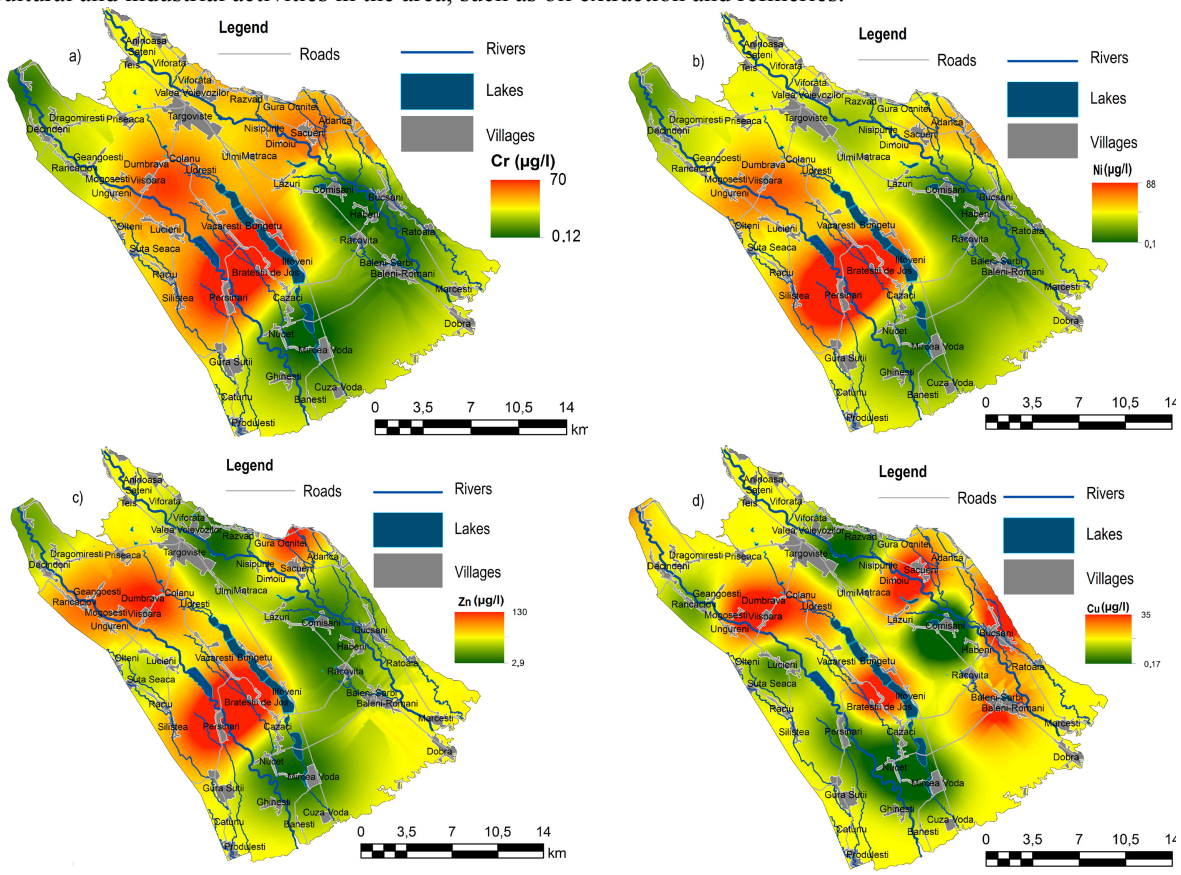

Figure. 4. Heavy metals concentrations (µg/l) present in the water samples (a) - Cr (µg/l); (b) - Ni (µg/l); (c) - Zn (µg/l); (d) - Cu(µg/l)

Fluorescence spectroscopy

Fluorescence spectroscopy was used in order to identify the presence of protein-like and humic-like components of OM. A graphical illustration of the geographical distribution of the fluorescence spectroscopy data is presented in Figure 5. The protein-like signature in the fluorescence spectra is given by peaks T (tryptophan-like) and B (tyrosine-like), while the humic-like marker is exhibited by peaks A, C and M (Coble, 1996). Peak T was recorded in the region λ_{ex}=230-240 nm/λ_{em}=325-345 nm, while peak B was determined in the region λ_{ex}=230-240 nm/λ_{em}=300-310 nm. In the case of humic-like substances, the wavelengths domains were λ_{ex}=230-250 nm/λ_{em}=405-430 nm for peak A, λ_{ex}=300-350 nm/λ_{em}=410-435 nm for peak C (Carstea et al., 2013) and λ_{ex}=312 nm/λ_{em}=380-420 nm for peak M (Carstea et al., 2013; Hudson et al., 2007).

The acquired data revealed that the humic signature (peaks A and C) was more intense than the proteic one for most of the samples. The highest values registered for these peaks originated from the sample wells W26 and W41 located near forests or pastures, while the lowest values corresponded to the water collected from W38 where arable lands and construction sites could be found. Peak M, usually found in areas that have recent biological activity (Coble, 1996) had the highest intensity for sample W22 situated on the green area, while the lowest value corresponded to a well situated in an area where the land was predominantly used for vegetable plantation and greenhouses. Lapworth et al. (2012) showed that greater quantities of OM reach shallow water

tables (~1.5 m below ground) compared to deep aquifers. Apart from a natural OM contribution, nutrients from the agricultural activities could infiltrate into shallow water beds through rainfall and surface runoff.

Peaks T and B were commonly associated to microbial activity (Hudson et al., 2007), and recently, Sorensen et al. (2015) found a relationship between peak T and enteric pathogens in drinking water sources. This relationship depended on the water source proximity to toilets, the depth of the well, the type of bedrock and season. The highest intensities for peaks T and B were registered at the water sample W26. According to Sorensen et al. (2016), 91% of water sources contaminated with thermotolerant coliforms were located within 10 m of a toilet. Pit latrines and septic tanks are commonly used in the rural area of the Targoviste Plain, and therefore it could explain the results.

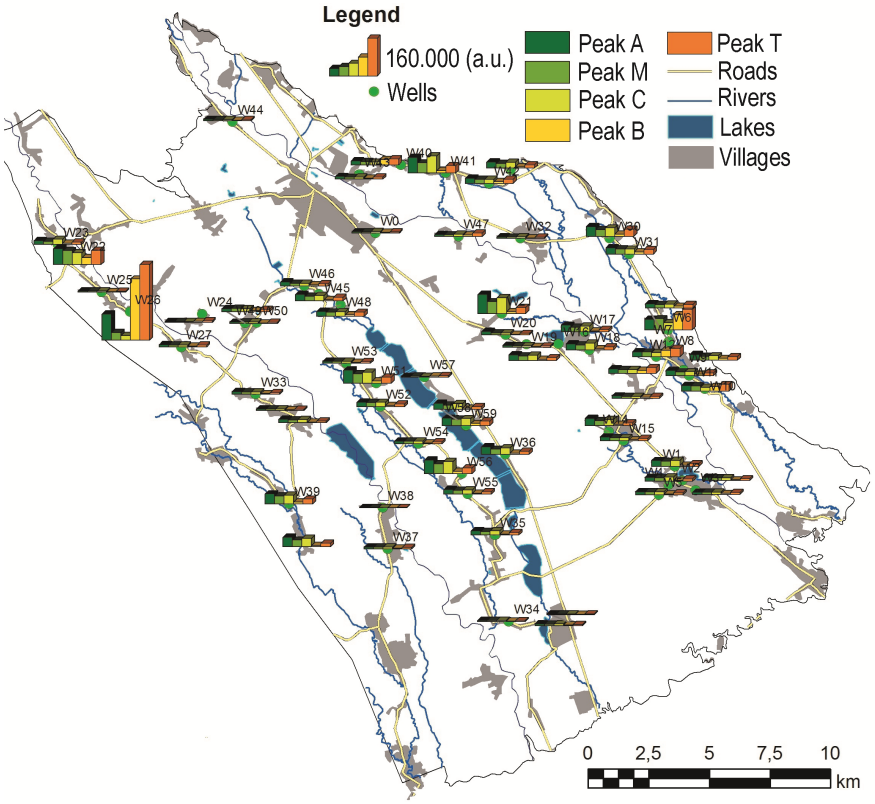

Figure 5. The distribution of fluorescence peaks associated with protein-like and humic-like substances

For determining the predominant OM fraction of each water sample, the ratio between peaks T and C was evaluated (Figure 6). As mentioned before, the results suggested that the majority of the tested samples were predominantly comprised of humic or fulvic-like material with the T/C ratio less than 1. Only twelve out of 60 samples presented values higher than 1 for the T/C ratio, suggesting that in the case of these samples, the microbial signature was more significant. We observed that the sites where the water samples presented the highest T/C values (W6, W12, W24, W26, W40 and W57) were located in the vicinity of mostly arable lands. In the region where the samples were collected, there were also a few construction sites, but the arable lands were predominant. This could explain the contamination of the groundwaters with soil enriched with organic fertilizer which may have led to an increase of bacterial activity in the soil. Another possible explanation could be the use of organic fertilizer, thus causing higher fluorescent intensities for protein-like peaks. This assumption was supported by studies which suggested that in recent years, the focus has been directed toward organic farming, using animal waste among other practices (Lori et al., 2017). In the case of wells W6 and W12, there was another possible explanation for the high intensities registered for peaks T, B and M. These wells were located in an area with former oil exploitation activities. Previous studies (Carstea et al., 2012) demonstrated that water samples containing traces of petroleum had characteristic fluorescence signatures, giving rise to higher intensities of peaks T, M and B. Therefore, with regard to samples W6 and W12, the most probable explanation for high values of the peaks B, T and M was the presence of petroleum in the groundwater samples. This hypothesis was supported by the chemical analysis performed on samples W6 and W12. Also, there were high concentrations of heavy metals usually found in the composition of petroleum products (Akpoveta and Osakwe, 2014). Moreover, sample W6 had the highest concentrations of Co and Cd from all the tested samples, while the concentration of Pb from sample W12 was high. These results, along with the knowledge of the previous use of

the land suggested that the intensity of peak T might have been influenced by petroleum content, microbial content, or even both.

The lowest values of T/C ratio (T/C <0.5) were registered for samples W14, W17, W21, W23, W56 and W58. In these cases, the surrounding environment was comprised of forests (W14 and W56), pastures (W17, W21, W23 and W58) and inland waters (W17 and W58). Well W57, which had a prevalent microbial-like signature, was closer to the forest, while well W58, which exhibited predominant humic-like markers, was situated in a region of the same village, farther to the forest land. It could be concluded that forests, pastures and inland waters had an important contribution on the groundwater systems, in these cases, the humic-like signature found in the fluorescence spectra being more prominent than the microbial-like markers.

In the region where the highest concentration of protein-like OM was registered, the lands were used for agricultural purposes (arable land and a vineyard) as depicted in Figure 1. In contrast, the area where the T/C ratio was lowest, thus suggesting a high concentration of humic-like OM, a region with reduced human interaction was remarked, a forest being located in there.

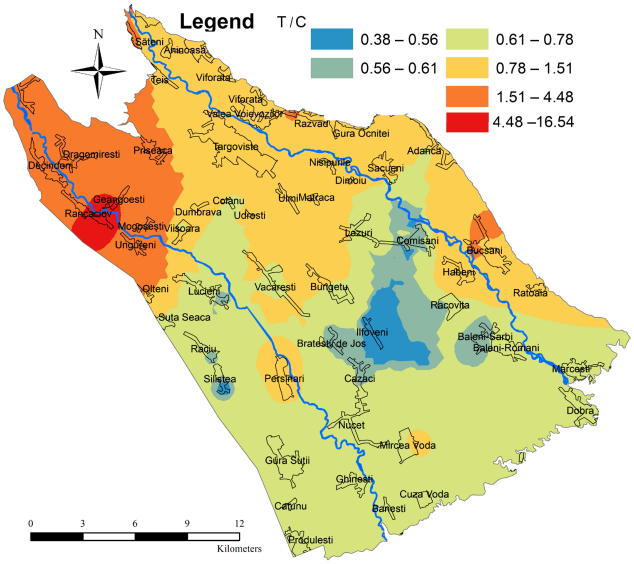

Figure 6. T/C ratio, evidencing the protein-like and humic-like character of the studied wells.

In order to evaluate the degree of OM hydrophobicity, the emission wavelength of peak C was determined for each sample (Figure 7). According to the studies conducted by Baker et al. (2018) low wavelengths, registered in the 400-420 nm range, are associated to relatively hydrophilic OM, while high wavelengths, ranging from 430 nm to 450 nm, are characteristic to waters with hydrophobic OM tendencies (Baker et al., 2008). Most of the samples presented a tendency towards hydrophilic OM. Mixed hydrophilic – hydrophobic and mostly hydrophobic matter was predominant in areas with fruit trees, forests, meadows and vineyards.

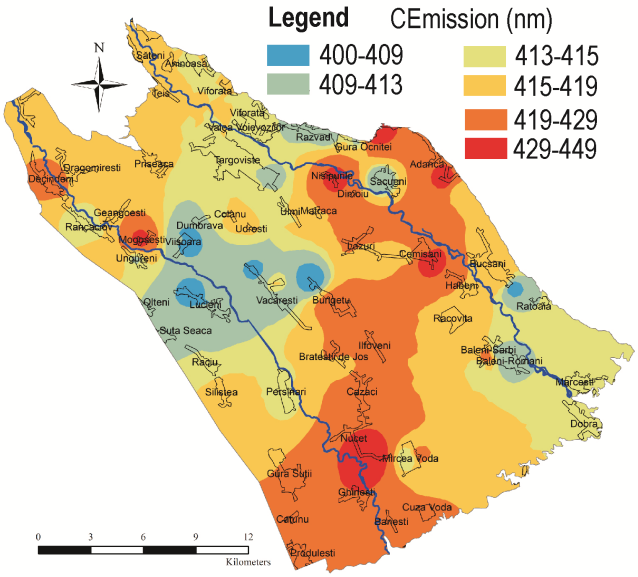

Figure 7. The distribution of the hydrophobicity degree of groundwater OM.

Table 3. Correlation matrix of the selected 23 Physico-chemical parameters determined for the left bank of Ialomita River.

	Conductivity	*Salinity*	*TDS*	*SO_4*	*HCO_3*	*Na*	*Mg*	*Fe*	*Co*	*Ga*	*Sr*	*Cd*	*In*	*Ba*	*Tl*	*Pb*	*PeakA (a.u.)*	*PeakM (a.u.)*	*PeakC (a.u.)*	*PeakB (a.u.)*	*PeakT (a.u.)*	*CEmission (nm)*	*T/C*
Conductivity	***1***																						
Salinity	***1***	***1***																					
TDS	***1***	***1***	***1***																				
SO_4	*0.59*	*0.59*	*0.59*	***1***																			
HCO_3	*0.27*	*0.28*	*0.28*	*0.63*	***1***																		
Na	*0.33*	*0.33*	*0.34*	*0.64*	***0.95***	***1***																	
Mg	*0.64*	*0.62*	*0.64*	*0.36*	*0.19*	*0.30*	***1***																
Fe	*0.40*	*0.38*	*0.40*	*0.23*	*0.30*	*0.42*	***0.84***	***1***															
Co	***0.75***	***0.74***	***0.76***	*0.31*	*0.39*	*0.48*	***0.78***	***0.76***	***1***														
Ga	***0.85***	***0.85***	***0.85***	*0.55*	*0.51*	*0.56*	*0.67*	*0.46*	***0.80***	***1***													
Sr	***0.87***	***0.86***	***0.87***	*0.43*	*0.17*	*0.34*	*0.67*	*0.56*	***0.82***	***0.73***	***1***												
Cd	***0.87***	***0.87***	***0.87***	*0.55*	*0.54*	*0.62*	*0.63*	*0.51*	***0.88***	***0.93***	***0.81***	***1***											
In	***0.84***	***0.84***	***0.85***	*0.50*	*0.53*	*0.62*	*0.65*	*0.58*	***0.93***	***0.90***	***0.83***	***0.99***	***1***										
Ba	*0.61*	*0.61*	*0.62*	*0.24*	*0.44*	*0.48*	*0.60*	*0.68*	***0.86***	*0.67*	***0.73***	***0.76***	***0.83***	***1***									
Tl	***0.86***	***0.86***	***0.87***	*0.49*	*0.52*	*0.58*	*0.62*	*0.52*	***0.90***	***0.91***	***0.84***	***0.98***	***0.99***	***0.85***	***1***								
Pb	*-0.08*	*-0.09*	*-0.09*	*-0.04*	*-0.21*	*-0.22*	*0.28*	*0.05*	*0.02*	*-0.03*	*-0.04*	*-0.08*	*-0.11*	*-0.14*	*-0.13*	***1***							
PeakA(a.u.)	*0.17*	*0.18*	*0.17*	*0.11*	*0.21*	*0.21*	*0.20*	*0.12*	*0.09*	*0.29*	*-0.03*	*0.28*	*0.24*	*0.17*	*0.24*	*-0.24*	***1***						
PeakM(a.u.)	*0.43*	*0.44*	*0.43*	*0.31*	*0.43*	*0.46*	*0.40*	*0.33*	*0.41*	*0.57*	*0.27*	*0.59*	*0.57*	*0.46*	*0.56*	*-0.31*	***0.92***	***1***					
PeakC(a.u.)	*0.02*	*0.03*	*0.02*	*-0.07*	*0.00*	*-0.02*	*0.04*	*-0.06*	*-0.08*	*0.13*	*-0.21*	*0.10*	*0.05*	*-0.02*	*0.05*	*-0.17*	***0.96***	***0.80***	***1***				
PeakB(a.u.)	***0.78***	***0.78***	***0.78***	*0.50*	*0.57*	*0.63*	*0.51*	*0.50*	***0.81***	***0.81***	***0.78***	***0.90***	***0.92***	***0.86***	***0.94***	*-0.36*	*0.33*	*0.65*	*0.12*	***1***			
PeakT(a.u.)	***0.77***	***0.77***	***0.78***	*0.51*	*0.55*	*0.62*	*0.58*	*0.53*	***0.77***	***0.83***	***0.71***	***0.89***	***0.90***	***0.80***	***0.91***	*-0.34*	*0.55*	***0.81***	*0.34*	***0.96***	***1***		
CEmission (nm)	*0.05*	*0.05*	*0.05*	*0.25*	*0.09*	*0.01*	*0.21*	*0.00*	*-0.08*	*0.12*	*-0.17*	*0.01*	*-0.08*	*-0.16*	*-0.05*	*0.62*	*0.04*	*-0.02*	*0.06*	*-0.18*	*-0.11*	***1***	
T/C	***0.72***	***0.72***	***0.73***	*0.40*	*0.36*	*0.40*	*0.45*	*0.47*	***0.74***	*0.65*	***0.82***	***0.73***	***0.79***	***0.86***	***0.83***	*-0.34*	*-0.03*	*0.30*	*-0.22*	***0.89***	***0.77***	*-0.27*	***1***

Due to the various industrial activities that occurred in the surrounding area of the villages situated on the left bank of the Ialomita River, a correlation between the chemical analysis and the fluorescent data has been made and is presented in Table 3. This particular region was subjected to oil exploitations, and there might be some residual pollution related to this type of land use. On the other hand, there are villages, such as Razvad (W40-W42) and Bucsani (W6-W12) where the water quality of the wells could have been impaired due to the diverse industrial influences in the region. From agricultural practices to waste resulted from the pharmaceutical industry and the manufacture of mechanical equipment, the soil and groundwater system were exposed to contamination with various chemical compounds, dangerous for human consumption.

As it could be observed, there was a good correlation ($r>0.7$) between peaks T and B and some heavy metals (Co, Ga, Sr, Cd, In, Ba and Tl). It was interesting to mention that the best correlation was registered between peaks T and B and Cd, In and Tl. These heavy metals are a major concern when found in drinking water sources, and their strong relationships with specific fluorescence signatures could signify that fluorescence spectroscopy could be used as a forefront investigation for determining the quality of groundwater sources, although more research should be undertaken before affirming with absolute certainty that there is a direct link between them. The concentrations of Tl, In and Cd in this area could be linked to the activities performed in the nearby plant that is specialized in manufacturing mechanical components.

It is important to monitor the groundwater quality, especially in regions where people rely on this kind of water supply for their daily use. The present studies generated a platform for further data, regarding the ability to monitor and identify potential health threats that people might come in contact to. The increased number of studied wells as well as the extent of the area which was investigated, bring new light into the mechanisms that influence the contamination of groundwater systems by external influences, such as soil or land use activities. In this context, our results offered new information on the status of various wells distributed across an extended rural area that relies mostly on well water for daily consumption of household and agricultural endeavours. It is necessary to maintain permanent control of these wells, considering the agricultural activities and exploitations undertaken in the surrounding area, which can lead to alteration of the water quality.

Conclusions

This study presented an evaluation of well water quality from private and public wells located in a rural area from Romania, with industrial and agricultural inputs. The study of chemical parameters and fluorescence indicators was useful to illustrate the impact of soil particularity and anthropogenic activities on groundwater quality. Environmental information regarding the land use in the vicinity of the wells suggested that due to agricultural activities and former oil exploitations, the water quality decreased, in some areas posing a real danger to the population who uses the wells for drinking water.

It was observed that external influences such as soil and land use had a major effect on the chemical content of the groundwater that supplies the wells from Targoviste Plain. Thus, in 95% of the cases, high concentrations of Ni were detected, as a result of ore-bearing rocks found in the vicinity of the water sources. Moreover, the present and former exploitations of the land could have determined an excess or a lack of chemical compounds in the water. An example was the impact of vineyards on the water quality parameters, different types of grapes needing different types of nutrients, influencing the concentration found in the soil and the underground water. In the same manner, the water coming from wells found in regions where oil extractions are common practices had traces of heavy metals.

Low concentrations of hydrogen carbonate, and high concentrations of lead (50.48 μg/L) and nitrate were found as the result of anthropogenic activities in construction sites and arable lands. High registered values for the sulphate, chloride and nitrate compounds were determined by the soil enriched with organic fertilizer, which also may have led to an increase of bacterial activity in the soil. In the region where the highest concentration of protein-like OM was registered, the lands were used for agricultural purposes, while a high concentration of humic-like OM was present in a region with reduced human interaction, a forest being located there. It could be concluded that there was a strong connection between land uses surrounding wells in rural areas and the water quality they provided. Moreover, the large number of analysed wells spread throughout an extended area provided an overall image on the status of surface underground water sources in a particular area of Romania. These findings could create the premises for even larger experiments in order to gain an accurate understanding of the mechanisms that influence water quality in rural areas.

Acknowledgements: *This work was supported by a grant of Ministry of Research and Innovation, CNCS - UEFISCDI, project number PN-III-P1-1.1-TE-2016-0646, within PNCDI III, by the Core Program 33N/2018 PN18-28/2018, under the support of ANCS.*

References

Akpoveta, O. V., & Osakwe, S. A. (2014). Determination of heavy metal contents in refined petroleum products. *IOSR Journal of Applied Chemistry, 7(6), 01-02.*

Andronache, I., Fensholt, R., Ahammer, H., Ciobotaru, A. M., Pintilii, R. D., Peptenatu, D., Draghici, C-C., Diaconu, D.C., Rudolvic, M., Pulighe, G., Azihou, A.F., Toyi, M.S., & Sinsin, B., (2017). Assessment of textural differentiations in forest resources in Romania using fractal analysis. *Forests, 8(3), 54.*

Avram, M., Mititelu-Ionuş, O., Niculae, M.I., Pătroescu, M., Badiu, D.L. & Avram S. (2018). The role and importance of water bodies for the structure and functions of urban oxygenating surfaces. Case study: South-West Oltenia development region, Romania. in: Gastescu, P., Bretcan, P., (edit.) *4th International Conference Water Resources and Wetlands, 5-9 September, 2018 Tulcea, Romania, pp. (42-47)*

Bain, R., Cronk, R., Hossain, R., Bonjour, S., Onda, K., Wright, J., Yang, H., Slaymaker, T., Hunter, P., Rüss-Ustün, A., & Bartram, J. (2014). Global assessment of exposure to faecal contamination through drinking water based on a systematic review. *Tropical Medicine & International Health, 19(8), 917-927.*

Baker, A., Tipping, E., Thacker, S. A., & Gondar, D. (2008). Relating dissolved organic matter fluorescence and functional properties. *Chemosphere, 73(11), 1765-1772.*

Boengiu, S., Ionuş, O., & Marinescu, E. (2016). Man-made changes of the relief due to the mining activities within Husnicioara open pit (Mehedinţi County, Romania). *Procedia Environmental Sciences, 32, 256-263.*

Carstea, E. M., Ghervase, L., Pavelescu, G., & Tautan, M. (2012). Real-time monitoring of an urban river contaminated with petroleum products. *Environmental Engineering & Management Journal (EEMJ), 11(2).*

Carstea, E. M., Ioja, C. I., Savastru, R., & Gavrilidis, A. (2013). Spatial characterization of urban lakes. Romanian Reports in Physics, 65(3), 1092-1104.

Cartwright, I., Werner, A. D., & Woods, J. A. (2019). Using geochemistry to discern the patterns and timescales of groundwater recharge and mixing on floodplains in semi-arid regions. *Journal of Hydrology, 570, 612-622.*

Chelarescu, E. D., Radulescu, C., Stihi, C., Bretcan, P., Tanislav, D., Dulama, I. D., Stirbescu, R.M., teodorescu, S., Bucurica, A.,Andrei, R. & Morarescu, C. (2017). Analysis of elements in lake sediment samples by PIXE spectrometry. Nuclear Instruments and Methods in Physics Research Section B: Beam Interactions with Materials and Atoms, 406, 58-60.

Chica-Olmo, M., Luque-Espinar, J. A., Rodriguez-Galiano, V., Pardo-Igúzquiza, E., & Chica-Rivas, L. (2014). Categorical Indicator Kriging for assessing the risk of groundwater nitrate pollution: the case of Vega de Granada aquifer (SE Spain). Science of the Total Environment, 470, 229-239. https://doi.org/10.1016/j.scitotenv.2013.09.077

Coble, P. G. (1996). Characterization of marine and terrestrial DOM in seawater using excitation-emission matrix spectroscopy. Marine chemistry, 51(4), 325-346. https://doi.org/10.1016/0304-4203(95)00062-3

Costache, A.& Sencovici, M. (2015). Influence of the socio-demographic variables on environmental perception. Case study: Targoviste (Dambovita county, Romania) 15th International Multidisciplinary Scientific Geoconference (SGEM) Ecology, Economics, Education And Legislation, Vol I Book Series: International Multidisciplinary Scientific GeoConference-SGEM JUN 18-24, 2015 (pp: 431-438)

Costache, A., Sencovici, M., & Murarescu, O. (2014). Land use and land cover change in Dambovita county, Romania (1990-2012). 14th SGEM GeoConference on Ecology, Economics, Education And Legislation, 2 (SGEM2014) Conference Proceedings, ISBN 978-619-7105-17-9/ISSN 1314-2704, June 19-25, 2014, Vol. 1, 405-412 pp), 405-412.

D'Aniello, A., Cimorelli, L., Cozzolino, L., & Pianese, D. (2019). The Effect of Geological Heterogeneity and Groundwater Table Depth on the Hydraulic Performance of Stormwater Infiltration Facilities. *Water Resources Management, 33(3), 1147-1166.*

Diaconu, D. C., Andronache, I., Ahammer, H., Ciobotaru, A. M., Zelenakova, M., Dinescu, R., Pozdnyakov, A.V. & Chupikova, S. A. (2017). Fractal drainage model-a new approach to determinate the complexity of watershed. *Acta Montanistica Slovaca, 22(1).*

Diaconu, D. C., Bretcan, P., Peptenatu, D., Tanislav, D., & Mailat, E. (2019a). The importance of the number of points, transect location and interpolation techniques in the analysis of bathymetric measurements. *Journal of Hydrology, 570, 774-785.*

Diaconu, D. C., Andronache, I., Pintilii, R-D., Bretcan, P., Simion, A.G., Draghici, C.C., Gruia, K.A., Grecu, A., Marin, M., & Peptenatu. D. (2019b). Using fractal fragmentation and compaction index in analysis of the deforestation process in Bucegi Mountains Group, Romania. *Carpathian Journal of Earth and Environmental Sciences 14 (2), 431-438.*

Dontu, S. I., Popa, C. L., Ioja, C. I., Tautan, M., & Carstea, E. M. (2018). Spatial and temporal variability of organic matter from an urban lake. in: Gastescu, P., Bretcan, P., (edit.) 4th International Conference Water Resources and Wetlands, 5-9 September, 2018 Tulcea, Romania, pp. 34-41

Drăghici, C. C., Andronache, I., Ahammer, H., Peptenatu, D., Pintilii, R. D., Ciobotaru, A. M., Simion, A.G., Dobrea, R.C., Diaconu, D.C., Vișan, M -C.& Papuc, R. M. (2017). Spatial evolution of forest areas in the northern Carpathian Mountains of Romania. *Acta Montanistica Slovaca, 22(2).*

Drinking water regulations and contaminants. https://www.epa.gov/dwregdev/drinking-water-regulations-and-contaminants (accessed 12 September 2018)

Dulama ID, Radulescu C, Chelarescu ED, Stihi C, Bucurica IA, Teodorescu S, Stirbescu RM, Gurgu IV, Let DD, Stirbescu NM (2017) Determination of heavy metal contents in surface water by inductively coupled plasma–mass spectrometry: a case study of Ialomita River, Romania. Rom. J. Phys. 62, 807.

Dunca, A. (2018). Monitoring Long-Term Air Temperature Regime in Banat (Romania). Annals of Valahia University of Targoviste, *Geographical Series, 18(1), pp. 74-83. doi:10.2478/avutgs-2018-0009*

Dunea, D., Tanislav, D., Stoica, A., Bretcan, P., Muratoreanu, G., Frasin, L.N., Alexandrescu, D. & Iliescu, N. (2018). ECO-PRACT: A project for developing the research competences of students regarding the monitoring of floristic composition in mountain grasslands. *Journal of Science and Arts, 18(1), 225-238.*

Gohar, A. A., Cashman, A., & Ward, F. A. (2019). Managing food and water security in Small Island States: New evidence from economic modelling of climate stressed groundwater resources. *Journal of Hydrology, 569, 239-251.*

Grigoraș, G. & Urițescu, B. (2018). Spatial Hotspot Analysis of Bucharest's Urban Heat Island (UHI) Using Modis Data. Annals of Valahia University of Targoviste, *Geographical Series, 18(1), pp. 14-22. doi:10.2478/avutgs-2018-0002*

Hudson, N., Baker, A., & Reynolds, D. (2007). Fluorescence analysis of dissolved organic matter in natural, waste and polluted waters-a review. River research and applications, 23(6), 631-649. https://doi.org/10.1002/rra.1005

Ionuș, O. (2011). The characteristics of the chemical flow within the Motru catchment area, South-West Romania. *Central European Journal of Geosciences, 3(1), 39-43.*

Jacks G, Sharma VP (1983) Nitrogen circulation and nitrate in ground water in an agricultural catchment in southern India. *Environmental Geology, 5(2):61–64.*

Jang CS (2013) Use of multivariate indicator kriging methods for assessing groundwater contamination extents for irrigation. *Environ. Monit. Assess. 185, 4049-4061.*

Journel AG (1983). Nonparametric estimation of spatial distributions. J. Int. Ass. Math. Geol. 15, 445-468.

Lapworth, D. J., Baran, N., Stuart, M. E., & Ward, R. S. (2012). Emerging organic contaminants in groundwater: a review of sources, fate and occurrence. *Environmental pollution, 163, 287-303.*

Lead in Drinking-water, Background document for development of WHO Guidelines for Drinking-water Quality, WHO/SDE/WSH/03.04/09/Rev/1, World Health Organization 2011

Lori, M., Symnaczik, S., Mäder, P., De Deyn, G., & Gattinger, A. (2017). Organic farming enhances soil microbial abundance and activity—A meta-analysis and meta-regression. *PLoS One, 12(7), e0180442. doi: 10.1371/journal.pone.0180442*

Marinică, I. (Oprea) Constantin, D.M., Marinică, A.F., & Vătămanu, V.V., (2016). Considerations on climate variability in south-western Romania in 2015, in: Gastescu, P., Bretcan, P. (edit) 3rd International Conference Water resources and wetlands Conference Proceedings, 120-127, 8-10 September, 2016 Tulcea, Romania, pp. 120-127.

Minea, I. (2017). Streamflow-base flow ratio in a lowland area of North-Eastern Romania. *Water Resources, 44(4), 579-585.*

Minea, I., & Croitoru, A.E., (2017). Groundwater response to changes in precipitations in North-Eastern Romania, *Environ. Eng. Manag. J. 16, 643-651.*

Minea, I., Hapciuc, O. E., Bănuc, G., & Jora, I. (2016). Trends and variations of the groundwater level in the north-eastern part of Romania. International Multidisciplinary Scientific GeoConference: SGEM: Surveying Geology & mining Ecology Management, 1, 1053-1060.

Nitrate and nitrite in drinking-water Background document for development of WHO Guidelines for Drinking-water Quality, WHO/SDE/WSH/07.01/16/Rev/1, World Health Organization 2011

Nitrate and nitrite in drinking-water Background document for development of WHO Guidelines for Drinking-water Quality, WHO/SDE/WSH/07.01/16/Rev/1, World Health Organization 2011

Nowicki, S., Lapworth, D. J., Ward, J. S., Thomson, P., & Charles, K. (2019). Tryptophan-like fluorescence as a measure of microbial contamination risk in groundwater. *Science of the Total Environment, 646, 782-791.*

Official Report of the Ministry of Health, regarding the quality of drinking water in Dambovita County in 2016, http://www.dspdambovita.ro/files/Informatii%20utile/calitatea%20apei%20 potabile/DSP_DB__ Raport_ calitate_apa_2016.pdf

Othman, S.T., Ismail, Z., Hashim, R. & Mohd, N.S. (2018) The application of geoelectrical and environmetric techniques in assessing the impacts of seawater intrusion on the groundwater of Carey Island, Malaysia in: Gastescu, P., Bretcan, P., (edit.) 4th International Conference Water Resources and Wetlands, 5-9 September, 2018 Tulcea, Romania, pp. 217-223

Palmiotto, M., Castiglioni, S., Zuccato, E., Manenti, A., Riva, F., & Davoli, E. (2018). Personal care products in surface, ground and wastewater of a complex aquifer system, a potential planning tool for contemporary urban settings. *Journal of environmental management, 214, 76-85.*

Patel-Sorrentino, N., Mounier, S., & Benaïm, J. Y. (2002). Excitation-emission fluorescence matrix to study pH influence on organic matter fluorescence in the Amazon basin rivers. *Water Research, 36(10), 2571-2581.*

Pavelescu, G., Ghervase, L., Ioja, C., Dontu, S., & Spiridon, R. (2013). Spectral fingerprints of groundwater organic matter in rural areas. *Romanian Reports in Physics, 65(3), 1105-1113.*

Prăvălie, R., Zaharia, L., Bandoc, G., Petrişor, A. I., ionus, O., & Mitof, I. (2016). Hydroclimatic dynamics in southwestern Romania drylands over the past 50 years. *Journal of Earth System Science, 125(6), 1255-1271.*

Radulescu, C., Bretcan, P., Pohoata, A., Tanislav, D., & Stirbescu, R. M. (2016). Assessment of drinking water quality using statistical analysis: a case study. *Romanian Journal of Physics, 61(9-10), 1604-1616.*

Radulescu, C., Pohoata, A., Bretcan, P., Tanislav, D., Stihi, C., & Chelarescu, E. D. (2017). Quantification of major ions in groundwaters using analytical techniques and statistical approaches. *Romanian Reports in Physics, 69, 705.*

Reynolds, D., Ahmad, S.R. (1995). Effect of metal ions on the fluorescence of sewage wastewater. *Water Research 29(9): 2214–2216.*

Rotaru A, Răileanu P (2008) Groundwater contamination from waste storage works. *Environ. Eng. Manag. J. 7, 731–735.*

Rylander, R. (2008). Drinking water constituents and disease. *J. Nutr. 138, 423S-425S.*

Sakizadeh M, Mohamed MM, Klammler H (2019) Trend Analysis and Spatial Prediction of Groundwater Levels Using Time Series Forecasting and a Novel Spatio-Temporal Method. *Water Resources Management, 1-13.*

Secu, C.V., Minea, I., & Stoleriu, I., (2015). Geostatistical modeling of water infiltration in urban soils. *Carpath. J. Earth Env. 10, 95-104.*

Sencovici, M. (2014) . Aspects concerning the biodiversity of the lakes of Târgovişte Plain, in: Gastescu, P., Marszelewski, W., Bretcan, P., (edit.) 2nd International Conference Water Resources and Wetlands, 11-13 September, 2014 Tulcea, Romania, pp. 146-151

Sencovici, M., & Costache, A. (2012). Methods and means of evaluating the perception concerning the environmental condition. Case study: the urban ecosystem of Târgoviste (Romania). International Multidisciplinary Scientific GeoConference: SGEM: Surveying Geology & Mining Ecology Management, 5, 571.

Shaad, K., & Burlando, P. (2019). Monitoring and modelling of shallow groundwater dynamics in urban context: The case study of Jakarta. Journal of Hydrology. Volume 573: 1046-1056 https://doi.org/10.1016/j.jhydrol.2018.01.005

Soler, D., Menció, A., Zamorano, M., Quintana, X., Compte, J., Casamitjana, X., Martinoy, M. & Pascual, J. (2018) Imaging the effect of dynamic interactions between fresh and sea water on the salinity of an aquifer-coastal wetland system: the restored la Pletera Salt Marsh Lagoons (Catalonia, NE Spain) in: Gastescu, P., Bretcan, P., (edit.) 4th International Conference Water Resources and Wetlands, 5-9 September, 2018 Tulcea, Romania, pp. 203-210

Sorensen, J. P. R., Lapworth, D. J., Marchant, B. P., Nkhuwa, D. C. W., Pedley, S., Stuart, M. E., Bell, R.A., Chirwa, M., Kabika, J., Liemisa, M., & Chibesa, M. (2015). In-situ tryptophan-like fluorescence: a real-time indicator of faecal contamination in drinking water supplies. *Water research, 81, 38-46.*

Sorensen, J. P. R., Sadhu, A., Sampath, G., Sugden, S., Gupta, S. D., Lapworth, D. J., Marchant, B.P., & Pedley, S. (2016). Are sanitation interventions a threat to drinking water supplies in rural India? An application of tryptophan-like fluorescence. *Water research, 88, 923-932.*

Sorensen, J. P., Baker, A., Cumberland, S. A., Lapworth, D. J., MacDonald, A. M., Pedley, S., Taylor, R.G., & Ward, J. S. (2018). Real-time detection of faecally contaminated drinking water with tryptophan-like fluorescence: defining threshold values. *Science of the Total Environment, 622, 1250-1257.*

Spencer, R. G., Bolton, L., & Baker, A. (2007). Freeze/thaw and pH effects on freshwater dissolved organic matter fluorescence and absorbance properties from a number of UK locations. *Water research, 41(13), 2941-2950.*

Thomas, B.F., & Famiglietti, J.S. (2015). Sustainable groundwater management in the arid Southwestern US: Coachella Valley, California. *Water resources management, 29(12), 4411-4426.*

Total dissolved solids in Drinking-water, Background document for development of WHO Guidelines for Drinking-water Quality, Originally published in Guidelines for drinking-water quality, 2nd ed. Vol. 2. Health criteria and other supporting information. World Health Organization, Geneva, 1996.

van Engelenburg, J., Hueting, R., Rijpkema, S., Teuling, A. J., Uijlenhoet, R., & Ludwig, F. (2018). Impact of changes in groundwater extractions and climate change on groundwater-dependent ecosystems in a complex hydrogeological setting. *Water resources management, 32(1), 259-272.*

Wittenberg, H., Aksoy, H., & Miegel, K. (2019). Fast response of groundwater to heavy rainfall. *Journal of Hydrology, 571, 837-842.*

Yang, X. D., Qie, Y. D., Teng, D. X., Ali, A., Xu, Y., Bolan, N., Liu, W-G., Lv, G-H., Ma, L-G., Yang, S-T., & Zibibula, S. (2019). Prediction of groundwater depth in an arid region based on maximum tree height. *Journal of Hydrology, 574, 46-52.*

Zhou, Y., Jeppesen, E., Zhang, Y., Shi, K., Liu, X.& Zhu, G., (2016) Dissolved organic matter fluorescence at wavelength 275/342 nm as a key indicator for detection of point-source contamination in a large Chinese drinking water lake. *Chemosphere. 144, 503-509. https://doi.org/10.1016/j.chemosphere.2015.09.027.*

The Influence of Parameters of Drilling and Blasting Operations on the Performance of Hydraulic Backhoes at Coal Open Pits in Kuzbass

Maxim Tyulenev[1], Oleg Litvin[1], Sergey Zhironkin[2] *and* ***Magerram Gasanov[3]***

The article describes a problem of increasing hydraulic backhoes performance on the open coal pits depending on the parameters of drilling and blasting operations. When developing coal-bearing zones of complex-structured coal deposits, due to the design features of working equipment, mobility and autonomy, hydraulic backhoe excavators are able to perform both mining and overburden operations more efficiently than rope shovels. Hydraulic backhoe excavators are extracting machines with downward scooping, which determines the working out of shotpile of the blasted rock in several layers. Therefore, the primary technological directions of increasing the efficiency of backhoes' operations are the justification of parameters of drilling and blasting operations to ensure a rational degree of rock crushing and rational parameters of the face for maximum realisation of the design features of excavators. As a result of research, the specific consumption of explosive and the diameter of explosive boreholes are among the most significant controlled technological factors that affect the quality of rock crushing. The substantiation and practical application of rational technological parameters for hydraulic backhoes at the open coal pits can provide higher technical and economic indicators on the backhoes application, compared to the rope shovels. The research was based on the data from Kuzbass (Kemerovo region, Russia) coal deposits being developed by open pits.

Keywords: *drilling and blasting operations, the performance of backhoes, the diameter of boreholes, specific consumption of explosive, excavators*

Introduction

More than 110 excavators of hydraulic backhoe type with a bucket capacity of more than 5 m^3 are currently in operation at Russian open-pit mines at overburden operations (Kolesnikov et al., 2018). About 60 machines of this type operate in the open-pit mining of Kuzbass coal deposits. In particular, at the open-pit mines of coal company "Kuzbassrazrezugol", the number of overburden mining and transport complexes based on hydraulic backhoes (produced by Liebherr, Caterpillar, Terex, Hitachi) with a geometric bucket capacity of more than 5 m^3 was about 20 or 12% of the total excavators' pool at the end of 2011. During 2015, they have excavated and loaded more than 100 million m^3 of the rock mass (Tyulenev et al., 2019). Over the coming years, the number of excavators of hydraulic backhoe type is expected to significantly increase and bring the annual volume of work with their use to 150 million m^3 of the rock mass. The average bucket capacity will be more than 14 m^3.

At the initial stage of implementation at Kuzbass open-pit mines, the performance of backhoes for stripping work was significantly less than the productivity declared by the manufacturers. This was explained not only by the lack of practical experience in operating hydraulic backhoes, but also by the lack of recommendations on the basis of which it would be possible to create the most favorable conditions for the realisation of the high potential of backhoe-type excavators (only a few researches in this area were performed) (Bhaveshkumar and Prajapati, 2013; Prakash et al., 2013; Nam and Drebenstedt, 2004; Nam and Drebenstedt, 2009; Conigliaro et al., 2009; Moore and Paredis, 2010; Zhang et al., 2011).

The functional dependence of the performance of the excavator on the parameters of drilling and blasting operations is a necessary element of the optimisation model for substantiating its rational value (Hrehová et al., 2012; Mattis et al., 2012). There are various methods of establishing the dependence of the performance of an excavator on the parameters of drilling and blasting operations, differing in the detail of taking into account the initial factors. For example, the excavator's performance is calculated depending on the diameter of the middle piece of the blasted rock mass and the associated excavation parameters (rock loosening coefficient, bucket filling ratio, duration of individual operations of the excavator's production cycle) (Matushenko, 1975; Litvin and Nikiforova, 2008). Along with this, there is a less detailed approach, in which only the average diameter of the rock piece, the coefficient of rock loosening in the shotpile and the share of the oversized fraction are involved in the calculation (Alabuzhev et al., 1966; Molotilov et al., 2009). The use of a particular approach determines the range of factors that can be researched using an appropriate calculation model and, therefore, has the defined purpose.

Therefore, the challenge remains to justify the dependence of the excavator's performance on the parameters of drilling and blasting operations based on the specific consumption of explosive, which, in turn, is determined by the strength of the explosive rock, the diameter of the borehole charge, and the model of the excavator. Correct determination of specific consumption, in turn, can allow achieving the optimum degree of

[1] *Maxim Tyulenev, Oleg Litvin,* Kuzbass State Technical University, Kemerovo, 650000, Vesennyaya Street, 28, Russia, tma.geolog@kuzstu.ru, litvinoi@kuzstu.ru
[2] *Sergey Zhironkin,* Siberian Federal University, 79 Svobodny pr., 660041 Krasnoyarsk, Russia, zhironkin@inbox.ru
[3] *Magerram Gasanov,* National Research Tomsk Polytechnic University, Tomsk, 634050, Lenin Avenue 30, Russia, hursud1@yandex.ru

crushing of overburden, which is an essential factor determining the performance of excavators.

Passport excavator performance (Q_p, m^3 / hour) is set from the formula (1):

$$Q_p = \frac{3600 \times E}{t_{cp}} \quad (1)$$

where E is the geometric capacity of the excavator bucket, m^3;

t_{cp} is the passport cycle duration when rotated through an angle of 90°, sec.

The technical performance of the excavator (Q_t, m^3 / hour) depends on many factors, the main of which are the characteristics of the size and state of the exploded rock mass. In turn, the characteristics mentioned above of the quality of explosion preparation of the rock mass are determined by the combination of technological parameters and the strength properties of the rocks. These include:

- specific consumption of explosive (q);
- borehole diameter (d_w);
- the geometric capacity of the excavator bucket (E);
- coefficient of rock hardness by Protodyakonov (f).

The indicator of the efficiency of the excavation process is the ratio of the technical performance of the excavator in specific mining conditions to the passport performance (excavation efficiency coefficient, C_{ee}):

$$C_{ee} = \frac{Q_t}{Q_p} \quad (2)$$

The excavation efficiency coefficient has the following properties.

1. The efficiency coefficient is an asymptotically increasing function up to 1 according to the parameters of specific consumption of explosive and the capacity of the excavator bucket.

2. The efficiency coefficient is a decreasing function according to the parameters of the diameter of boreholes and the strength of rocks.

3. The partial derivatives of specific consumption and the capacity of excavator bucket with $q = 0$ and $E = 0$ are equal to zero.

4. The mathematical design of specific consumption of explosives, borehole diameter and rock strength in combination with the dimensional magnitude of the acceleration of gravity are the dimensionless value and characterises the ratio of the significance of these factors, which is experimentally confirmed by the overburden crushing model (Katsubin and Makridin, 2018). It should be borne in mind that the indicator of the rock hardness actually has the dimension of pressure.

On this basis, the functional dependence of the excavation efficiency coefficient C_{ee} is taken as an exponent (Litvin and Nikiforova, 2008):

$$C_{ee} = 1 - exp\left[-a \times \left(\frac{q}{d_w \times f}\right)^b \times E^c\right] \quad (3)$$

By mathematical transformations, the expression can be reduced to a linear model with three unknown parameters *a, b, c*, which were determined by multivariate analysis methods using actual data on 78 mass explosion projects at Kuzbass open pits in 2011-2015. These values were defined as the following: $a = 840$, $b = 2$, $c = 0.5$.

Materials and Methods

An important role in achieving the maximum performance of an excavator is played by the degree of crushing of rocks by an explosion. Imitation calculations confirmed that the rational degree of crushing depends mainly on the operational parameters of the excavator, the blockiness of the exploded rocks. The rational degree of crushing Z_r depending on these factors can be calculated by the formula (4) (Kovalev and Litvin, 2012):

$$Z_r = 1 + \frac{d_e^{n1}}{E^{n2} + n_3} \quad (4)$$

where d_e is the diameter of rock fracture without displacement, m (the distance between the adjacent cracks in the rock array);

n_1, n_2, n_3 are the constant parameters characteristic of the considered excavators (hydraulic backhoes), $n_1 = 2.0$, $n_2 = 0.13$, $n_3 = 0.93$.

The value of $n_2 = 0.13$ confirms the conclusion made when analysing the actual performance of hydraulic

backhoes and their power characteristics that, as the bucket capacity increases, the rational degree of crushing changes to a lesser extent than when using old models of rope shovels (for rope shovels $n_2 = 0.9$).

The rational values of the specific consumption of explosive in the preparation of overburden for hydraulic backhoes are 20–50% higher than the values, recommended for rope shovels with a corresponding bucket capacity (Scott et al., 2010; Hummel, 2012). Herewith the actual values of specific consumption of explosive are higher than calculated ones by 10–30%. For comparison, Table 1 presents data on a rational degree of crushing for the rope shovels (ECG excavators) with a bucket capacity of 5–20 m^3 with the most common rock hardness ratio for Kuzbass open pits f = 5-9 (Tyulenev et al., 2017).

Table 1 – Rational degree of crushing for explosive rock preparation for basic models of rope shovels

The rock hardness ratio by Protodyakonov	***The geometric capacity of the excavator bucket, m^3***		
	5	***10***	***20***
5	*1.40*	*1.36*	*1.32*
6	*1.58*	*1.52*	*1.46*
7	*1.79*	*1.71*	*1.63*
8	*2.03*	*1.92*	*1.82*
9	*2.30*	*2.17*	*2.04*

According to Table 1, in the considered bucket capacity and rock hardness, the degree of crushing for hydraulic backhoes Z_r = 1.53-2.53, and for basic models of rope shovels Z_r = 1.40-2.04. At the same time, as the bucket capacity increases from 5 to 20 m^3, the degree of rock crushing for hydraulic backhoes decreases by 4-6%, and for rope shovels by 9-24%.

Hydraulic backhoes require a higher quality of explosive crushing of overburden, which predetermines the need to increase the specific consumption of explosives by 4–15% compared with the basic models of rope shovels with comparable bucket capacity (Table 2).

Table 2 – Rational degree of crushing of explosive rock preparation for hydraulic backhoes

The rock hardness ratio by Protodyakonov	***Backhoe model, the geometric capacity of the excavator bucket, m^3***						
	Liebherr-984C			***Liebherr-994***		***Liebherr-9350***	***Terex***
	5.2	*6*	*7.5*	*10.3*	*11*	*13.8*	*20.6*
3	*0.9*	*0.9*	*0.9*	*1.18*	*1.18*	*1.18*	*1.17*
4	*1.34*	*1.34*	*1.33*	*1.32*	*1.32*	*1.31*	*1.30*
5	*1.53*	*1.53*	*1.52*	*1.50*	*1.50*	*1.49*	*1.47*
6	*1.77*	*1.76*	*1.74*	*1.72*	*1.72*	*1.70*	*1.68*
7	*2.04*	*2.03*	*2.01*	*1.98*	*1.98*	*1.96*	*1.92*
8	*2.36*	*2.35*	*2.32*	*2.28*	*2.28*	*2.25*	*2.21*
9	*2.72*	*2.70*	*2.67*	*2.62*	*2.62*	*2.58*	*2.53*
10	*3.13*	*3.10*	*3.06*	*3.01*	*2.99*	*2.95*	*2.89*
11	*3.58*	*3.54*	*3.50*	*3.43*	*3.41*	*3.36*	*3.28*
12	*4.07*	*4.03*	*3.97*	*3.89*	*3.87*	*3.81*	*3.71*

According to Table 2, the rational degree of crushing for the rock with higher Protodyakonov hardness ratio for hydraulic backhoes is 15-25% higher than for rope shovels. Compared to the same dependence for increasing the bucket capacity for both types of the excavators, it confirms the fact that hydraulic backhoes are the excavation equipment that is very sensitive to the quality and uniformity of explosive crushing of rock. It is known that the diameter of boreholes is a parameter of drilling and blasting operations, which significantly affects the quality of explosive preparation of the rock mass. Therefore, the justification of the model of drilling rigs, working in complex with hydraulic backhoes should be made taking into account the technical indicators of the drilling, blasting and loading operations.

In the theory and practice of explosive preparation of overburden to excavating and loading operations, there is a fundamental principle – more even distribution of explosive in the rock array contributes to improving the quality and uniformity of rock crushing. From this point of view, the use of explosive boreholes of smaller

diameter has a more favourable effect on the quality and uniformity of crushing of the exploded rock mass.

At the same time, at present, at Kuzbass coal open pits, there is a steady tendency to increase the volume of drilling of explosive using drilling rigs with relatively large diameter boreholes (more than 240 mm). The reason for this is considered to be the higher performance of powerful drilling rigs both in the total length of the boreholes and in the volume of drilled rock. Over the past 10 years, the average diameter of blast holes has increased by more than 15% (Fig. 1).

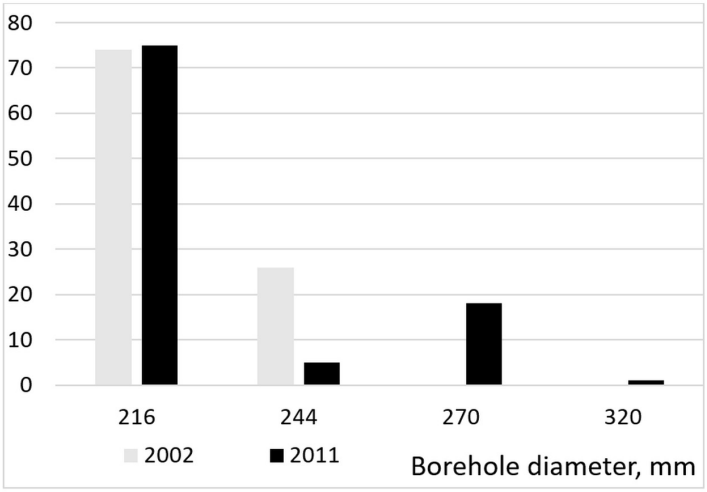

Fig. 1. Dynamics of drilling borehole diameter (the share in all boreholes – based upon the data from authors' surveys and calculations).

As can be seen in Fig. 1, by 2011, up to 20% of the boreholes at Kuzbass open pits had the diameter of 270-320 mm, while in 2002 there were none of them. The increase in the diameter of the boreholes entails an increase in the specific consumption of explosives. In addition, there is a need to increase the over-drill as a part of the borehole (Fig. 2). Over-drilling of boreholes is carried out with the purpose of developing the bench floor, which ensures the possibility of maintaining the horizontal level of the lower working platform. Low quality of the rock mass preparation at the bench floor is due to the low loosening rate of the array in this zone. The possibility of increasing the loosening rate at the floor level is possible, in particular, by increasing the length of the over-drill (l_{over}). It also means an increase in tamping length (l_{tamp}).

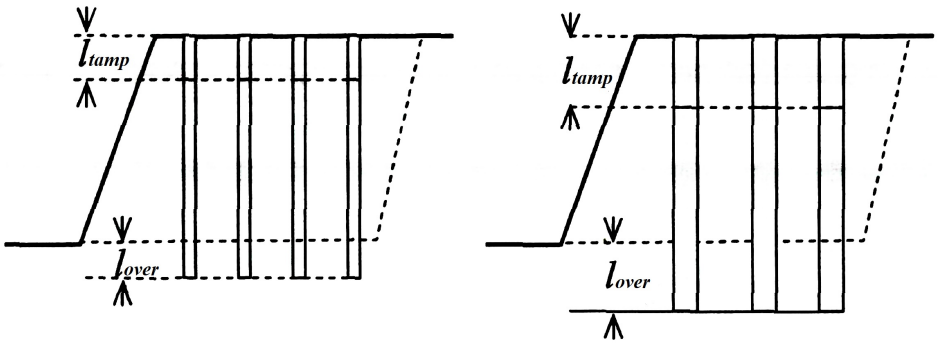

Fig. 2. Conventional charge pattern at different borehole diameters (source: own processing).

The diameter of the boreholes determines the uniform distribution of the total amount of explosives in the exploding rock array (Chung et al., 1991; Benselhoub et al., 2019). With the existing principles for calculating the tamping of boreholes, it is known that a more uniform distribution of explosives in the array corresponds to smaller values of the diameter of the boreholes (Wu et al., 2006; Sun and Deng, 2014; Wang et al., 2018).

Practical experience, experimental and theoretical studies indicate that the uniformity of placement of explosives in the array, achieved by reducing the diameter of the boreholes, contributes to increasing the uniformity and degree of crushing of the rock mass (Litvin and Nikiforova, 2008; Kovalev and Litvin, 2012). This fact applies to all categories of overburden and all types of explosives used at Kuzbass open pits. For illustration in Fig. 3, the qualitative influence of the diameter of the charge on the output of the oversized fraction of blasted rocks of various categories by explosiveness is shown.

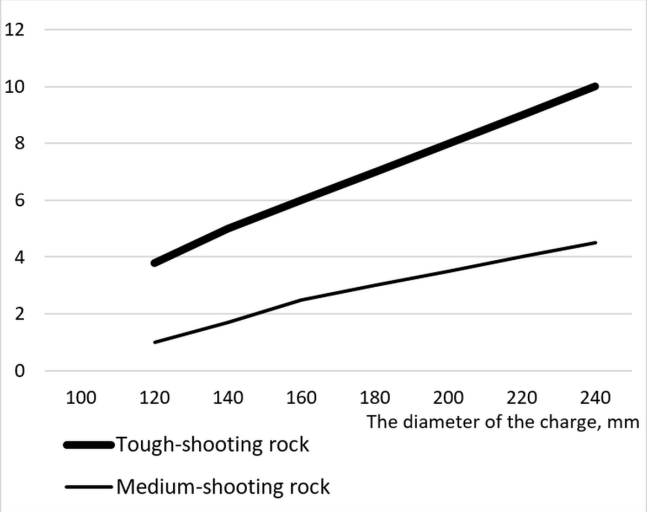

Fig. 3. Influence of charge diameter on the output of oversized fractions for hard and medium shooting rocks (based upon the data from authors' surveys and calculations), %.

As it can be seen in Fig. 3, the lower borehole diameter provides higher blasting quality both for tough-shooting and medium- tough- shooting rocks. The effect of charge diameter on the quality of crushing at different specific consumption of explosives manifests itself with different intensity, and in order to maintain the degree of crushing at a certain level with increasing borehole charge diameter, it is necessary to increase the specific consumption of explosive.

So far, in the methodological part of the standard projects of mass overburden rocks explosions in Kuzbass, the following recommendations were made for the use of boreholes of different diameters drilled by rigs developed for rope shovels in 1980-1990s (Oparin et al., 2012):

1. For easily shooting rocks of homogeneous blockiness, it is possible to use boreholes of relatively large boreholes diameter (250 - 350 mm).
2. For middle-shooting rock category, borehole diameters up to 250 mm are preferred.
3. For tough- shooting rocks that are not uniform in blockiness, the most appropriate are relatively small diameters (150-190 mm).

However, currently, there are no sound recommendations on the choice of the size of modern high-performance diesel drilling machines, working complete with hydraulic backhoes.

The increase in the specific consumption of explosives with an increase in the diameter of the boreholes is due to the existence of two regularities. The first is related to the need to ensure a rational degree of rock crushing for the applicable size of the excavator's bucket. This pattern is reflected in the previously established and statistically justified formula (3) (Litvin et al., 2009), which is the basis for calculating rational values of the specific consumption of explosives in the development of projects for mass explosions at many Kuzbass open pits.

The second regularity is that as the borehole diameter increases, it becomes necessary to increase borehole over-drill in order to maintain high-quality explosive development of the bench floor. In the methodological recommendations made for Kuzbass open pits, the length of the over-drilling of boreholes is related to their diameter in accordance with the formula (5):

$$l_{over} = 3d_w \times d_e + 1 \tag{5}$$

where d_w is borehole diameter, m;

d_e is the diameter of rock fracture without displacement, m

As the diameter of boreholes increases, not only the design specific consumption of explosives increases but also the actual specific consumption – the ratio of the mass of the charge in the borehole to the rock volume, bounded by the dimensions of borehole grid and the depth of borehole (not including over-drilling). Fig. 4 shows the calculated dependences of the design and specific consumption of explosives on the borehole diameter.

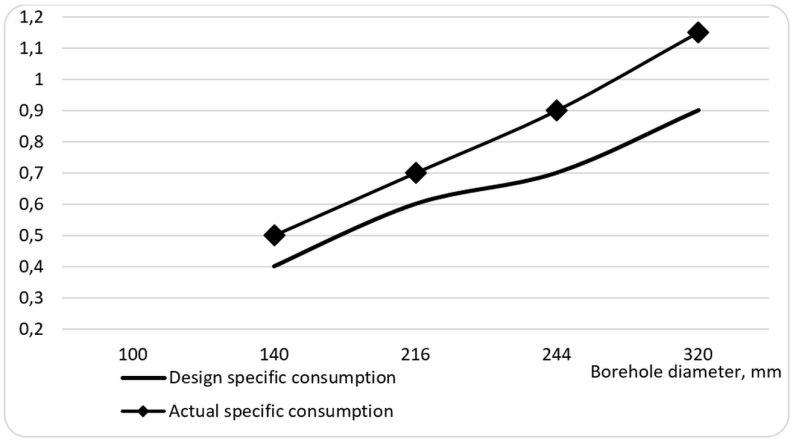

Fig. 4. The characteristic dependence of the specific consumption of explosives on the diameter of boreholes, kg / m³ (based upon the data from authors' surveys and calculations).

As can be seen in Fig. 4, both the design and actual specific consumption, providing the necessary degree of fragmentation, increase almost in proportion to the increase in the diameter of boreholes. It fully corresponds to the dependence shown in Fig. 3 (decrease in oversized fractions output with lowering the diameter of the boreholes).

Results

Regularities of changes in the specific consumption of explosives (Fig.4), the productivity of drilling machines depending on the diameter of boreholes, and the correspondence with the cost parameters of drilling and blasting allowed us to establish the pattern of its influence on the excavators' productivity.

The output of the rock mass can be calculated as:

$$v = \frac{P \times k_{fw}}{q} \tag{6}$$

where: p is the capacity of 1 m borehole, kg;
k_{fw} is the fill factor of the borehole 0.7 - 0.75);
q is the specific consumption of explosives, kg / m^3.

The capacity of 1 m borehole is defined as:

$$P = \frac{\pi d_w^2}{4} \times \rho \tag{7}$$

where ρ is the bulk density of explosives, kg / m^3.

The output of oversized fractions (φ) is set from the following expressions:

$$\varphi = exp(-0.8\lambda^{2.5}) \tag{8}$$

$$\lambda = \frac{l_N}{d_{av}} \tag{9}$$

$$l_N = 0.8E^{0.33} \tag{10}$$

where l_N is the average diameter of an oversized piece of the rock mass (along with an excavator bucket), m;
d_{av} is the diameter of the middle piece of the blasted rock mass, m;
E is the excavator bucket capacity, m^3.

The diameter of the middle piece of the blasted rock mass is determined by the formula (11):

$$d_{av} = \frac{5d_w \times d_e}{5d_w + q \times d_e} \tag{11}$$

The behaviour of the excavation efficiency coefficient C_{ee} and Technical performance of the hydraulic backhoe excavator (Q_t,) during the excavation of blasted rock was researched for the following conditions for drilling, blasting and excavation works:

- overburden rocks have the hardness ratio by Protodyakonov of 3-12;
- the drilling of rocks is made by boreholes with a diameter d_w = 0.216 m;
- regulation of the width of shotpile was carried out by the schemes of millisecond-delay blasting and with the use of explosions with a retaining wall;
- the specific consumption of explosives has its own range of changes depending on the category of rocks by blockiness (Markov et al., 2018) (Table 3).

Table 3 – Range of specific consumption of explosives

Indicators	***Category of rocks by blockiness (the distance between the adjacent cracks in the array, m)***				
	I (<0.1)	***II (0.1-0.5)***	***III (0.5-1.0)***	***IV (1.0-1.5)***	***V (>1.5)***
The lowest value of specific consumption of explosive, kg / m³	*0.1*	*0.2*	*0.3*	*0.4*	*0.5*
The biggest value of specific consumption of explosive, kg / m³	*0.5*	*0.8*	*1.0*	*1.2*	*1.4*

A comparative assessment of the actual (really achieved) and estimated technical performance of hydraulic backhoes Q_t is given in Table 4. The reliability of the approximation of technical performance is 85%.

Table 4 – Comparative evaluation of the calculated and actual performance of the excavator (based upon the data from authors' surveys and calculations)

Bucket Geometric Capacity E, m³	***The rock hardness ratio by Protodyakonov (f)***	***Specific consumption of explosives (q), kg / m³***	***The technical performance of the excavator, m³ / hour***	
			Actual	***Estimated***
5.2	*5*	*0.48*	*307*	*310*
6.0	*9*	*0.82*	*342*	*282*
7.5	*9*	*0.75*	*301*	*337*
10.3	*5*	*0.45*	*496*	*531*
11.0	*9*	*0.75*	*420*	*474*
	10	*0.66*	*499*	*430*
	11	*0.71*	*490*	*432*
	12	*0.8*	*533*	*444*
13.8	*5*	*0.41*	*607*	*700*
20.6	*5*	*0.29*	*842*	*901*
	6	*0.55*	*835*	*930*
	9	*0.75*	*791*	*870*
	10	*0.71*	*971*	*926*

Table 4 data analysis allows concluding that the discrepancy between actual and estimated data does not exceed 17% with an average value of 11%. The specific consumption of explosive is one of the most significant factors that affect the drilling and blasting preparation of rocks for excavation. The substantiation of the specific consumption of explosives is carried out taking into account the influence of the rock hardness (Fig. 5), as well as some other mining engineering factors.

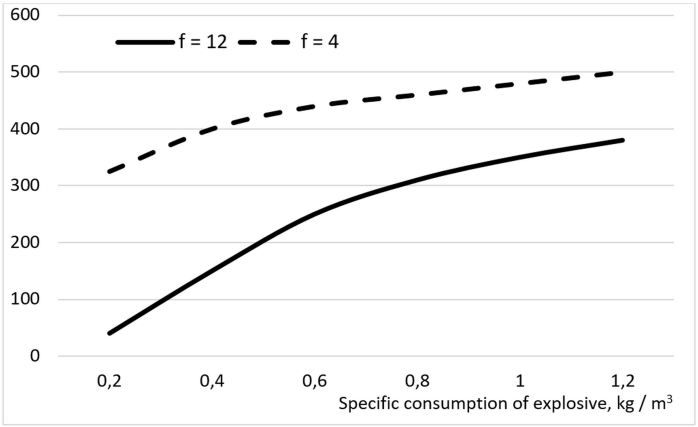

Fig. 5. Characteristic dependence of the passport excavator performance (m^3 / hour) on the specific consumption of explosives (based upon the data from authors' surveys and calculations).

As can be seen in Fig. 4, the growth of specific consumption of explosives influences on the backhoe performance in the maximum extent in the interval of 0.2-0.7 kg / m^3. It is true for both values of Protodyakonov rock hardness ratio f = 4 (sandstone of middle hardness) and f = 12 (very hard sandstone, siliceous schist). The following growth of specific consumption of explosives (0.8-1.2 kg / m^3) leads to a slight increase in backhoe productivity. This can be explained by the growth of borehole diameter, which causes the expanding of the boreholes grid and worsening the rock crush.

Discussion

Hydraulic backhoes – the excavators that actively replace rope shovels at Kuzbass open pits, are more depending on the quality of explosive preparation of rock mass, since the specific force on the cutting edge of the bucket of hydraulic excavators is 1.5-2.0 times less, and the force applied to 1 ton of rock is 3-4 times more compared with rope shovels. This makes hydraulic backhoes more productive machines, but their performance greatly depends on the accuracy of drilling and blasting parameters defining. So they require a higher quality of crushing of the blasted rock mass, which is less dependent on the model of the excavator as compared with rock shovels with comparable bucket capacity.

At present, there is no uniform regulatory framework for explosive consumption for various types of excavators in Kuzbass. Thus, for hydraulic backhoes Liebherr-994, Liebherr-9350, Terex (with a bucket capacity of 10.3-20.6 m^3) and the overburden rocks of the IInd blockiness category, the specific explosives consumption is 0.45-0.6 kg / m^3. At the same time, for a Liebherr-984C excavator in close conditions, the specific consumption is 0.45-0.52 kg / m^3. Reducing the borehole diameter makes it possible to reduce the specific consumption of explosives due to a more even distribution of explosives in the array and a shorter over-drilling length relative to the bench floor. However, there is a decrease in the productivity of drilling equipment both along the length of the drilled boreholes and in the volume drilled. On the other hand, an increase in the borehole diameter is associated with the need for an almost proportional increase in the specific consumption of explosives.

The expedient diameter of borehole charges in the preparation of overburden for excavation by hydraulic backhoes with a bucket geometrical capacity from 5 to 22 m^3 for small, medium and large blocks of overburden is respectively 170-240 mm, 170-220 mm and 170-190 mm.

Specific consumption of explosives, achieved on the basis of production experience of Kuzbass open pits, are characterised by significant fluctuations with a scope of this indicator reaching 1.5-2.33 times. For example, several explosions for a Liebherr-984C backhoe extracting the overburden rocks with Protodyakonov hardness ratio of 5 differ in specific consumption of explosives in 1.52 times. The explosions in the rock face for Liebherr-9350 backhoe, according to the rocks with Protodyakonov hardness of 5-6 differ in specific consumption of explosives in 1.74- 2.33 times. The wide scope of specific consumption of explosives, obtained for different blasts, allowed maintaining the constant backhoe productivity with the dispersion of values not less than 18%.

Acknowledgements: *The research is carried out at Tomsk Polytechnic University within the framework of Tomsk Polytechnic University Competitiveness Enhancement Program grant.*

References

Alabuzhev, P.M., Alimov, O.D., Ermolin, Y.N. and Shekhovtsov, B.A. (1966). The selection of characteristics for very large mechanical shovels. Soviet Mining, 2(2). pp. 183–187

Benselhoub, A., Remli, S. and Rouaiguia, I. (2019). Optimisation of blasting parameters in open cast quarries of El Hassa-Bouira (Northern Algeria). GeoScience Engineering. LXV(1). pp. 53-62. DOI: 10.35180/gse-2019-0006

Bhaveshkumar, P.P. and Prajapati, J.M. (2013). Kinematics of mini hydraulic backhoe excavator. International Journal of Mechanisms and Robotic Systems, 1(4). pp. 261-282

Chung, S.H., Lee, N.H. and Hunter, C.J. (1991). A Blast Design Analysis for Optimising Productivity at INCO Ltd's Thompson Open Pit. Proceedings of 17th Conference on Explosives and Blasting Techniques, 02. pp. 119–127.

Conigliaro, R.A., Kerzhner, A.A. and Paredis, C.J.J. (2009). Model-Based Optimisation of a Hydraulic Backhoe using Multi-Attribute Utility Theory. SAE International Journal of Materials and Manufacturing, 1. 0565. https://doi.org/10.4271/2009-01-0565

Hrehová, D., Cehlár, M., Rybár, P. and Mitterpachová, N. (2012). Mining technology with drilling-blasting operations, Proceedings of 12th International Multidisciplinary Scientific GeoConference SGEM2012. pp. 675–682

Hummel, M. (2012). Comparison of existing open coal mining methods in some countries over the world and in Europe. Journal of Mining Science, 48(1). pp. 146-153

Katsubin, A.V. and Makridin, E.V. (2018). Systematisation of the technological schemes of excavator faces at the central Kuzbass open pit mines. Journal of Mining and Geotechnical Engineering, 1. pp. 81-88. DOI: 10.26730/2618-7434-2018-1-81-88

Kolesnikov, V.F., Cehlár, M. and Tyuleneva, E.A. (2018). Overview of excavation and loading operations in the coal-bearing zones at Kuzbass open pit mines. Journal of Mining and Geotechnical Engineering, 2. pp. 36-49. DOI: 10.26730/2618- 7434-2018-2-36-49

Kovalev, V.A. and Litvin, O.I. (2012). Rational boreholes' diameter in preparation for overburden excavation by reverse hydraulic excavators. Bulletin KuzSTU, 5. pp. 15-17

Litvin, O.I. and Nikiforova, A.S. (2008). The results of processing time observations of the technological cycle of reverse hydraulic shovels. Bulletin KuzSTU, 3. pp. 10-11

Markov, S.O., Tyulenev, M.A. and Kuzin, E.G. (2018). Georadar research of the block structure for drilling and blasting operations on Zarechnyi open pit mine. Journal of Mining and Geotechnical Engineering, 1. pp. 56-63. DOI: 10.26730/2618-7434-201H-1-56-63

Mattis, A.R., Cheskidov, V.I. and Labutin, V.N. (2012). Choice of the hard rock surface mining machinery in Russia. Journal of Mining Science, 48(2). pp. 329-338

Matushenko, V.M. (1975). A method of comparing excavation equipment. Soviet Mining 11(5). pp. 576-578

Molotilov, S.G., Cheskidov, V.I., Norri, V.K. and Botvinnik, A.A. (2009). Methodical principles for planning the mining and loading equipment capacity for open cast mining with the use of dumpers. Part II: Engineering capacity calculation. Journal of Mining Science 45(1). pp. 43-58

Moore, R. and Paredis, C.J.J. (2010). Variable Fidelity Modeling as Applied to Trajectory Optimization for a Hydraulic Backhoe. Proceedings of ASME 2009 International Design Engineering Technical Conferences and Computers and Information in Engineering Conference. August 30–September 2 2009, San Diego. pp. 79-90. https://doi.org/10.1115/DETC2009-87522

Nam, B.X. and Drebenstedt, C. (2004) Use of hydraulic backhoe excavator in Vietnam open pit coal mines. Proceedings of the Thirteenth International Symposium on Mine Planning and Equipment Selection. Wroclaw, Poland, 1-3 September 2004. pp. 197-202.

Nam, B.X. and Drebenstedt, C. (2009). Use of hydraulic backhoe excavator in surface mining, Innovative Entwicklung und Konzepte in der Tagebautechnik. Freiberg, TU Bergakademie. pp. 175-189.

Oparin, V.N., Cheskidov, V.I., Bobyl'sky, A.S. and Reznik, A.V. (2012). The sound subsoil management in surface coal mining in terms of the Kansk-Achinsk coal basin. Journal of Mining Science, 48(3). pp. 585-594

Prakash, A., Mallika, V., Murthy, S.R. and Singh, K.B. (2013). Rock excavation using surface miners: An overview of some design and operational aspects. International Journal of Mining Science and Technology, 23(1). pp. 33-40

Scott, B., Ranjith, P.G., Choi, S.K. and Manoj, K. (2010). A review on existing opencast coal mining methods within Australia. Journal of Mining Science, 46(3). pp. 280-297

Sun, J. and Deng, J. (2014). Calculation of Hole Collapse Pressure Considering the Influence of Borehole Diameter. Journal of Industrial and Intelligent Information, Vol. 2, No. 4, pp. 264-269, DOI: 10.12720/jiii.2.4.264-269

Tyulenev, M.A., Zhironkin, S.A., Litvin, O.I. Tyuleneva, E.A, Zhironkina, O.V. and Markov, S.O. (2017). Safe and Productive Application of Hydraulic Backhoes in Coal-Bearing Areas of Complex Structured Deposits. Geotechnical and Geological Engineering, 35(5). pp. 2065–2077

Tyuleneva, E.A., Lesin, Yu.V. and Litvin, Ya.O. (2019). Research of the coal-bearing zones' mining technology at Kuzbass open pits using simple and complex faces. Journal of Mining and Geotechnical Engineering, 1. pp. 35-49. DOI: 10.26730/2618-7434-2019-1-35-49

Wang, M., Qiu, X. and Zhou, J. (2018). Multi-planar detection optimisation algorithm for the interval charging structure of large-diameter longhole blasting design based on rock fragmentation aspects. Engineering Optimisation. March 2018. https://doi.org/10.1080/0305215X.2018.1439943

Wu, L., Lu, W.B. and Zong Q. (2006). Distribution of Explosive Energy Consumed by Column Charge in Rock. Rock and Soil Mechanics. 27 (5): 735–739.

Zhang, J.-R. Wang, A.-L., Song, S.-T. and Cui D.-M. (2011). An analysis of trajectory in hydraulic backhoe excavators. Journal of North University of China (Natural Science Edition), 2011, 2. 007.

Reduction of NOx formation under the limit combustion conditions through the application of combined primary deNOx methods on the gas boilers

Miroslav Rimár[1], Marcel Fedák[1], Andrii Kulikov[1], Ivan Čorny[1], Milan Abaham[1] and Ján Kizek[2]

The article deals with the issue of reducing the formation of nitrogen oxides in the boundary conditions of combustion. These conditions occur at a high thermal load of the combustion chamber, while the amount of nitrogen oxides increases exponentially according to the Arrhenius formula. Due to this, special attention must be paid to the combustion of natural gas, especially because there is a constant demand for minimizing the formation of pollutants. The simulation model of a steam boiler with 4 industrial gas burners (heat output of each is 17.8 MW) and the high thermal load of the combustion chamber (0.59 MW.m-3) is presented in the paper.

Simulation modelling and subsequent experimental measurements on a real object show how classical primary de-NOx methods manifest themselves under extreme thermal loads. The result of the research is a significant reduction in NOx production, which was achieved by a combination of primary methods.

Keywords: *combustion, boiler, ANSYS, pollutants, NOx.*

Introduction

Optimizing of combustion processes is an important task, considering efficient energy production. An important area is the combustion of natural gas under the limiting/boundary conditions of the thermal load in the combustion chamber, which relates directly to the formation of nitrogen oxides. There are many scientific papers (Zeldovic 1947, Gurevich 1975, Segal 1966) which describe the mechanisms of NOx formation in the combustion process, as well as articles on the chemical kinetics of combustion (Semenov 1930) and flame heat relation to NOx formation (Fenimore 1972, Chen 2017).

As far as the combustion process itself is concerned, it is important to emphasize that high flame temperatures are an integral part of combustion and are critical parameters in terms of burner or boiler performance, as well as flame stability and heat transformation stability (Rimar 2014). Flames are more stable and more homogeneous when the combustion air is preheated compared to normal air temperature (Gopalokrishnan 2007, Lamoreux 2010).

Combustion in the thermal load limiting conditions of the combustion chamber is characterized by an extreme thermal load of the combustion chamber (ETLCCh). The extreme heat load of the combustion chamber means that there is a high temperature in the combustion chamber; this has a negative impact on the formation of nitrogen oxides (Glarborg 1995, Yeh 2013, Rimar 2014, Durdán and Kostúr, 2015).

According to the published works (Fackler 2015, Horbaj 2005, Yeromin 2018), the flame temperature is one of the most important factors influencing the formation of NOx. A particularly critical situation of NOx formation occurs under limiting combustion conditions. Since it is one of the European Union's objectives to alleviate the impact of human activity on the quality of the environment (Hayhurst 1980), the reduction of the formation of nitrogen oxides in the combustion devices is very actual (SR legislation 252/2016). According to European Union legislation, emissions of nitrogen oxides must be significantly reduced (SR Regulation 442/2013).

Recent findings point to the flame geometry as an effective factor in influencing flame temperature and flue gas presence time in the boiler combustion chamber (Basu 1999, Anderson 1995, Panda 2011, Xubo 2016, Duplakova 2014). By setting the flame geometry, it is possible to minimize zones with a temperature above 1775 K, which is limiting in terms of the exponential growth of nitrogen oxides. According to Holoubek (2002) and Rimar (2016), the geometry of the flame is one of the essential factors affecting the formation of nitrogen oxides during combustion.

1.1 Nitrogen oxides formation

Total NOx emissions in the flue gas of steam boilers can be divided into two main compounds NO and NO_2 (Miller 1996, Ferstl 2011, Flimel 2010, Jandačka 2015). Approximately 95-99% of NOx is NO, while the

[1] *Miroslav Rimár, Marcel Fedák, Andrii Kulikov, Ivan Čorny, Milan Abaham:* Department of Process Technique, Faculty of Manufacturing Technologies of the Technical University of Kosice with a seat in Prešov, Bayerova 1, 080 01 Prešov, Slovak Republic, miroslav.rimar@tuke.sk, marcel.fedak@tuke.sk, andrii.kulikov@tuke.sk, ivan.corny@tuke.sk, milan.abraham@tuke.sk

[2] *Ján Kizek,* Department of Thermal Technology and Gas Industry, Institute of Metallurgy, Faculty of Materials, Metallurgy and Recycling of the Technical University of Košice, Letná 9, 042 00 Košice, Slovak Republic, jan.kizek@tuke.sk

content of more toxic NO_2 is not more than 1-5%. Under the influence of natural factors, the largest part of NO after exhaust to the atmosphere is converted to NO_2. Therefore, the calculation of the NOx mass concentrations and emissions is carried out according to NO_2.

Thermal NO - the concentration of thermal NO is controlled by the molar concentrations of nitrogen and oxygen and the combustion temperature. Such processes have a high energy consumption of 561 kJ/mol and thus are dependent on the overall process temperature.

The required time for combustion of the methane/air mixture is approximately 10^{-2} to 10^{-3} s for the equilibrium NO concentration in complete combustion, but the required combustion time is 10 times less, i.e. 10^{-4} s. Nevertheless, hydrocarbon flames have sufficiently high NO concentration, as opposed to H_2 and CO flames in the combustion zone (Flagan 1988). C. Fennimore (1972), based on many reactions, suggests that the rapid NO formation scheme is caused due to the binding of nitrogen radical molecules with CH and C_2 in reactions with low energy barriers. Many scientists (Saheed 2016, Ben Rejeb 2017, Choong-Kil 2011, Boukhalfa 2016, Smeringai 2014, Jeffrey 2013) have conducted experiments and corresponding measurements in this area and it can be said that the rapid nitrogen oxide formation scheme in the flame front is a phenomenon that is organically linked to the properties of the hydrocarbon and carbon fuel flames (Klippenstein 2011, Salokyová 2016, Kristensen 1996). Targeted NOx reduction is not yet fully resolved. The rapid oxidation of nitrogen in the flame front is a reliable and well-known fact (Van Oijen 2016, Yu 2016, Fischer 2016, Panda 2014).

Known characteristics of rapid nitrogen oxidation in flames are: a) short process duration, resulting in the formation of a NO (nitrogen monoxide) zone that is located in a small space around the laminar flame front; b) combustion temperature; c) strong dependence on fuel/air input ratio (Zajac 2004, Wunning 1997).

The basic prerequisite for the formation of NOx as combustion products is the natural presence of atmospheric nitrogen, which is an integral part of the combustion air, or presence of fuel nitrogen, which occurs mainly in liquid and solid fuels. For this reason, the theory distinguishes between thermal nitrogen oxides and fuel nitrogen oxides (Myles 2015).

The basic factors influencing the formation of nitrogen oxides in the combustion process are these: a) flame temperature, b) flame geometry, c) partial pressure of oxygen, d) time of combustion mixture presence at NOx formation.

1.2 Methods of NOx reduction in natural gas combustion

Currently used methods of reducing nitrogen oxides released into the atmosphere from combustion processes are divided into primary and secondary methods. The application of primary methods is based on the reduction of nitrogen oxides formation by Govert S. (2015), and Hua P. (2016), in the combustion process itself.

Based on the knowledge of the causes of nitrogen oxide formation, several methods have been developed to eliminate them, of which the most important are: a) reduction of combustion air temperature, b) substoichiometric combustion, c) flue gas recirculation, d) cascade combustion, e) adjustment of oxygen partial pressure, f) reburning (Westbrook 2005, Bowman 1992, Boxiong 2004).

The above-mentioned articles (Varga 2015) have shown that the course of combustion temperatures in a real plant points to a critical zone of the heat field with temperatures above 1775 K. The results show that the nitrogen oxide growth zone corresponds to these temperature ranges (Young 2012, Adams 2016, Jablonský 2015, Terpák 2007). In a case when several burners are installed in the same combustion chamber, the interaction between them may occur (flames interact), thereby significantly increasing the high-temperature zone and exponentially increasing NOx formation.

Taking into account the temperature as the decisive factor for the formation of NOx, it is also necessary to consider the residence time of the flue gas in the combustion chamber of the boiler, in particular, the residence time of the combustion medium in the high-temperature zone. The effective factor that affects both the flame temperature and the residence time is the flame geometry. By adjusting the flame geometry, it is possible to reduce the area of exponential increase in the formation of nitrogen oxides, to reduce the time during which the combustion mixture remains in the high-temperature zone residence time, and to to minimize areas with temperature above 1775 K. It is obvious that when the flame length is reduced, the flame is expanding or, conversely, when it becomes narrower, its length increases. Shortening of the flame length has a positive effect on the residence time of the mixture in the high-temperature zone.

Another reduction method is combustion with low excess air, which has several advantages. Reduction of combustion air volume is made by the control before the burner. In this way, the oxygen partial pressure is reduced. However, it is important to note that in applying this method it is necessary to have flue gas control devices to avoid a drastic drop in oxygen in the combustion mixture, which would lead to over-limit CO formation. The disadvantage of this method is that simply reducing the volume of combustion air in the power industry burners will cause reduction of the swirling effect, as well as the fuel/air mixing. At the same time as the amount of combustion air decreases, the risk of flame instability increases, there is also a risk of increasing the formation of carbon monoxide and soot.

Cascade combustion is a cascade supply of combustion air or fuel to the burner that is used mainly in low emission burners, so-called LNB burners (Low NOx Burners) or cascade fuel feed and cascade air intake into the combustion chamber – system "over fire air" (OFA) (Dunn-Rankin 2008, Gavlas 2013). Cascade combustion technology not only reduces the amount of thermal NOx but also fuel NOx, as fuel and air can be more thoroughly mixed.

There is another way to reduce nitrogen oxides – injecting water into the combustion air supply. The use of this method is particularly suitable for burners (not LNB technologies) that use preheated combustion air (Trisjono 2016). Injecting water into the combustion air results in the catalytic decomposition of H_2O to hydrogen and atomic oxygen in the zones with high flame temperature. The oxygen reacts primarily with carbon, and the reaction produces carbon monoxide. Two hydrogen molecules from the original H_2O bond are able to reduce nitric oxide→ N2 + 2H $_2$O, thereby reducing NO content. The principle of this method is that atomic oxygen reacts primarily with carbon and not with nitrogen. The disadvantage of this method is the fact that chemically treated water must be available. Another disadvantage is the greater susceptibility to corrosion in the combustion part of the boiler, particularly in areas with insufficient air or flue gas circulation.

2. Materials and Methods

The aim of the research was to assess the effectiveness of particular primary deNOx methods and to find their optimal settings for real boiler operation under limiting combustion conditions. Also, the importance of the interaction of particular deNOx methods and their influence on the overall efficiency of NOx removal in the flue gas, as well as the efficiency of the boiler have been verified. The subject of the research was the heat production unit with four burners installed in the common combustion chamber, as shown in Figure 2. The criterion for comparing the efficiency of NOx reduction in combustion processes is the final concentration of nitrogen oxides in the flue gas under normal conditions.

2.1 Real Device Description

The NOx reduction under limiting combustion conditions using combined primary deNOx methods (CPdeNOx) were tested on a simulation model created in ANSYS Fluent, and simultaneously on a real device - Steam Membrane Boiler OK 60 ČKD Dukla (Figure 1).

There are 4 identical industrial burners installed in the boiler front wall. The burners can operate on natural gas (NG) or heavy fuel oil. In normal operation, natural gas is used as a fuel. Burners belong to low NOx type. The maximum content of nitrogen oxides, according to the manufacturer's technical documentation, per burner should not exceed 100 mg/m^3, provided that it is operated under normal conditions and operating on NG in full range.

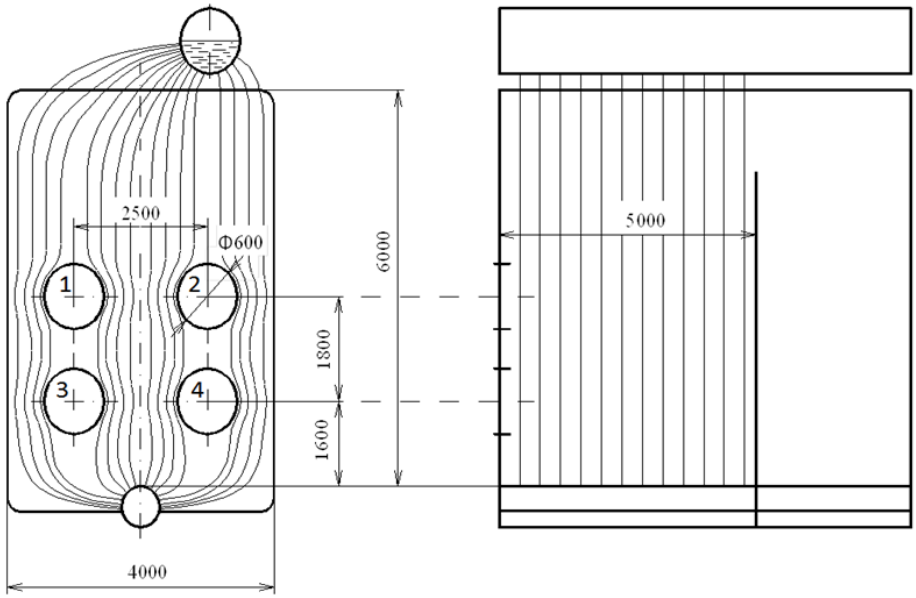

Figure 1. Scheme of boiler OK 60 ČKD Dukla.

The basic technical parameters of the boiler and burners are given in Table 1.

Table 1. Technical parameters of the boiler and burners.

Boiler type	OK 60 ČKD Dukla
Manufacturer	ČKD Tatra Kolín
Highest overpressure	4.5 MPa
Nominal overpressure	3.8 MPa
Designed overpressure	4.0 MPa
Hearth type	overpressure
Nominal steam output	60 $t.h^{-1}$
Efficiency at nominal parameters	90%
Fuel	NG/HFO
Minimum output	30 $t.h^{-1}$
Nominal steam temperature	720 K
Nominal feed water temperature	420 K
Burner type	VKH-17.8-1P
Manufacturer	PBS Třebíč a.s.
Nominal thermal output	17.8 MW
Gaseous fuel NG consumption	1 800 $m^3.h^{-1}$
Nominal pressure of gaseous fuel – NG	50 kPa
Liquid fuel HHO consumption	1.6 $t.h^{-1}$
Nominal pressure of liquid HHO fuel	3.2 MPa
Number of air fans	2
Output of air fans	2 x 12 $m^3.s^{-1}$
Output of smoke fan	37.6 $m^3.s^{-1}$
Designed under pressure in the hearth	20 Pa
Combustion air temperature	475 K
Number of burners	4
Burner type	VKH 17.8 1P
Burner manufacturer	PBS Třebíč
Max burner output	18 000 kW
Gaseous fuel consumption	1 820 $Nm^3.h^{-1}$
Burner regulating range at gaseous fuel	1:5
Gas overpressure before the burner	100 kPa
Combustion air pressure	1 600 Pa
Max. concentration of NOx (NG/HFO)	100/450 $mg.m^{-3}$
Max. concentration of CO (NG/HFO)	50/80 $mg.m^{-3}$

2.2 Description of the Measuring Device

Measurements of gaseous pollutant concentrations of CO, NOx, SO_2, CO_2 as well as O_2 were performed using the HORIBA ENDA 680P emission measurement system. The principles of measuring NOx, SO_2, CO_2, CO are based on modulated non-dispersive infrared detection in the gas flow cross section, and O_2 measurement is performed by magneto-pneumatic detection. The continuous measurement of the observed variables was performed on the basis of physical measurement principles and was evaluated as the average of half-hour values of mass concentrations. The measurement chain diagram is shown in Figure 2.

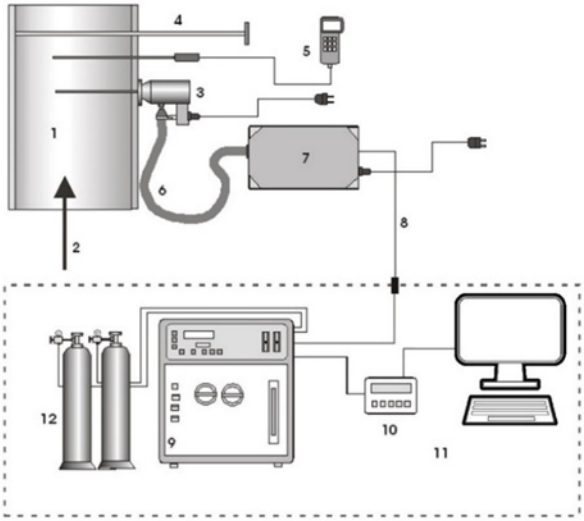

Figure 2. Measuring scheme: 1 – flue gas pipe, 2 – flue gas flow direction, 3 – probe with heated filter for solids, 4 – calibrated rod for measuring pipe dimensions, 5 – thermometer, 6 – heated sampling hose (up to 200°C), 7 – pre-treatment unit with sample cooler and water vapour separator, 8 – Teflon hose (unheated route of treated sample), 9 – HORIBA ENDA 680P multicomponent analyser with 2nd grade sample treatment and vacuum pump, 10 – data logger, 11 – PC, 12 – calibration gases.

The location of the sensor of HORIBA ENDA 680P analyzer, the burners and the boiler OK 60 ČKD Dukla are shown in Figure 3. The probes of the measuring device were placed in the upper part of the boiler flue duct.

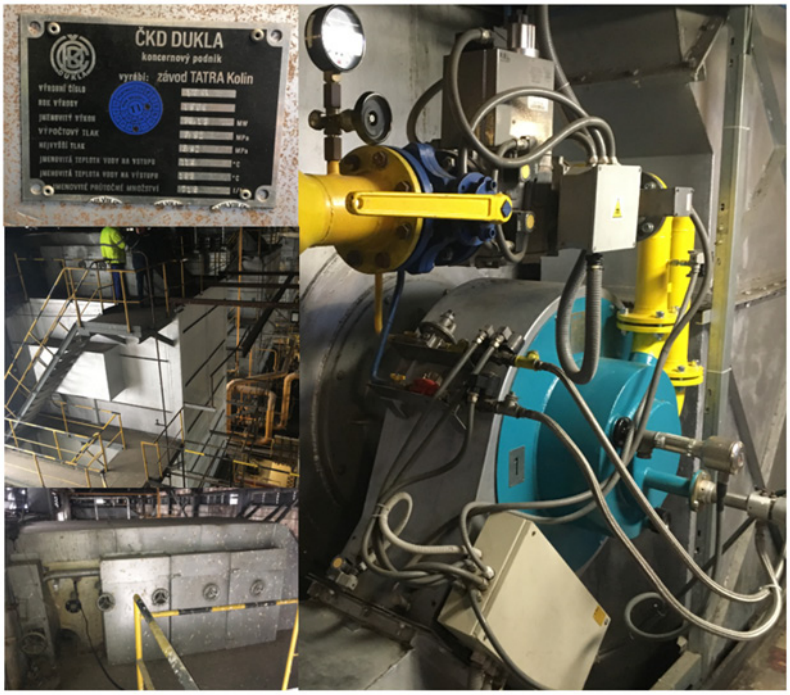

Figure 3. Boiler OK 60 ČKD Dukla. Clockwise: one of 4 gas burners; the top of the boiler duct; height view of the boiler; label with technical parameters of the boiler.

2.3 Description of the Experiment

The main idea of the experiment was to determine the boiler efficiency and to compare all primary deNOx methods suitable for implementation on a given boiler type.

The following primary denitrification methods were selected for processing the experiment:

- Adjustment of oxygen partial pressure
- Cascade combustion
- Injection of auxiliary substances
- Circulation

Each of the methods was tested separately, to determine its effectiveness in the combustion process in terms of nitrogen oxides formation. The whole experiment was divided into four stages.

The first stage is the creation of an accurate simulation model of the membrane boiler OK 60 ČKD Dukla with four burners VKH-17.8-1P using the ANSYS software tool.

The main objective of the first stage is to create an accurate model of the combustion plant with the following validation of the simulation results. Within this validation, the real measurements were performed on the device under different conditions.

The second stage includes the implementation and testing of the primary deNOx methods using the simulation model. The effect of the implementation of each method was evaluated separately by comparing the simulation results with appropriate reference simulation.

In the third stage, the interaction effect of the combination of primary deNOx methods and their impact on NOx formation and overall boiler performance was monitored and evaluated using the simulation environment. Also, the measures have been proposed and simulated to reduce nitrogen oxides in the real plant.

The aim of the last stage was to confirm/validate the results of stage 3 using a series of measurements that were performed in the semi-operational mode.

The diagram of the experiment is shown in Figure 4.

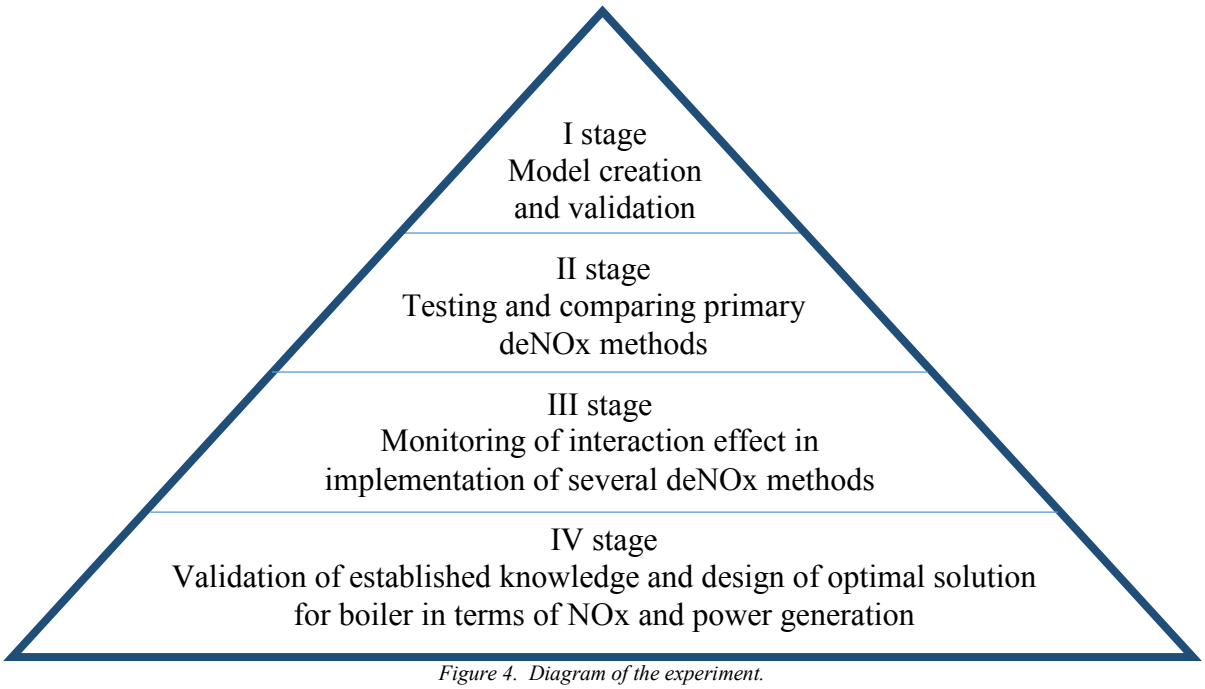

Figure 4. Diagram of the experiment.

3 Experiment

The main idea of the experiment was to determine the efficiency and compare all the primary deNOx methods, which are suitable for implementation on the given type of boiler.

3.1 Modelling

In order to compare the effectiveness of each deNOx method, a computer model was developed. Non-premixed combustion was solved using the ANSYS Fluent simulation software. The CAD models of the boiler and burners were created in ANSYS Design Modeller according to the technical documentation.

As a part of a model, the network has been created for Computational Fluid Dynamics (CFD) Fluent Solver with Proximity, and Curvature Advanced Size functions. Due to the difference in input and output dimensions, the minimum size of the element side was proposed 1.455 mm according to Proximity function, and the maximum size was 500 mm. The element growth rate parameter was set to the value of 1.35. In accordance with these settings, 60% of all elements had an orthogonal quality of more than 0.76, and the lowest value was 0.13, with less than 1% of the elements. According to the skewness statistic, 80% of the elements had the quality of 0.38, with less than 1% of the elements belonging to the worst quality group of 0.7-0.97. The total number of simulation model elements was 18,923,062.

When defining the turbulence model, verification simulations were implemented using integrated modules RANS and then LES. The results of the boiler simulations showed that from the point of view of the calculation stability, the realizable k-epsilon model, which was also applied for the simulations, was the best.

The solved transport equation for the realizable k-epsilon model has the following form:

$$\frac{\partial}{\partial t}(\rho k) + \frac{\partial}{\partial x_j}(\rho k u_j) = \frac{\partial}{\partial x_j}\left[\left(\mu + \frac{\mu_t}{\sigma_k}\right)\frac{\partial k}{\partial x_j}\right] + G_k + G_b - \rho\varepsilon - Y_M + S_k \quad (1)$$

and

$$\frac{\partial}{\partial t}(\rho\varepsilon) + \frac{\partial}{\partial x_j}(\rho\varepsilon u_j) = \frac{\partial}{\partial x_j}\left[\left(\mu + \frac{\mu_t}{\sigma_\varepsilon}\right)\frac{\partial \varepsilon}{\partial x_j}\right] + \rho C_1 S_\varepsilon - \rho C_2 \frac{\varepsilon^2}{k+\sqrt{\varepsilon v}} + C_{1\varepsilon}\frac{\varepsilon}{k}C_{3\varepsilon}G_b + S_\varepsilon \quad (2)$$

where

$$C_1 = max\left[0.43, \frac{\eta}{\eta+5}\right], \eta = S\frac{k}{\varepsilon}, S = \sqrt{2S_{ij}S_{ij}} \quad (3)$$

- In these equations, G_k represents the generation of the kinetic energy of turbulence due to mean velocity gradients.
- G_b is the generation of kinetic energy by turbulence considering buoyancy.
- YM represents a manifestation of fluctuating dilation in compressible turbulence to the overall scattering rate.
- $C_{1\varepsilon}$, $C_{3\varepsilon}$, and C_2 are constants.
- σ_k and σ_ε are turbulent Prandtl numbers for *k* and *e*.
- S_k and S_ε are user-defined source formulas.

The formula for normal Reynolds stress of incompressible average flow results from the combination of Boussinesq approximation and the definition of eddy viscosity.

$$\overline{u^2} = \frac{2}{3}k - 2v_t\frac{\partial U}{\partial x} \quad (4)$$

Eddy viscosity is calculated as:

$$\mu_t = \rho C_\mu \frac{k^2}{\varepsilon} \quad (5)$$

In the case of the realizable k-epsilon model, Cμ is not a constant value:

$$C_\mu = f(k, \varepsilon, \Omega, \omega) \quad (6)$$

Where
Ω – rotation speed tensor,
ω – angular velocity.

The PDF model for non-premixed combustion had additional settings: equilibrium state relation, non-adiabatic energy treatment with 102 325 Pa combustion chamber operating pressure, number of mean mixture fraction points 40, the maximum number of components 30, number of enthalpy points 45.
The PDF compositions, like Laminar Finite-Rate and model, should be used to simulate chemical kinetic effects with a finite extent in turbulent reaction flows. With a suitable chemical mechanism, kinetically controlled elements such as CO and NOx, as well as flame extinction and ignition can be predicted (Boukhalfa 2016).
The transport equation PDF is derived from the Navier-Stokes equation as (Smeringai 2014):

$$\frac{\partial}{\partial t}(\rho P) + \frac{\partial}{\partial x_i}(\rho u_i P) + \frac{\partial}{\partial \psi_i}(\rho S_k P) = -\frac{\partial}{\partial x_i}\left[\rho\langle u_i'' | \psi\rangle P\right] + \frac{\partial}{\partial \psi_i}\left[\rho\left\langle\frac{1}{\rho}\frac{\partial J_{i,k}}{\partial x_i}\middle|\psi\right\rangle P\right] \quad (7)$$

Where
P – common composition of PDF and Favre,
ρ – average liquid density,
u_i – Favre velocity vector,
S_k – the rate of reaction of *k* elements,
ψ – space composition vector,
u_i'' – vector of fluid velocity fluctuation,
J_{ik} – molecular diffusion flow vector.

Notation ⟨…⟩ indicates expectations, and ⟨A | B⟩ is the conditional probability of event A when event B occurs. The turbulent scalar flow is not closed and is modelled by the assumption of diffusion gradient transition (Song 2012):

$$-\frac{\partial}{\partial x_i}\left[\rho\langle u_i^{''}|\psi\rangle P\right] = \frac{\partial}{\partial x_i}\left(\frac{\rho\mu_t}{Sc_t}\frac{\partial P}{\partial x_i}\right) \quad (8)$$

Where
μ_t is turbulent viscosity,
S_{ct} is Schmidt number.

The Turbulence model specifies μt for the composition of PDF simulation.
For all flows, ANSYS Fluent solves the mass and momentum conservation equations. For flows that include heat transfer or compressibility, another energy conservation equation is solved. For flows involving mixing or reactions of the components, the component conservation equation is solved or, if the model is applied for non-premixed combustion, the conservation equations for the mixture fraction and its dispersion are solved. In the case of turbulent flow, additional transport equations are solved.

For the external surfaces of the model, boundary conditions of the second kind were selected. The heat dissipated through the boiler peripheral wall was calculated using a separate model, the determined value is 0.57 MW.

To reduce the computational time, a steady model of combustion and turbulence was chosen. The time processes were chosen as less important because the stationary calculation shows the most likely variation of the combustion processes, as well as the most likely processes of the regular boiler operation mode.

The velocity specification for air and gas inputs has been proposed as a value perpendicular to input with an absolute reference value; the turbulence specification was determined according to the intensity and hydraulic diameter.

Figure 5 shows the CAD model of the burner. The geometry of the combustion chamber and part of the flue gas duct was optimized in terms of calculation time without significant influence on the calculation accuracy.

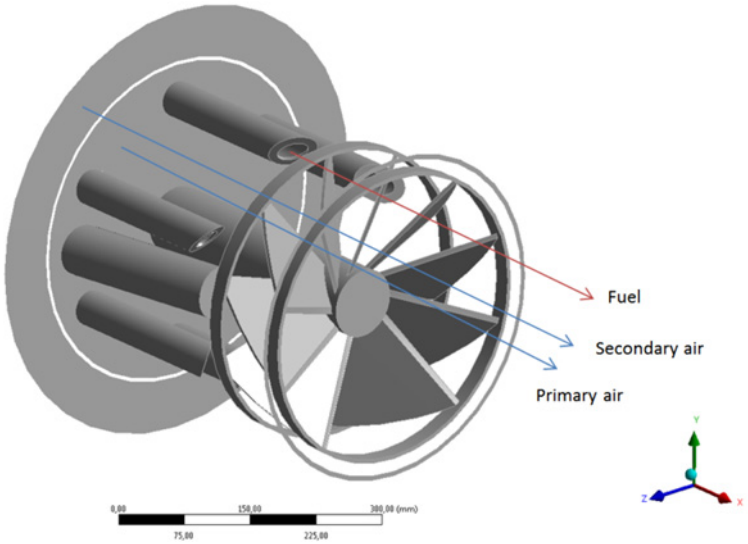

Figure 5. The CAD model of the burner.

3.2 Model Simulation

The geometry of the simulation model was drawn precisely according to the technical parameters and dimensions of the burners and the boiler combustion chamber (Fig. 2 and Table 1), as well as the distances between the burners in the horizontal and vertical planes. The combustion simulation parameters were determined from the burner performance ratios and the corresponding amount of natural gas consumed as the fuel and combustion air as the oxidant. The average composition of the natural gas used in the simulation model (Table 2) was determined from the values representing the volume ratios of the individual components in the real operating conditions of the boiler.

Table 2. Composition of natural gas.

Composition of natural gas [mol %]							
Methane	Ethane	Propane	Butane	Pentane	Hexane +other	Carbon dioxide	Nitrogen
95.361	2.5231	0.6437	0.8504	0.0407	0.0255	0.2351	0.3205

The model validation was done by comparing the simulation output parameters with the real measured values and the calculated values. All monitored parameters of the simulation can be divided into three basic groups:

• Basic physical parameters such as temperature, velocity, pressure, density, viscosity, turbulence energy, heat and mass flows;

• Input parameters: gas and air composition, the content of fuel and air partial elements;

• Output parameters: the content of CO, CO_2, O_2, N_2, NO, NO_2, N_2O, H_2O and other flue gas components.

A series of simulations (j) were performed with increasing iteration number (j * 10E3). The results of which are shown in Table 3. With respect to the measurement method, the concentration values were determined as the mean values at the output of the simulation model.

Table 3. Simulation results.

Exp.	Max. temperature [K]	Min. temperature [K]	NO [mg/m^3]	NO_2 [mg/m^3]	N_2O [mg/m^3]	The volume of high temperature, [m^3]	Number of iterations
1	2155.5	287	347,2	16.32	0.00088	24	1000
2	2156.2	287	347,8	16.45	0.00091	24	2000
3	2156.1	287	348,1	16.67	0.00094	24	3000
4	2156.2	287	348,3	16.68	0.00096	24	4000
5	2156.3	287	348,5	17.14	0.00097	25	5000
6	2156.6	287	348,6	17.18	0.00098	25	6000
7	2156.8	287	348,9	17.21	0.0010	25	7000
8	2157	287	349,1	17.22	0.0010	25	8000
9	2157.1	287	349,1	17.23	0.0011	25	9000
10	2157.1	287	349,2	17.23	0.0011	25	10000

The graphical visualization of the combustion chamber interior displays processes taking place in the boiler. Figures 6 and 7 show the simulation characteristics. The temperature field patterns are shown in Figure 6, and the NO concentrations and kinetic energy are shown in Figure 7 in the horizontal and vertical plane inside the combustion chamber.

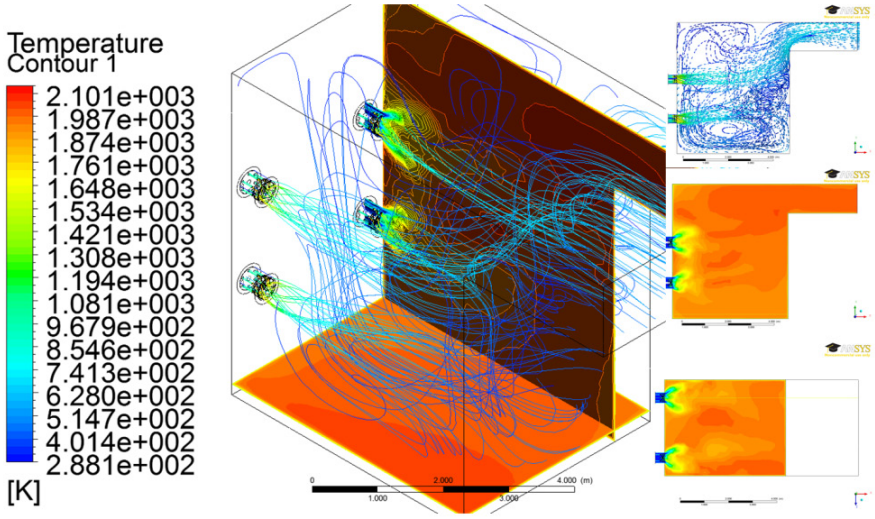

Figure 6. Temperature field patterns.

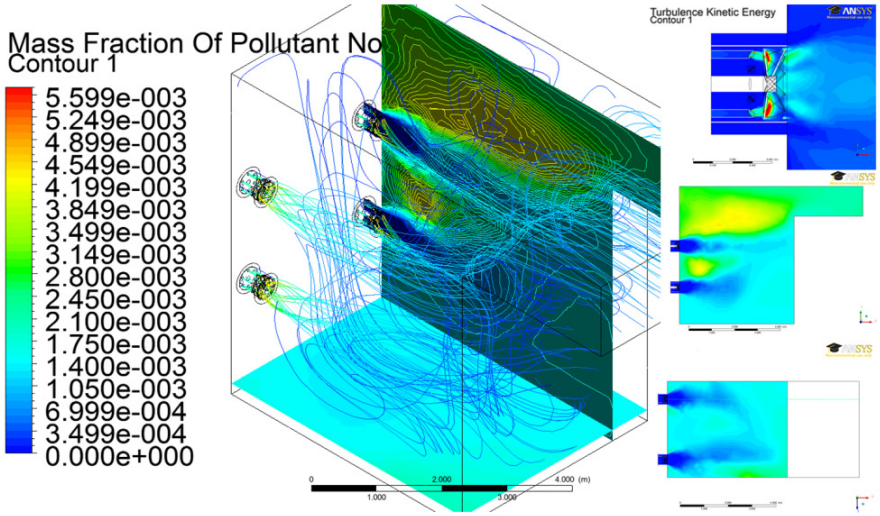

Figure 7. The NO concentrations and kinetic energy patterns.

For the analysis of the mechanism, as well as for the determination of the worst spot for the formation of nitrogen oxides in the boiler, the diagrams of NOx content were created along the horizontal axis of each of the 4 burners, as well as along the horizontal axis of the boiler in the area between the burners.

Figure 8 shows the distribution of the NO mass fraction in dependence on the horizontal distance from the burner and from the horizontal axis of the boiler.

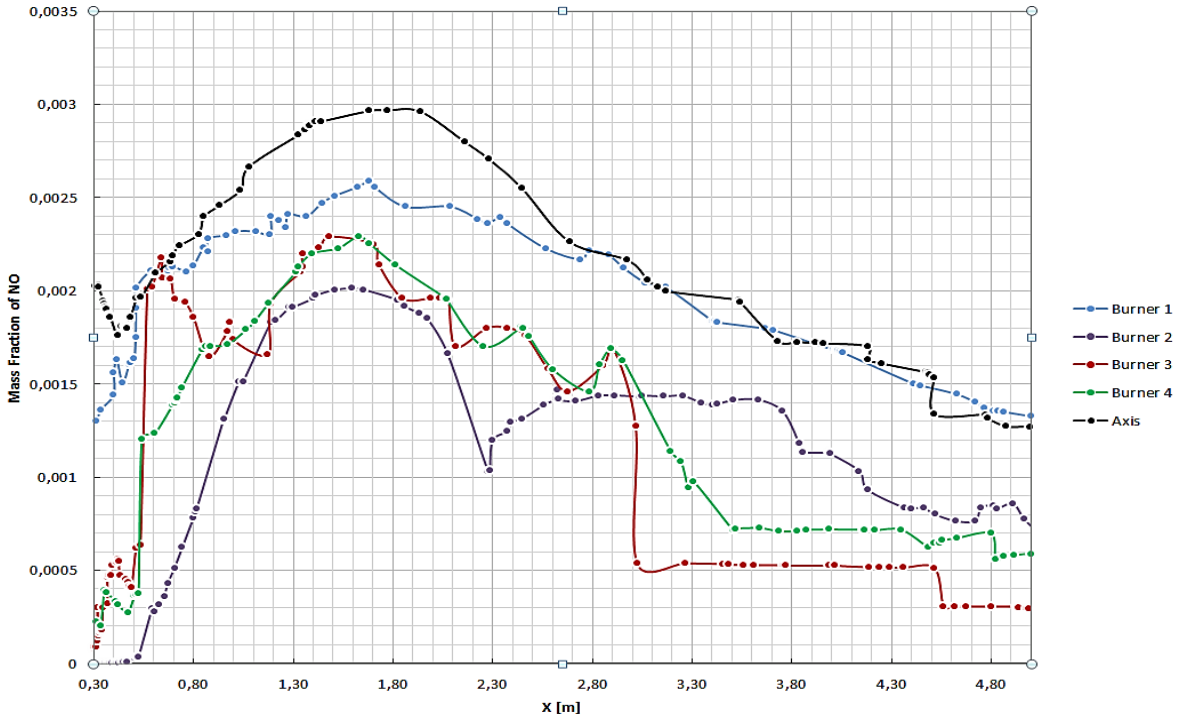

Figure 8. The distribution of the NO mass fraction in dependence on the horizontal distance from the burner and from the horizontal axis of the boiler.

3.3 Model Validation

With regard to the list of standard controlled values and the possibilities of the measuring technique, the flue gas temperatures, oxygen content, carbon dioxide content, as well as the mass concentration of nitrogen oxides in the flue gas were compared.

Table 4 lists the measured values as the mean half-hour values of volumetric and mass concentrations of pollutants calculated for normal pressure, temperature, and the oxygen reference value of 3% at full boiler load.

Table 4. Real measurement results.

Measurement time [h:min]	8:45-9:15	9:15-9:45	9:45-10:15	10:15-10:45	10:45-11:15	Value	
						max	mean
Content [% vol.]							
O_2	7,27	7,15	7,08	6,87	6,85	7,27	7,04
CO_2	7,34	7,41	7,44	7,53	7,53	7,53	7,45
Mass concentration [mg.m^{-3}]							
NO_x	351	353	353	344	348	353	350
CO	3	2	2	6	3	6	3

When comparing simulation model output data with real data, the model was classified as appropriate, including its boundary conditions, the number of repetitions, selected calculation modules, etc. From the comparison of the simulation model results (Table 3) and the measured values (Table 4) of the mass concentrations calculated for reference conditions (normal temperature T_n = 293.15 K, normal pressure p_n = 101,325 Pa) it can be seen that the simulation model shows high compliance level of parameters, especially temperatures, also O_2, CO, CO_2, and NOx concentrations.

It can be seen in Figures 4 and 5 that the dimensions of the combustion chamber and the axial distances between the boiler burners can cause the formation of limiting conditions. These conditions are characterized by the extreme heat load of the combustion chamber Q_n = 0.59 MWm^{-3}. The graphical visualization of the interior of the combustion chamber shows that the burner flames have a direct impact on the back wall of the combustion chamber and confirm the theoretical assumptions regarding the combustion under the limiting conditions formulated in the previous section. Simulations have also confirmed that, because of the short distance between the burners, the high-temperature area increases due to the interaction of the flames, especially when the boiler operates at maximum power.

4 The Results

4.1 Simulation Results

In order to determine the effectiveness of separate primary deNOx methods, a series of simulations were performed in ANSYS Fluent.

4.1.1 Oxygen Partial Pressure

One of the important parameters in terms of combustion stoichiometry, as well as flow and mixing dynamics, is the ratio of combustion air and fuel. From the literature (Varga) it is known that by setting the correct combustion air/fuel ratio, nitrogen oxides production can be reduced by 10 to 15%. From the physic-chemical point of view, the optimum amount of air in the combustion of natural gas is within the range of 102 to 107% of the amount required for complete burning (n = 1.02 - 1.07).

Series of simulations was performed varying amounts of combustion air. On the basis of theoretical knowledge, the effect of the combustion air ratio ranging from 90% to 110% of the stoichiometrically required (complete burning) amount was tested. Based on the results of the simulations, the characteristic diagram (Figure 9) was created.

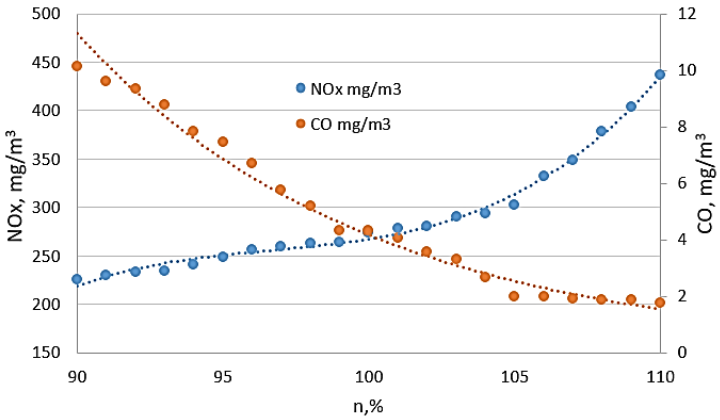

Figure 9. Characteristic diagram of the effect of combustion air ratio ranging from 90% to 110%.

Based on the results of the simulation, it can be concluded that from the viewpoint of the stoichiometry of combustion and NOx formation, the optimal combustion is at 105% from stoichiometrically needed air. At the given value of *n* it is possible to use the fuel efficiently and also, in view of the NOx curve, there is no rapid NOx increase due to higher temperatures in the combustion chamber, and there is no increase of oxygen amount. The graphical visualization of the processes in the combustion chamber is shown in Figure 10.

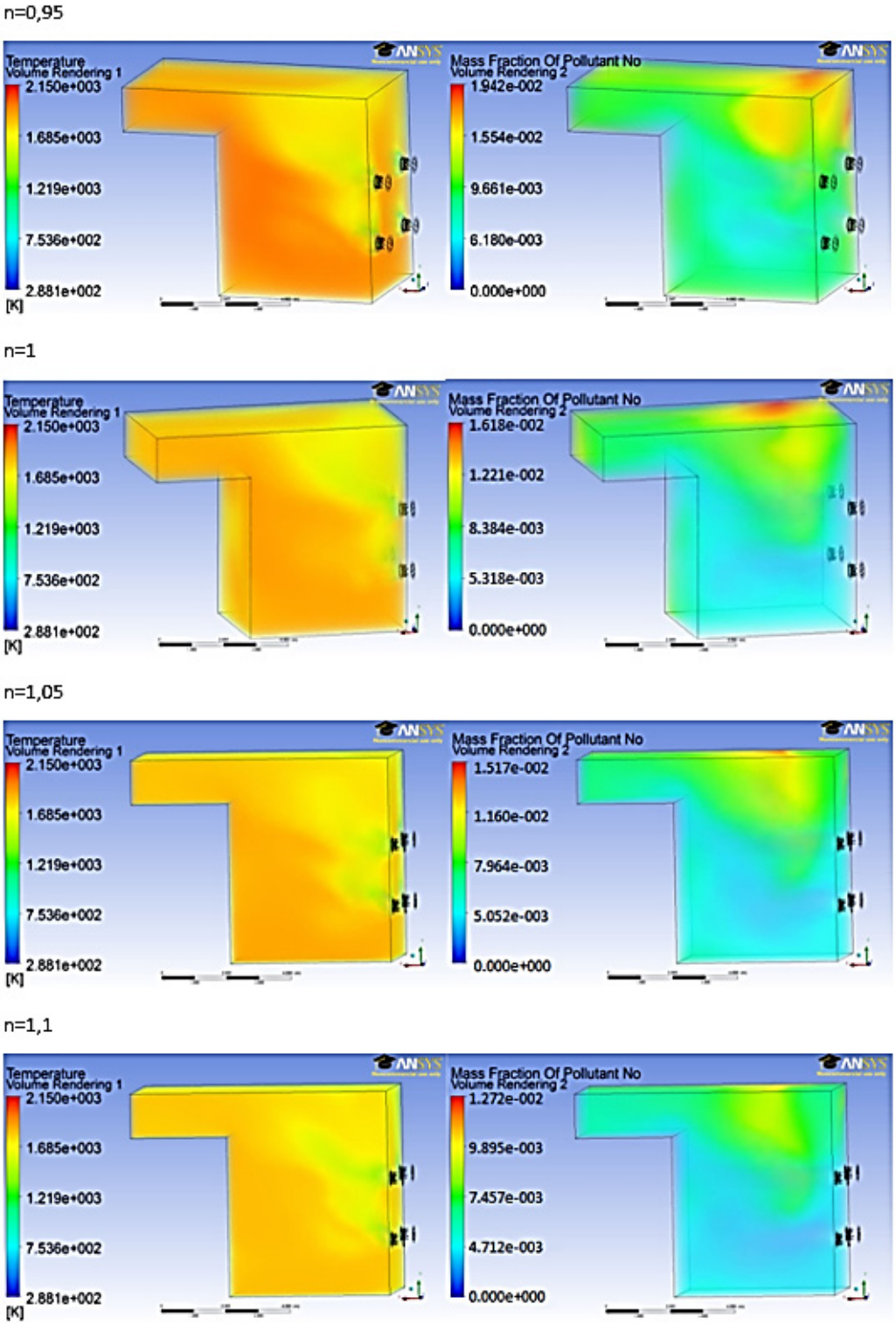

Figure 10. Graphical visualization of processes in the boiler combustion chamber, at different O_2 partial pressures.

In comparison with the validation model, it is evident that the NOx content decreased by 12.5% to about 305 mg/m^3. This decrease is mainly due to the reduction of the oxygen partial pressure, resulting in a decrease of high-temperature range, and hence in the decrease of the thermal NOx. In this case, the CO content increased

only by 1%, i.e. by 2.2 mg/m^3, and the overall boiler output (calculated on the basis of thermal balance) decreased by 0.5% to 59.5 MW.

4.1.2 Cascade Combustion

Using modern burners with combustion air distribution to the primary and the secondary air (cascade air supply), it is very important to maintain their proper ratio. It has been established (Rimar) that, depending on the shape of the combustion chamber, flame shape and other parameters, the ratio should be in the range of 65-35% to 80-20%. Simulation without cascade air supply has also been proposed to determine efficiency in particular conditions. Table 5 shows the values of primary/secondary air ratios for each simulation.

Table 5. Primary/secondary air ratio for simulations.

Ratio	50:50	65:35	70:30	75:25	80:20
Primary air [m^3/s]	2.5	3.25	3.5	3.75	4
Secondary air [m^3/s]	2.5	1.75	1.5	1.25	1

Simulation with the same primary and secondary air ratio is applied to determine the efficiency of the cascade air supply in the boiler. Figure 11 shows the results of cascade air supply simulations.

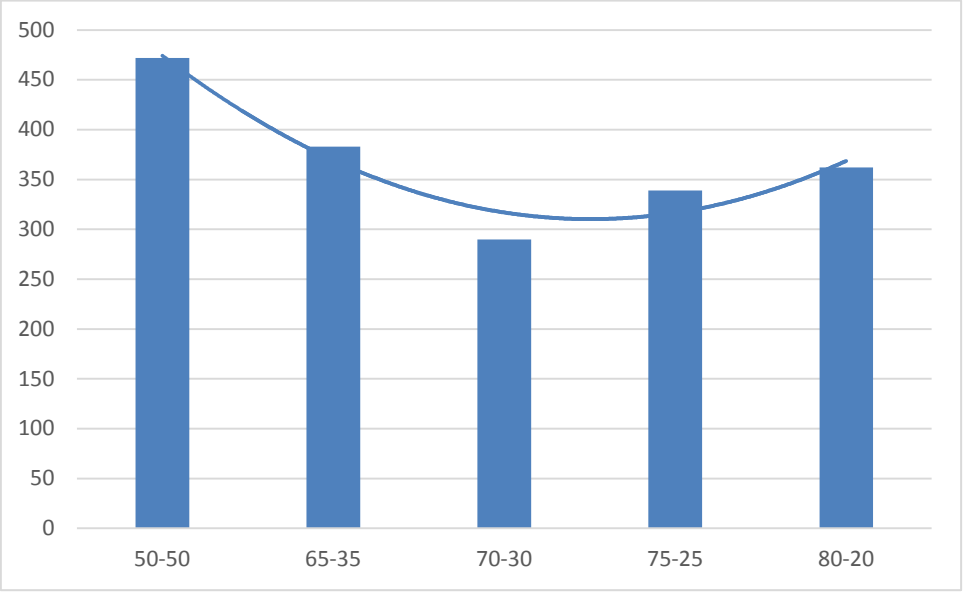

Figure 11. Effect of cascade air supply.

Based on the results of the simulation, it can be stated that the optimum ratio of cascade air supply is 70-30%. When comparing the reference simulation of combustion with a cascade air supply of 70-30%, it was possible to reduce the nitrogen oxides content by 20%, i.e. up to 290 mg/m^3. At the same time, the boiler output did not change. The NOx reduction is associated with lower temperature in the flame centre, and with an increase of the flame length. The graphical visualization of the processes in the combustion chamber is shown in Figure 12.

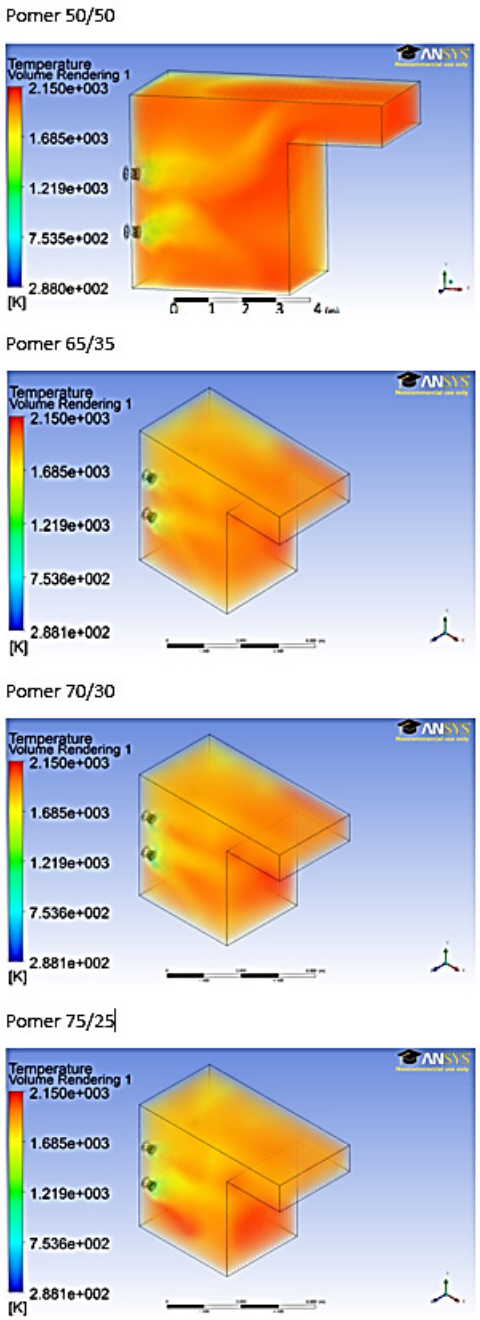

Figure 12. Graphical visualization of processes in the boiler combustion chamber, at different combustion air ratios.

4.1.3 Injection of Auxiliary Substances

The analysis of the possibilities of applying the method of auxiliary substances injection in the real device has lead to the following conclusions:

- Reducing the temperature of the combustion air or fuel would lead to a significant drop in boiler performance.
- The addition of reacting agents into the combustion process has been assessed to be very cost-intensive in most boilers because it requires the installation of a whole range of additional equipment.

For these reasons, the method of reducing the flame temperature of the burners by the addition of cooling agents was chosen as appropriate. Water vapour was chosen as the cooling agent at 300 K, due to the type of used equipment and the water vapour availability.

Discrete analysis of the effect of vapour injections was performed to demonstrate NOx reduction efficiency and to test theoretical assumptions in the simulated environment. The injection water vapour volume for impact analysis was applied from 0 kg/h to 120 kg/h with the step of 10 kg/h. The limit value of 120 kg/h was determined as maximum possible on the given type of burner, in order to avoid a significant change of flow and hence the flame dimensions.

Table 6. Outputs of combustion simulation with water vapour injection into primary air of burners.

No.	Water vapour volume [kg/h]	Maximum temperature in boiler [K]	Boiler power ratio [%]	NO [mg/m^3]	N_2O [mg/m^3]	High-temperature volume [m^3]
1	0	2157	99.37336	349	0.001	25.3
2	10	2143	98.75864	346	0.001	25
3	20	2131	98.92435	344	0.001	23.7
4	30	2120	98.12938	339	0.001	22.2
5	40	2089	97.40332	335	0.001	20.6
6	50	2064	96.52132	328	0.001	18.3
7	60	2012	95.70154	321	0.0009	16.2
8	70	1971	95.10803	312	0.0009	14.6
9	80	1929	94.33792	305	0.0009	12.9
10	90	1885	93.25225	299	0.0009	10.1
11	95	1839	92.89907	295	0.0008	9
12	100	1818	91.96816	290	0.0008	8.5
13	105	1783	91.28704	288	0.0008	7.9
14	110	1707	89.67808	274	0.0007	4.2
15	120	1643	85.03848	262	0.0006	3.1

It can be seen from the table that the critical point for the given boiler is at 100 kg/h of injected water vapour. On the basis of acquired values, the analysis was carried out for the dependence of NOx amount on water vapour amount, maximum flame temperature, and boiler output (Figure 13).

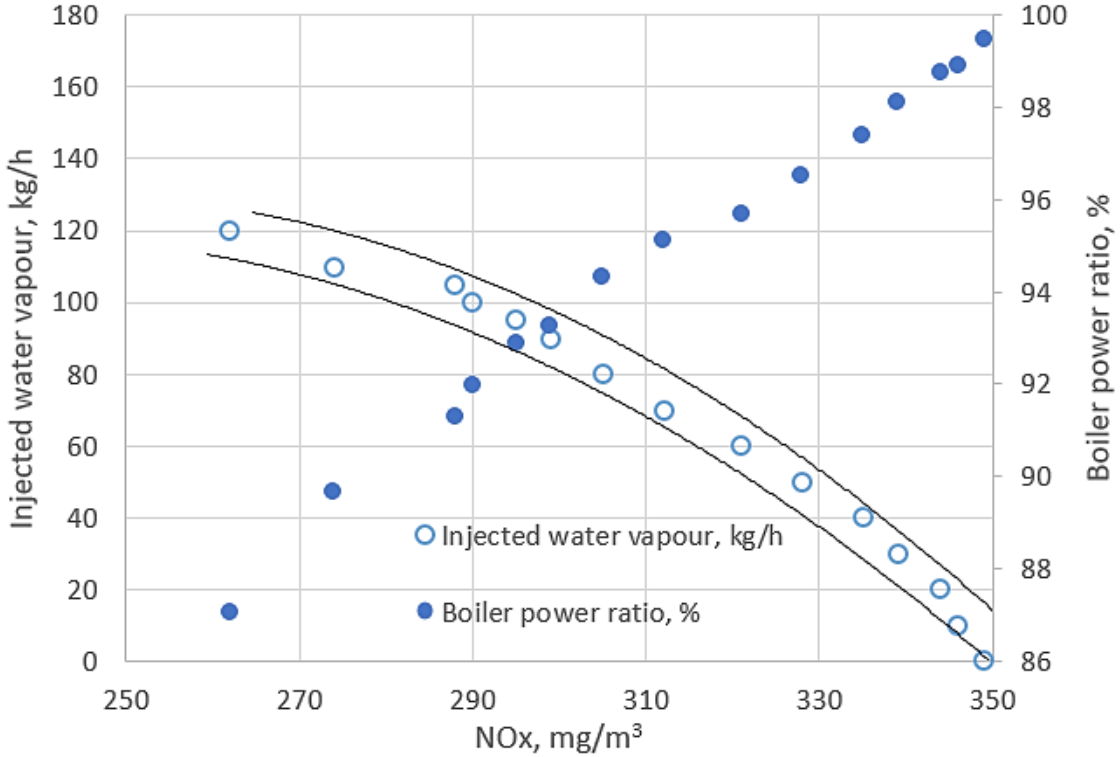

Figure 13. Dependence of water vapour injection and maximum burner flame temperature on nitrogen oxide formation.

The area of overlap of dependence curves of the boiler power ratio and water vapour injection on the NOx formation indicates the optimal level of water vapour injection in terms of boiler performance and nitrogen oxide formation.

On the one hand, the injection of less than 90 kg/h of water vapour in the boiler results in a small reduction in nitrogen oxides formation but does not substantially affect boiler performance. On the other hand, injection of more than 110 kg h of water vapour has a significant impact on the formation of nitrogen oxides but also has a significant negative impact on boiler performance.

By injecting 120 kg/h of water vapour, the NOx content could be reduced by 25% to approx. 260 mg/m^3 but with such a volume of injected water vapour, there was also a significant reduction of the boiler output by about 15%.

Injection 10kg/h

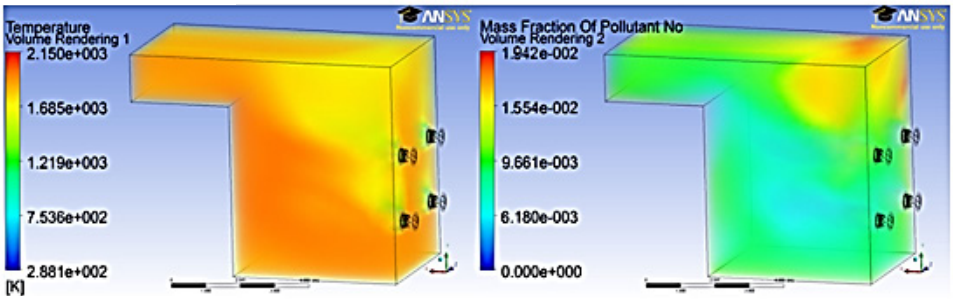

Injection 50kg/h

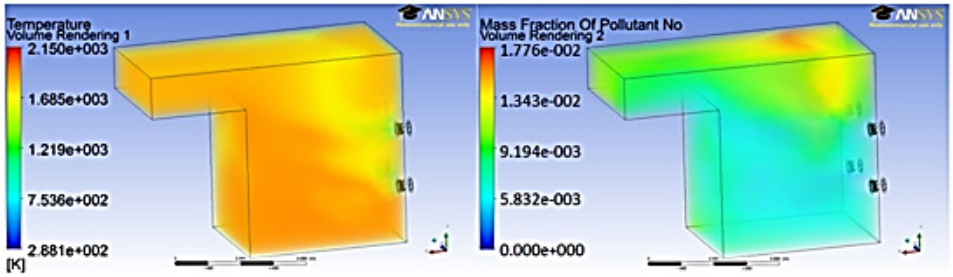

Injection 100kg/h

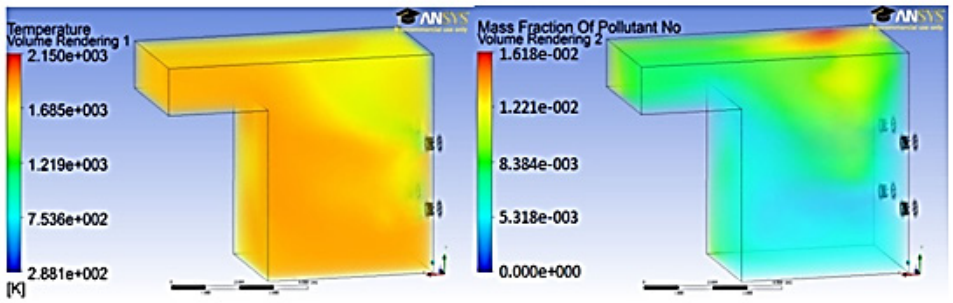

Injection 120kg/h

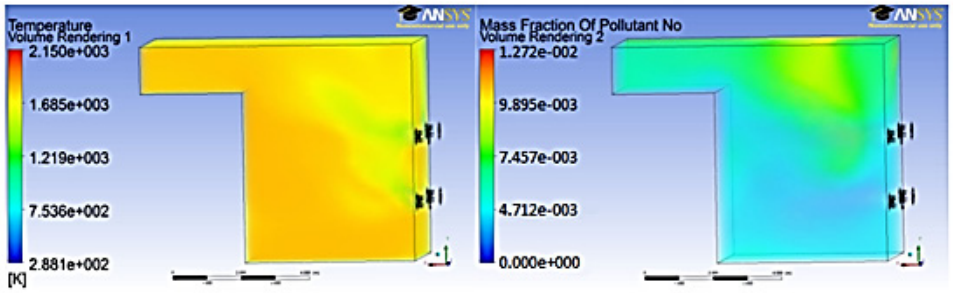

Figure 14. Graphical visualization of the processes in the boiler combustion chamber, with different volumes of injected water vapour.

According to the results of the simulations and the theoretical review, the analysis of the effect of water vapour injection at different thermal loads of the combustion chamber is shown in Figure 15.

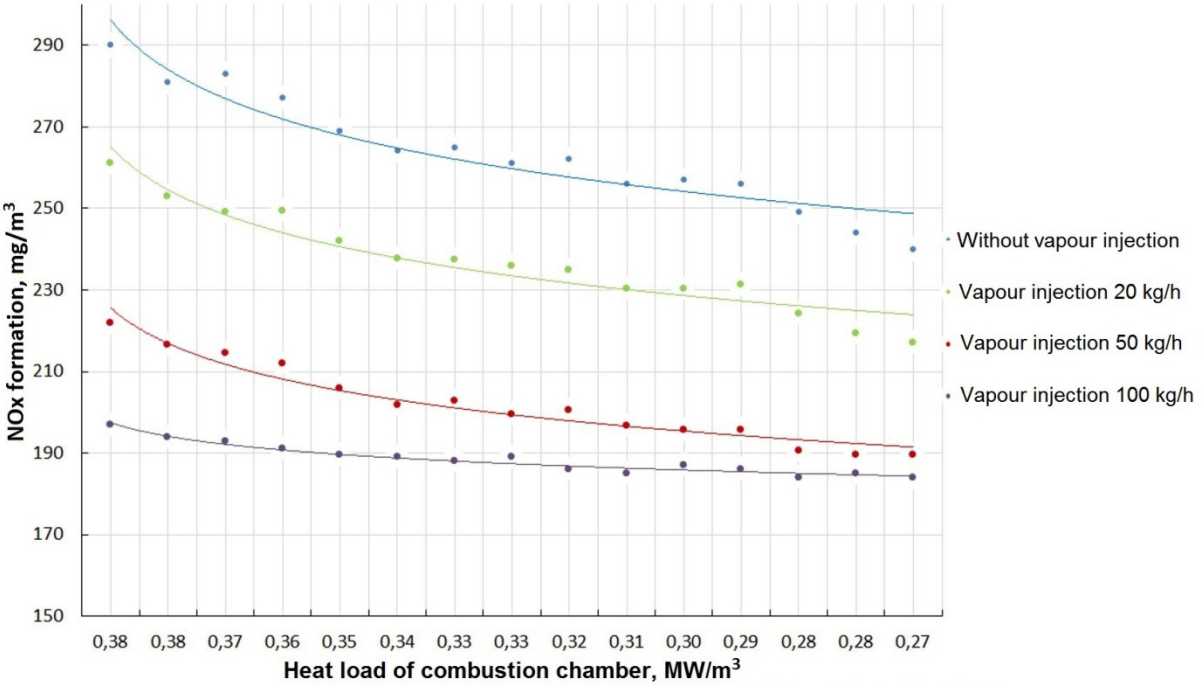

Figure 15. Influence of water vapour injection at different thermal loads of the combustion chamber.

From the results of the simulation, it was found that the decisive parameter in solving the problem of the formation of thermal nitrogen oxides is the thermal load of the boiler combustion chamber. The critical value with respect to the formation of nitrogen oxides was set at 0.33 MW/m^3.

4.1.4 Flue Gas Circulation

The main idea of flue gas circulation is to increase the time which the flue gas retains in the combustion chamber of the boiler. Based on the carried-out analysis, it was determined that one of the essential ways of improving circulation is the boiler design change related to the location of the burners, or to the shape of the combustion chamber.

The mass flow analysis in the combustion chamber has shown that the flames of the upper pair of burners tend to bend upwards due to the influence of the lower pair, and thus about 40% of the flue gases go straight to the exhaust of the combustion chamber. It was proposed to solve this problem by reducing the power of the lower pair of burners by 150 to 300 kW, which is 1% to 2%. The simulation results are shown in Figure 16.

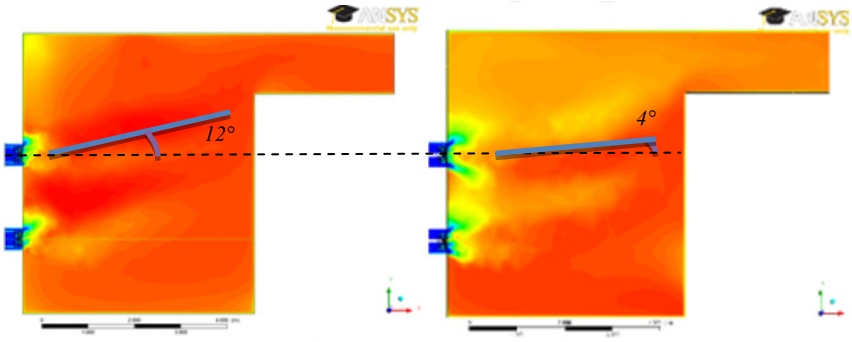

Figure 16. Results of simulations when changing flue gas circulation.

From the figure, it can be seen that decreasing the power of the lower pair of burners by 1% resulted in moving the flames of the upper pair of burners closer to the boiler axis. The improvement in flue gas circulation associated with this effect has resulted in a reduction of NOx content by 2% while reducing performance by only 0.5%. Further reduction of the lower burners performances had the opposite effect in terms of NOx formation, due to the flame interaction.

4.2 Proposal for Burner Setting

On the basis of simulations described in the previous chapters (4.1.1-4.1.4), optimum boiler settings have been proposed in terms of performance and nitrogen oxide formation. The following settings have been selected:

- Excess air coefficient: $n = 1.05$
- Primary to secondary air ratio: 70/30%
- Amount of injected water vapour: 100 kg/h
- Performance of lower burners: 99%

The simulation was carried out to confirm the boiler settings. The results of the simulation are shown in Table 7.

Table 7. Simulation results (settings 1).

Maximum temperature in boiler [K]	Boiler power ratio [%]	NO [mg/m^3]	N_2O [mg/m^3]	High-temperature volume [m^3]
1812	90.87336	191	0.001	7.5

From the results of the simulation it is evident, that by the means of the proposed settings, the nitrogen oxide content at the exhaust of the boiler combustion chamber decreased by 45%, while the boiler's relative output decreased by about 9%. This reduction of NOx was mainly due to the significant reduction of the flame temperature and hence the reduction of high-temperature volume where thermal nitrogen oxides are formed. Even though by combining primary deNOx methods, the NOx content could be significantly reduced, the effectiveness of each separate method in combination was reduced. Further analysis has shown that the initially selected optimal settings for NOx reduction are no longer optimal due to their combination. The main problem has arisen in reducing of the oxygen partial pressure in the primary flame burning zone. In this respect, simulation with the modified primary/secondary air ratio of 72/28% was carried out. Table 8 shows the simulation results.

Table 8. Simulation results (settings 2).

Maximum temperature in boiler [K]	Boiler power ratio [%]	NO [mg/m^3]	N_2O [mg/m^3]	High-temperature volume [m^3]
1812	90.63691	185	0.001	7.,4

Table 8 shows that, by increasing the primary air ratio, a further NOx reduction of 3% to 185 mg/m^3 was achieved, although this led to an increase of NOx content in the stand-alone simulations.

Based on settings 1 and 2, a series of simulations were carried out to determine the effects of interactions of primary deNOx methods. The simulation results are shown in Figure 17.

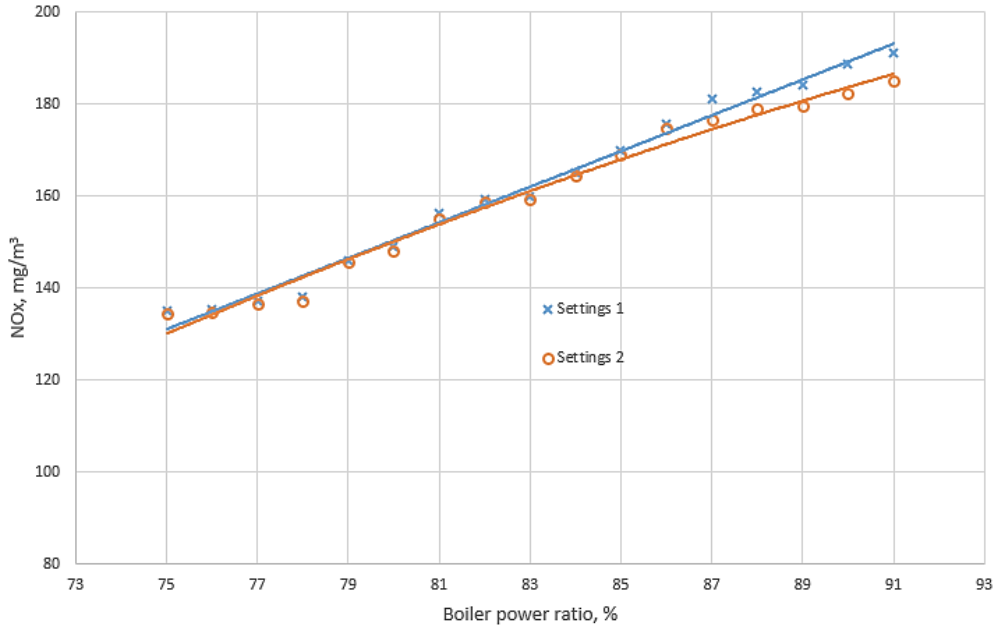

Figure 17. Effects of interaction of primary deNOx methods at different boiler performance.

The curves in the diagram show that the interaction effect is most pronounced at higher boiler output (from 85%). These performances result in a greater thermal load in the combustion chamber, creating a more sensitive environment for the formation of nitrogen oxides. Consequently, combustion plants with the thermal load of the combustion chamber of less than 0.25 MW are less "sensitive", which, in most cases, allows their pattern-setting according to the defined parameters. In contrary, combustion plants with the thermal load of the combustion chamber greater than 0.25 MW require individual approach and accurate operation parameters setting.

4.3 Measurement Results for Proposed Boiler Settings

Based on the selected optimal settings, a series of measurements were made to validate the results of both groups of settings. The measurement results are shown in Table 9 and 10.

Table 9. NOx concentration measurement results for the first settings.

Measurement time [h:min]	8:45-9:15	9:15-9:45	9:45-10:15	10:15-10:45	10:45-11:15	Value	
						max	mean
Contents [% vol.]							
O_2	7.31	7.23	7.22	7.75	6.88	7.75	7.28
CO_2	7.32	7.42	7.38	7.48	7.54	7.54	7.43
Mass concentration [$mg.m^{-3}$]							
NO_x	198	196	196	187	191	198	193
CO	3	6	2	2	3	6	3

Table 10. NOx concentration measurement results for the second settings.

Measurement time [h:min]	14:00-14:30	14:30-15:00	15:00-15:30	15:30-16:00	16:00-16:30	Value	
						max	mean
Contents [% obj.]							
O_2	7.34	7.32	7.33	7.22	7.33	7.34	7.31
CO_2	7.26	7.30	7.27	7.38	7.27	7.38	7.30
Mass concentration [$mg.m^{-3}$]							
NO_x	189	181	186	185	189	189	186
CO	2	2	2	2	3	3	2

The results of the measurements confirmed the accuracy of the selected settings described in chapter 4.2 and also the presumption of the interaction of primary deNOx methods in their combination.

5 Conclusions

The performed experiments, simulations and discussions pointed to several important aspects, as well as the facts about NOx reduction, verified by using a combination of primary methods in the limiting conditions of the thermal load of the combustion chamber.

The simulation model was developed to determine the characteristics of boiler operation and the efficiency of primary deNOx methods. This model was compared to the measurement results. The model showed a high degree of conformity in particular measured parameters.

The model has confirmed the predicted causes of excessive NOx formation, especially in the conditions of the extreme thermal load of the combustion chamber $Q_V \geq 0.3$ MW/m ^{3}. The results obtained by the standard primary methods of reduction of nitrogen oxides applied in this work, pointing to their effectiveness even under conditions of high thermal load in the combustion chamber, are as follows :

- Oxygen partial pressure – NOx decrease by 12.5%
- Cascade air supply – NOx decrease by 20%
- Water vapour injection – NOx decrease by 25% (the level of reduction was affected by boiler performance)
- Flue gas circulation – NOx decrease by 2%

The third stage of the research pointed to the problem of interactions of primary deNOx methods, especially the effectiveness of the reduction of individual methods. Thus, in the case of boiler operation according to the

settings from section 4.1, the NOx content was reduced by 45% to 190 mg/m^3. Further correlation of settings resulted in a further 3% reduction of nitrogen oxides.

The most effective method for NOx reduction has been the water vapour injection method. Vapour injection reduced the maximum temperature, eliminating the volume of high-temperature zones in the boiler combustion chamber by approximately 65%. Injecting approximately 100 kg of vapour per hour reduces NOx by 20 to 25% below the limit of 198 mg/m^3.

The most appropriate parameters of primary deNOx methods can be better identified by simulation programs than by direct measurements on the boiler because they are time efficient.

The results show that at present, the amount of NOx in large heat-producing plants will not be reduced by using just a single primary NOx reduction method. To successfully reduce NOx emissions in these units, a combination of two or more primary methods must be applied. According to the results presented in this paper, the best option is to use the following methods: (a) improve the circulation of gases in the combustion chamber, (b) adjust the partial pressure of oxygen, (c) inject water or steam or other compounds that lower the flame temperature, (d) adjusting the cascade supply of combustion air.

Acknowledgement: *This work was supported by the Slovak Research and Development Agency under the contract No. APVV-16-0192*

References

Adams T. (2016). Off-design point modelling of a 420 MW CCGT power plant integrated with an amine-based post-combustion CO_2 capture and compression process. *Applied Energy*, 178, pp. 681–702.

Anderson JD. (1995). Computational Fluid Dynamics: The Basics with Applications, 1st ed., Science, Engineering, Math. USA: McGraw-Hill Science, p.574.

Basu P, Kefa C and Jestin L. (1999). Boiler and Burners. Design and Theory. Berlin: Springer-Verlag

Ben Rejeb S. (2017). Thermal radiation modeling using the LES–ODT framework for turbulent combustion flows. *International Journal of Heat and Mass Transfer*, 104, pp. 1300–1316.

Boukhalfa N. (2016). Chemical Kinetic Modeling of Methane Combustion. *Procedia Engineering*, 148, pp. 1130–1136.

Bowman TC. (1992). Control of combustion – generated nitrogen oxid emissions: Technology driven by regulation. *Proc. of Combustion Institute*, 24(1), pp. 859-878.

Boxiong S. (2004). Kinetic model for natural gas reburning. *Fuel Processing Technology*, 85(11), pp. 1301–1315.

Dunn-Rankin D, Miyasato MM. and Trinh Pham K. (2008). Introduction and Perspectives. In Dunn-Rankin D (ed.) Lean Combustion Technology and Control. California, USA, pp. 1–18.

Dupláková D. and Husár J. (2014) Využitie simulácie procesov ako nástroj optimalizácie výrobných časov a nákladov. In:*Management of manufacturing systems 2014. Zborník vybraných vedeckých prác,* Starý Smokovec, TU of Košice, pp.32-37.

Durdán, M. and Kostúr, K. (2015). Modeling of temperatures by using the algorithm of queue burning movement in the UCG Process. *Acta Montanistica Slovaca*, 20(3), pp.181-191.

Fackler KB. (2015). NOx Behavior for Lean-Premixed Combustion of Alternative Gaseous Fuels. *Journal of Engineering for Gas Turbines and Power*, 138(4), p.11.

Fennimore CP. (1972). Formation of nitrik oxide from fuel nitrogen in ethylene flames. *Combustion and Flame*, 19(2), pp. 289-296.

Ferstl, K. and Masaryk, M. (2011). Heat transfer book. (Prenos tepla). 1st ed. Bratislava: Slovak University of Technology in Bratislava, p.424.

Fischer M. (2016). A chemical kinetic modelling study of the combustion of CH4–CO–H2–CO2 fuel mixtures. *Combustion and Flame*, 167, pp. 274–293.

Flagan, Richard C. and Seinfeld. (1988) *Fundamentals of air pollution engineering.* Prentice-Hall, Englewood Cliffs, New Jersey.

Flimel M. (2010). Problematika určovania skutočnej hodnoty súčiniteľa prechodu tepla stavebných konštrukcií budov metódou merania tepelného toku. *Vytápění, větrání, instalace*, 19(4), pp. 166-169.

Gavlas S, Lenhard R. and Jandacka J. (2013). Design and numerical simulation of the heat exchanger for heat recovery system with melting furnaces for melting secondary aluminums. In: Dancova, P., Novonty, P. (Eds.), *EFM12 - Experimental Fluid Mechanics 2012*, 7th International Conference on Experimental Fluid Mechanics (EFM), E D P SCIENCES, Cedex A, p. UNSP 01033.

Glarborg P. (1995). The thermal DeNOx process: Influence of partial pressures and temperature. *Chemical Engineering Science*, 50(9), pp. 1455-1466.

Gopalakrishnan P. (2007). *Controlling mechanisms for low NOx emissions in a non-premixed stagnation point reverse flow combustor.* Proceedings of the Combustion Institute, 31(2), pp. 3401–3408.

Gövert S. (2015). Turbulent combustion modelling of a confined premixed jet flame including heat loss effects using tabulated chemistry. *Applied Energy*, 156, pp. 804–815.

Gurevich, H.A. and Aksenov, V.L. (1976). *Investigation of the yield of nitrogen oxides in the furnace of the DKVR boiler with large excess air.* In the book: Formation of nitrogen oxides and ways to reduce their release into the atmosphere. Sb.nauch.tr. Kiev: Nauchna Dumka, pp.106-109.

Hayhurst AH. and Vince M. (1980). Progress in Energy and Combustion Science. Oxford Pergamon Press, 6, pp. 35-51.

Holoubek D. (2002) *Spaľovacie zariadenia, výmeníky tepla a kotly.* 1st ed. Košice, TU of Košice, p.2015.

Horbaj P. (2005). Some notes on basic parameters, determination of empirical formula and incineration of solid municipal waste. *Chemicke Listy*, 99(10), pp. 694-702.

Hua P. (2016). Promotional mechanism of propane on selective catalytic reduction of NOx by methane over In/H-BEA at low temperature. *Applied Surface Science*, 390, pp. 608–616.

Chen Z. (2017). Anthracite combustion characteristics and NOx formation of a 300 MWe down-fired boiler with swirl burners at different loads after the implementation of a new combustion system. *Applied Energy*, 189, pp. 133–141.

Choong-Kil S. (2011). De-NOx characteristics of a combined system of LNT and SCR catalysts according to hydrothermal aging and sulfur poisoning. *Catalysis Today*, 164(1), pp. 507–514.

Jablonský G, Pástor M and Dzurňák R. (2015). *Obohacovanie horľavej zmesi kyslíkom v praxi*. 1st ed. Košice: TU of Košice, p.92.

Jandacka J, et al. (2015). Performance and emission parameters change of small heat source depending on the moisture. *Manufacturing Technology*, 15(5), pp. 826-829.

Kristensen PG, Glarborg P. and Dam-Johansen K. (1996). Nitrogen Chemistry during Burnout in Fuel-Staged Combustion. *Combustion and Flame*, 107(3), pp. 211-222.

Lamoureux N. (2010). Experimental and numerical study of the role of NCN in prompt-NO formation in low-pressure CH4–O2–N2 and C2H2–O2–N2 flames. *Combustion and Flame*, 157(10), pp. 1929–1941.

Miller JA. and Glarborg P. (1996). Modeling the Formation of N2O and NO2 in the Thermal De-NOx Process. *Series in Chemical Physics*, 61, pp. 318-333.

Myles Bohon D. (2015). Experiments and simulations of NOx formation in the combustion of hydroxylated fuels. *Combustion and Flame*, 162(6), pp. 2322–2336.

Panda A, Prislupčák M. and Pandová I. (2014). Progressive technology diagnostic and factors affecting to machinability. *Applied Mechanics and Materials*, 616, pp. 183-190.

Panda A. (2011). Analysis of the process production. *Studia i materialy,* 29(2), pp. 22-28.

Rimar M. and Fedak M. (2014). Combustion processes. (Spaľovacie procesy.). 1st ed. Prešov: Technical University of Košice, p.144.

Rimar M. and Kulikov A. (2016). *NOx Formation in Combustion of Gaseous Fuel in Ejection Burner*, In: Lenhard, R., Kaduchova, K. (Eds.), Application of Experimental And Numerical Methods In Fluid Mechanics And Energy 2016: XX Anniversary of International Scientific Conference, Amer Inst Physics, Melville, p. 020051.

Saheed Ismail O. (2016). Modelling combustion reactions for gas flaring and its resulting emissions. *Journal of King Saud University - Engineering Sciences*, 28(2), pp. 130–140.

Salokyová Š. and Krenický T. (2016). Analysis of the effects of factors in relation to vibration of technological head during the splitting of construction steels through hydro-abrasive splitting. *Key Engineering Materials,* Volume 669, pp. 216-219.

Segal IJ and Lyubeznikov DA. (1966) The study of heat transfer gas torch at different degrees of pre-mixing the gas with air. *Inzhenerno Physics Journal*, 10, pp. 163-166.

Semenov NN (1929). Kinetics of Chain Reactions. *Chem.Rev.*, 61(3), pp.347-379.

Smeringai P, Rimár M. and Fedák M. (2015). Optimization of combustion process with respect to the assessment of nitrogen oxides formation. In: *Energetické premeny v priemysle 2015, Zborník vedeckých prác*. TU of Košice, pp. 190-194.

Smeringai P. and Rimár M. (2014). Simulácia procesov v spaľovacích zariadeniach s viacerými priemyselnými horákmi. In: *Management of Manufacturing Systems2014. Zborník vybraných vedeckých prác,* Starý Smokovec, pp.116-119.

Stephen Klippensteina J, Lawrence Hardinga B. and Glarborg P. (2011) The role of NNH in NO formation and control. *Combustion and Flame*, 158(4), pp. 774–789.

Terpák, J., Dorčák, Ľ. and Maduda, V. (2007). Combustion process modelling and control. *Acta Montanistica Slovaca,* 12(3), pp.238-242.

Trisjono P. (2016). Modeling turbulence–chemistry interaction in lean premixed hydrogen flames with a strained flamelet model. *Combustion and Flame*, 174, pp.194–207.

Van Oijen JA. (2016) State-of-the-art in premixed combustion modeling using flamelet generated manifolds. *Progress in Energy and Combustion Science*, 57, pp. 30–74.

Varga A, Kizek J. and Dudrik M. (2015). *Oxidačné činidlo v procese spaľovania*. 1st ed. Košice: TU of Košice, p.92.

Vyhláška Ministerstva životného prostredia SR č. 252/2016 Z. z., ktorou sa mení a dopĺňa vyhláška Ministerstva životného prostredia Slovenskej republiky č. 410/2012 Z. z., ktorou sa vykonávajú niektoré ustanovenia zákona o ovzduší v znení vyhlášky č. 270/2014 Z.z. [online] Available at: https://www.slov-lex.sk/static/pdf/2016/252/ZZ_2016_252_20161001.pdf [Accessed 2 May 2019].

Vyhláška Ministerstva životného prostredia SR č. 442/2013 Z.z., ktorou sa mení vyhláška Ministerstva pôdohospodárstva, životného prostredia a regionálneho rozvoja Slovenskej republiky č. 360/2010 Z. z. o kvalite ovzdušia. [online] Available at: https://www.slov-lex.sk/static/pdf/2013/442/ZZ_2013_442_20140101.pdf [Accessed 2 May 2019].

Westbrook KC. (2005). Computational combustion. *Proceedings of the Combustion Institute*, 30(1), pp. 125–157.

Wu Jeffrey CS. (2013). Removal of NOx by photocatalytic processes. *Journal of Photochemistry and Photobiology. C: Photochemistry Reviews*, 14(1), pp. 29–52.

Wünning JA. and Wünning JG. (1997). Flameless oxidation to reduce thermal no-formation. *Progress in Energy and Combustion Science*, 23(1), pp. 81-94.

Xubo G. (2016) Modeling and simulation of urea-water-solution droplet evaporation and thermolysis processes for SCR systems. *Chinese Journal of Chemical Engineering*, 24(8), pp. 1065–1073.

Yeh CL. (2013). NOx Reduction in a Carbon Monoxide Boiler by Reburning. *Procedia Engineering*, 67, pp. 378-387.

Yeromin, A., Yeromina O., Lukáč L., Kizek J. and Dzurňák R. (2018). The possibility of increasing the efficiency of temperature distribution control in reheating furnaces. *Acta Montanistica Slovaca*, 23(2), pp.175-183.

Young Kim H. (2012) Investigation of fuel lean reburning process in a 1.5 MW boiler. *Applied Energy*, 89(1), pp. 183–192.

Yu JCC. (2016). NOx abatement from stationary emission sources by photo-assisted SCR: Lab-scale to pilot-scale studies. Applied Catalysis, A: General, 523, pp.294–303.

Zajac J. and Čorný I. (2004). *Monitoring of processing fluids.* Science Report, Kielce, pp. 215-229.

Zel'dovich BJ and Frank-Kamenetskiy DA. (1947). *The oxidation of nitrogen during the combustion*. Kyiv: Nauka, p.146.

Positive Environmental and Economic Impact of Polyvinyl Butyral Waste Material after Recycled Windscreen

***Marián Albert*[1], *Jana Čitbajová*[1], *Lucia Knapčíková*[2], *Marcel Behún*[1] *and* *Annamária Behúnová*[2]**

The development of the economy and the continual competition for the customer brings new impulses in the area of production, trade, and consumption. Manufacturers are increasingly looking to meet customers, wanting to meet the needs of a wider range of consumers with their manufacturing and sales strategy, with an emphasis on the environmental and economic impact of their products. Therefore, recycling and re-use of raw materials are very important today. The paper is focused on experimental studying and testing of material relaxation of recycled polyvinyl butyral (PVB). Polyvinyl butyral foil is one of the most important parts of the windscreen or safety glass as an interlayer. Polyvinyl butyral carries a large amount of chemically bonded energy. Less harmful vapours are released during combustion of PVB than when combustion of heating oil. However, the price of energy obtained from such a waste product is sometimes lower than the price of energy obtained from oil. Given the global polyvinyl butyral waste production, the price for this attractive commodity is very reasonable. It ranges from 0.25 € to 0.50 € per kilogram of this thermoplastics. After homogenization, the mixture polyvinyl butyral was compressed to the test samples of prescribed shape and size under action of pressure and heat. Recycled polyvinyl butyral was investigated under tensile test and material stress relaxation. Based on the results, it can be stated that the material had the max. values of a tensile stress 0.78 MPa, the strain of the material subject to tensile strain was from 410 % to 520 %.

Keywords: *Polyvinyl butyral (PVB), Safety glass, Cost savings, Sustainability, Mass Customization.*

Introduction

The changes in the economic, socio-cultural, political, competitive and technological environment that have taken place in the world in recent years have forced many companies to acclimatize in the "new economy" environment, bringing new approaches to production strategies and a new philosophy in the marketing´s field (Kotler, 2003). The long-term production focusing of the company, i.e. the production strategy of the company, represents a summary of not only production but also commercial, innovative and other long-term prospective tasks to ensure the strategic goals of the company. (Zhao et al., 2006) The frameworks are created for a very specific production content of the company, whether in terms of product quality, volume, product mix and other requirements (EuroEkonóm.sk, 2015; Mandičák et al., 2018). The implementation of materials from secondary raw materials and their application to possible components reduces the economic and environmental aspects that are very important today (Industrial Property Office of the Czech Republic, 2019; 2. Recycled polyvinyl butyral, Schirmbeck GmbH, 2018). The aim of the work is to find areas of use of recycled polyvinyl butyral (PVB) product, which is the product of windshield recycling (Figure 1), regarding the investigation of material relaxation.

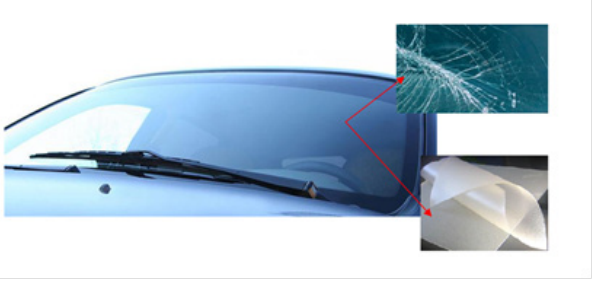

Fig.1. Polyvinyl butyral safety layer in the car windshield Source: own processing

Nowadays, every vehicle and its windscreen are equipped with a polyvinyl butyral film that secures the safety of the glass. The worldwide patent research (Recycled polyvinyl butyral, Schirmbeck GmbH, 2018; Dhaliwal and Hay, 2002) shows the possible use of recycled polyvinyl butyral in practice. PVB film does not contain additives classified as dangerous or harmful. PVB is primarily used as a multilayer foil in the windscreen, all modern vehicles, passenger cars, trucks. (Asik, 2003) PVB film protects the glass from grinding,

[1] *Marián Albert, Jana Čitbajová, Marcel Behún*, Technical University of Košice, Technical University of Košice, Faculty of Mining, Ecology, Process Control and Geotechnology, Letná 9, 042 00, Košice, Slovak republic marian.albert@mail.com, jana.citbajova@tuke.sk, marcel.behun@tuke.sk

[2] *Lucia Knapčíková, Annamária Behúnová*, Technical University of Košice, Faculty of Manufacturing Technologies with a seat in Prešov, Department of Industrial Engineering and Informatics, Prešov, Slovak Republic, lucia.knapcikova@tuke.sk, annamaria.behunova@tuke.sk

damage, crash, and the like. In some cases, PVBs are part of the glazing of buildings, especially in areas where hurricanes are frequent, or, of course, in security windows of buildings. (Hidallana-Gamage et al., 2014) At the Michigan Molecular Institute, for years, they have been trying to find applications for the use of PVB waste, these applications are moving further into the automotive industry with efficiency in the US countries (Barry and Orroth, 2000). After the separation itself, the PVB waste still contains glass particles, which, while decreasing its use, but are still widespread in several industries. External storage of PVB material is dissuaded because moisture and ultraviolet radiation generally degrade the properties of PVB (Sekisui chemical.com, 2018). Also, the possibility of primary PVB contamination is increased. Due to the sticky and soft surface of the recycled PVB film, it is assumed that when unsuitable for storage, the number of impurities can be easily adhered to the surface, thereby reducing the quality of the use of the recycled product (Polyvinyl butyral, Kuraray, 2019). PVB storage capacities are limited in many countries (Fischer and Häring, 2009). Accordingly, some countries are already increasing storage costs and are trying to make producers of PVB encourage, that this type of waste to be re-used, they returned it to the production process again. With regard to solar energy, there is a prediction that the fastest growing area of the PVB end-user, with regard to the compound annual growth rate, is projected to increase by more than 6% between years 2015 and 2023 (Mitaľová et al., 2016; Knapčíková et al., 2016). In terms of volume of PVB produced, Asia, in the year 2014, has contributed to more than 35% of PVB use within the global market (Sekisui chemical.com, 2018; Mitaľová et al., 2016). The use of PVB film on the market in Latin America, the Middle East, and Africa is expected to grow significantly over the next eight years, mainly due to the increase in land transport and construction as end-users (Mohammadian-Kohol et al., 2016).

As we can see from the classification of PVB's usability in individual countries of the world, PVB has a wide range, application variability in production conditions with an emphasis on the requirements of the final consumer, the PVB processor to the final products. (Sridhara and Satapathy, 2015) Based on this differentiation of countries, companies and their specific needs, it is possible to apply a targeted customization strategy where pure customization cannot be achieved for the entire product portfolio, but the company can reach it for more than one production area segment. (Iwasaki et al., 2007) The strategy is focused on the demands of consumers, where the company produces its customers based on the specific requirements, but only in certain, targeted markets. Analysing targeted mass customization explains why in some market's companies produce a range of just basic types, while in other markets businesses produce an expanded range of their products to meet customer requirements. This means that a company that offers only a limited number of its products in one country allows its consumers to "tailor to their products" (Cavusoglu et al., 2007).

Materials and methods

Polyvinyl butyral (PVB) (Mitaľová et al., 2016) is a special resin, mainly used as a raw material for laminated safety glass in cars (Figure 1) and in the building construction industry. Application is mainly for skyscrapers. PVB currently produces several companies in Europe and the world, each under its trademark. In addition to the main application and thus the use of PVB films, PVB resins are used for the production of paints, structural adhesives, dry toner paints and as binders for ceramics and composite fibres (Farzana et al., 2016). The PVB foil has many excellent features such as high tensile strength, impact resistance, transparency and flexibility, which is particularly useful in producing safety glass. Due to the alcohol, ester and acetate bond content, PVB foil (Zhang et al., 2016; Valášek et al., 2016) can hold the glass firmly, even if the glass breaks. The glass can adhere to the PVB film interlayer to prevent breakage. Sales of primary end-users of polyvinyl butyral are dependent on the performance of the general economy, especially for safety glass, which is so necessary for the automotive industry and in the construction industry - in architecture (Knapčíková, 2015; Knapčíková et al., 2016). The PVB is exported to the countries with widespread automotive production, which is characterized by a high level of mass customization - customization. According to Lampel and Mintzberg (Lampel and Mintzberg, 1996), the last type of mass customization is customizing customization, in which customers directly interfere with the production process and modify their "products" themselves. The consumer here affects distribution, assembly and production, which has a significant impact on the company's final production. Ultimately, by consuming the recycled PVB in the required condition, quality and characteristics, the consumer obtains the feedstock, which is an essential ingredient for his further transformation process (production). In his publication, D. Anderson (2004) divided mass customization into three primary groups: dimensional, modular and customized. For this process is typically dimensional, this type of MC brings constant changes in mixing ratios, scales, and can have infinitely many options. (Vasiliev and Morozov, 2001) Examples of such customization with an infinite number of possibilities are shearing sheets, mixing chemicals, sewing clothes, etc. Dimensional customization can be applied using CNC (Saad et al., 2006) machines that receive instructions based on orders received.

Recycled polyvinyl butyral

The key material of this study is polyvinyl butyral (Figure 2), which was obtained after windscreens recycling. The flakes have a size from 2 mm to 20 mm, and the thickness is from 0.5 mm to 1.5 mm.

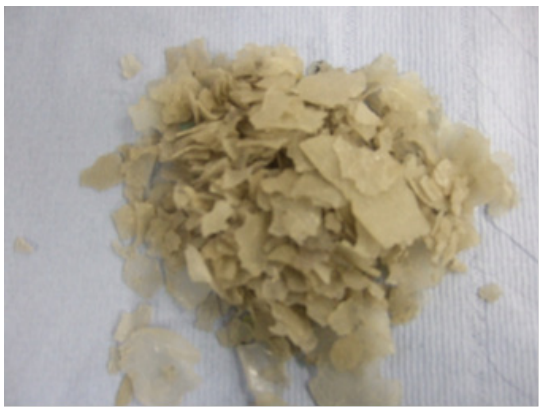

Fig.2. Recycled polyvinyl butyral Source: own processing

This recycled polyvinyl butyral is contaminated with dust, glass fragments, so it is important to thoroughly wash the material and dry it before starting laboratory work. Polyvinyl butyral as the thermoplastic material is soluble in ethanol, butanol, ethyl acetate, butyl acetate, in a mixture of chlorinated hydrocarbons and insoluble in aliphatic hydrocarbons (in gasoline) (Knapčíková et al., 2016). The polyvinyl butyral density used by the research was 1.07 g.cm^{-3}, and the sales price of recycled polyvinyl butyral is from 0.25 € to 0.50 € per kilogram. The economic potential of this "waste" material is very high.

Tab. 1. Material Advantages of recycled polyvinyl butyral for manufacturing

Recycled polyvinyl butyral	
• Form	flakes
• Size	20-30 mm
• Purity	more than 97%
• Fire point	None
• Glass temperature transition	130°C -170°C
• Viscosity (dynamic)	100 – 175 m Pa*s According to DIN 53015
• MVR (Melt Volume Rate)	6 -7 cm³. 10 min^{-1}
• MFR (Melt Flow Rate)	5 – 6 g.10 min^{-1}

Source: own processing

Material preparation

Before to compression moulding process technology, the thermoplastic material was homogenized used double screw machine (Del Linz et al., 2016; Botko et al., 2018; Kulikov et al., 2018). Continuous mixing was used to prepare the homogenized mixture (Knapčíková et al., 2016; Valášek et al., 2016). Homogenization of the material (Figure 3) was carried out on a Brabender Plasti-Corder W 350 E (Valášek et al., 2016). Laboratory investigations were performed at room temperature 22 ° C and 60% humidity. The homogenization process lasted 15 min. The material was thoroughly mixed, and the formation of air bubbles that were undesirable during the moulding process (occurring during compression, incomplete mixing, or incomplete filling of the thermoplastic mould cavity) was avoided. (Sheng and Zhang, 2016) After homogenization of the recycled polyvinyl butyral on a Brabender Plasti-Corder W 350 E, the material was carefully selected and prepared for moulding. In compression moulding, thermoplastic or thermoset material (in the form of granules or flakes) is melted in the mould cavity under heat and pressure, followed by cooling and part removal after it is cured (Knapčíková et al., 2010). Table 2 shows the moulding characteristics used Brabender W 350 mould equipment.

Tab. 2. Moulding specifications

Equipment	Brabender W350
• Molding temperature	190 °C
• Pre-heating time	20 min
• Molding time	20 min
• Cooling time	20 min
• Molding pressure	10 MPa

Source: own processing

Stress relaxation of recycled polyvinyl butyral

Stress relaxation means the degradation of the material by cyclic (repetitive) stress and mechanical load (Figure 3) (Knapčíková et al., 2016; Telišková et al., 2018). If the amplitude of the stress is greater than the fatigue limit of the material, it ultimately leads to crack initiation. If a crack is predicted or spread, then the test specimen can break (Knapčíková, 2015).

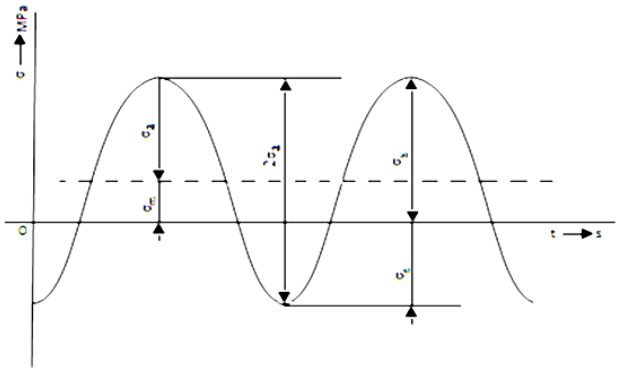

Fig.3. Repeated cyclic relaxation of recycled polyvinyl butyral material. Source: Mitaľova et al.,2016

The following characteristics are known from the above mentioned Figure 3(Mitaľova et al., 2016):

σ_h - maximum stress [MPa]
σ_n - minimum stress [MPa]
σ_m - medium stress [MPa]
σ_a - stress amplitude [MPa]
R - cycle asymmetry parameter [MPa]

Material relaxation was performed on the Zwick Z020 Universalpruefungsmaschine (Figure 4) (Valášek et al., 2016), using a climate chamber where test conditions were set. The temperature ranges from -80 °C to + 250 °C was used for the climate chamber tests. (Cormie et al., 2009) The choice of temperature is given by the internal and external factors of the investigation, whether the tests are at controlled temperature or the ambient temperature test (Knapčíková et al., 2016).

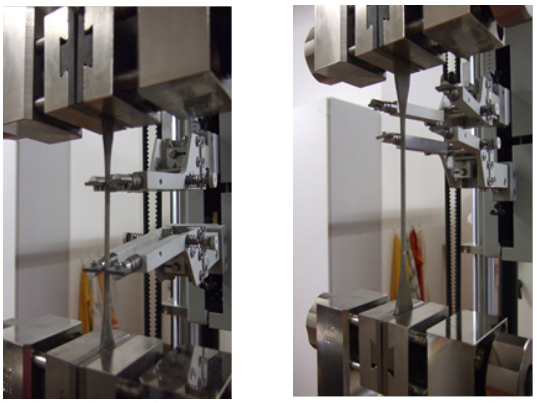

Fig.4. Fixturing a sample of recycled polyvinyl butyral at relaxation during 5 min, 15 min and 25 min period. Source: Knapčíková et al., 2016

Results and discussion

The investigation of material relaxation was carried out according to the standard EN ISO 4892. In the case of testing of samples from recycled polyvinyl butyral, a constant temperature of 23 °C was set in the climate chamber (Farzana et al., 2016; Liu et al., 2012; Botko et al., 2018). The duration of the maximum stress at the material relaxation is always 10 minutes (5 min, 15 min and 25 min for all tested period). All experiments were repeated 10 times with triplicate samples for each group. Significant differences between two groups were evaluated using a one-way analysis of variance (ANOVA) with a 95 % confidence interval. Underneath, graphical representations presented the result of a tensile test carried out on a Zwick Z020 Universalpruefungsmaschine equipment.

Tab. 3. Measured material characteristics of recycled polyvinyl butyral during the relaxation test

No.	Period	Tensile stress [MPa]	Strain [%]	Stress at break [N]	Strain at break [%]
1.	0	0	0	0	0
	5	0.451	400	234.597	281.358
	15	0.255	260	68.381	330.848
	25	0.301	400	214.633	289.634
2.	0	0	0	0	0
	5	0.350	550	196.74	394.727
	15	0.350	480	168.185	179.929
	25	0.300	500	240.024	343.954

Source: own processing

Tab. 4. Measured force characteristics of recycled polyvinyl butyral material during the relaxation test

No.	Period	Max. force after relaxation F´εges [N]	Max. force before relaxation F εges [N]	Strain after relaxation ε´ges [mm]	Strain before relaxation ε ges [mm]
1.	0	0	0	0	0
	5	4.708	9.775	21.120	21.121
	15	4.628	9.175	21.031	21.020
	25	3.754	8.173	21.080	21.070
2.	0	0	0	0	0
	5	5.643	10.614	21.032	21.031
	15	4.278	11.332	20.980	20.980
	25	4.350	11.740	21.111	21.100

Source: own processing

By introducing the above measurement conditions (Telišková et al., 2018; Botko et al., 2018), the material manufactured by compression moulding from recycled polyvinyl butyral was tested for its ability to withstand a continuous load of 10 cycles. The relaxation time (Farzana et al., 2016) was 10 minutes in all cases. It can be seen from the graph that with a period of 5 minutes, the relaxation time of 10 minutes and a total number of cycles at this stress, the sample was ruptured by strain results between 410% and 570%, tensile stress from 11.2 MPa to 11.5 MPa. By 15 min period testing, the relative strain values were from 260% to 460% and the tensile stress from 9.3 MPa to 9.5 MPa. The testing cycle, which lasted 25 min, had a relative strain value from 435% to 520% and tensile stress from 10.1MPa to 11.9MPa (Figure 5).

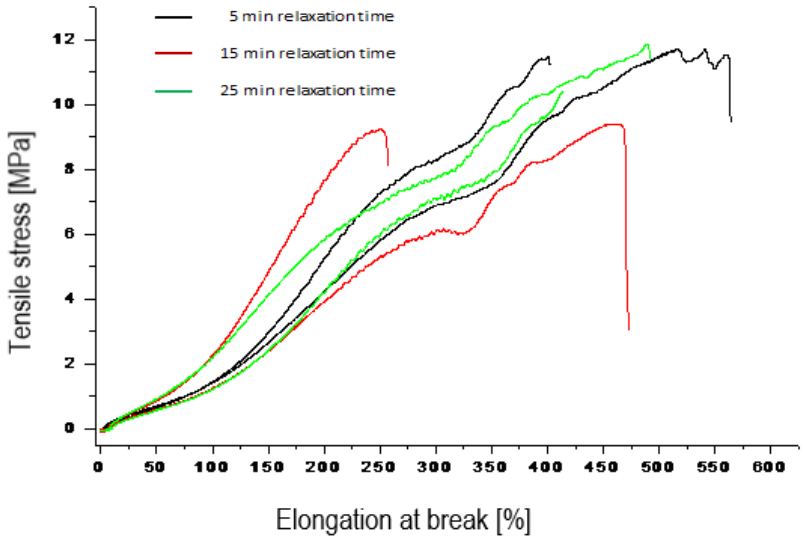

Fig. 5. Graphical representation of recycled polyvinyl butyral stress relaxation (by 5-, 15- and 25-min relaxation time)
Source: own processing

In Figure 6, the view of relaxation by 5-min and the number of cycles 10 can be seen. The tensile stress has the max. value of 0.65 MPa by 5-min relaxation time. All presented curves; i.e. dependencies of individual variables were evaluated by Origin Ver.6.

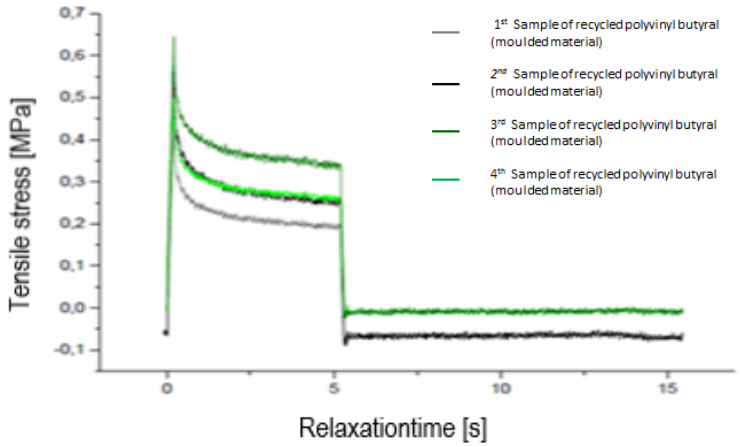

Fig.6. Graphical representation of recycled polyvinyl butyral stress relaxation (by 5 min relaxation time)
Source: own processing

The cyclic relaxation of the material was by the regular relaxation of the material at a constant speed, and a force of 5.01 N. Orange colour presented correction of curves (optimal condition) in dependence on the strain and tensile stress. Neon green colour by 25-min relaxation is presented an optimal condition. Figures 7 and 8 show the material relaxation for 10 cycles and for all tested samples together.

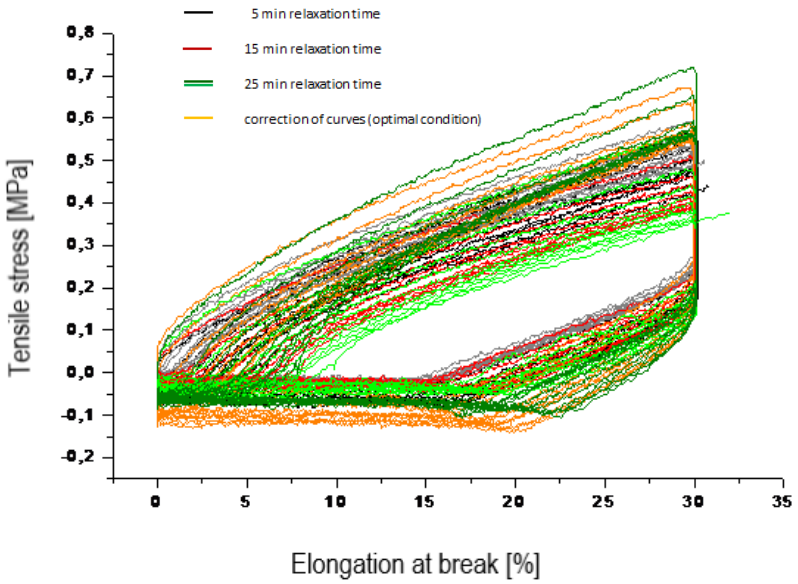

Fig.7. Graphical representation of material relaxation by the 5-min, 15-min and 25-min testing period (10 cycles)
Source: own processing

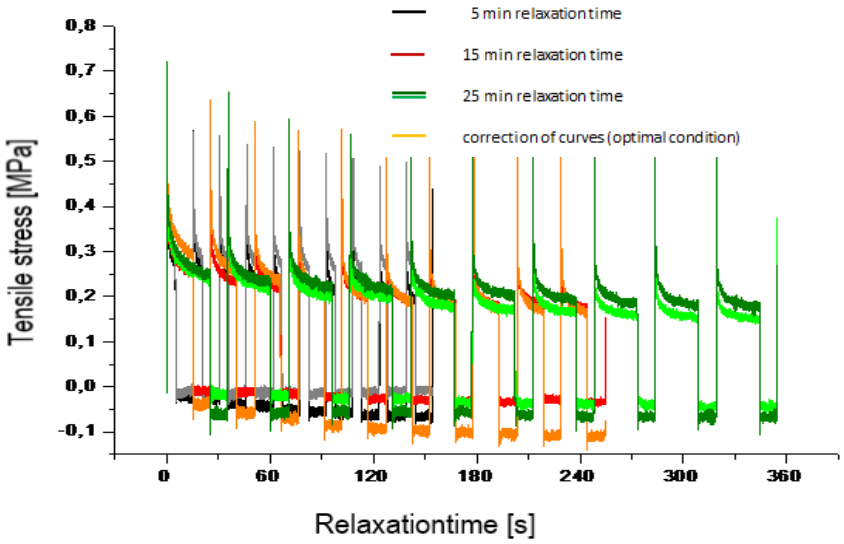

Fig.8. Graphical representation of material relaxation under 10 cycles
Source: own processing

According to ISO 3384-1:2011 performed laboratory testing of recycled polyvinyl butyral show less manual work and measurement can continue throughout the test after it is started. Advantages of this measurement are no physical movement of the rigs after the test is started. With a comparison of our obtained results and already published results, we have to observe the completion of regular cycles of 5-min, 15-min, and 25-min, the material was brought to a state where it reached the tensile stress of the test material at failure. This is mainly because the tensile stress amplitude was greater than the fatigue limit of the material. Ultimately, this led to crack initiation. This phenomenon arises especially when there is a certain presumption of crack formation or its potential, and there is a presumption of its assumption. After that, a test sample of moulded recycled polyvinyl butyral was broken. We see the novelty of the presented paper in the testing of material manufactured with recycled polyvinyl butyral.

Conclusions

Recycled polyvinyl butyral, as one of the most important parts of safety (for example, automotive) glass, was investigated under material stress relaxation. Based on the results, it can be stated that:

1. The material had the max. values for tensile stress of 0.78 MPa, the strain of the material for the tensile strain was up 410% to 520%.
2. Upon completion of regular cycles of 5-min, 15-min, 25-min, the material was brought to a state where it reached tensile stress at break σ_B which is also characterised as the tension of the test material in the tensile stroke of the test sample.
3. The amplitude of the tensile stress was greater than the material fatigue limit. In the end, it has led to crack initiation.

Recycled PVB is an important part of the production of new materials, and we can say that the variation in the use of this type of material is high. It is characterized by very well:

- elasticity,
- adhesion to various surfaces,
- good water resistance,
- economic investment,
- environmental friendly material.

According to the presented results, the advantage of this material is high compatibility with other polymers, as well as very good processing and subsequent production of composite materials. Last but not least, the economic potential of this new material is very important. Given the cost of this alternative commodity, which is in the range of 0.25-0.50 € per kilogram of this thermoplastic and its physical, chemical and ecological properties make it a very desirable raw material for the end-user.
Obtained results of our research:

- minimise deficiencies or problems with the raw material of car windscreens.
- Can be reused in the production process.
- New material can be implemented in selected engineering production, for example, indoor and outdoor.
  material´s cap, and not only there. According to its own of properties and processing is an open application to the construction industry,
  garden construction, road construction, for example, insulation material, facing panel,
- Manufactured materials based on recycled polyvinyl butyral save the company's initial investment

.

As part of the mass customization strategy, the manufacturer has the opportunity to apply this recycled raw material to a wide portfolio of its products in order to maximise customer satisfaction, minimize production costs while paying attention to the environmental ecology.

References

Barry, C. M. F. and Orroth, S. A. (2000). Processing of thermoplastics, USA.

Cavusoglu, H. and Cavusoglu, H. and Raghunathan, S. (2007). Selecting a Customization Strategy Under Competition: Mass Customization, Targeted Mass Customization, and Product Proliferation. IEEE TRANSACTIONS ON ENGINEERING MANAGEMENT, 54(1).

Del Linz, P. and Wang, Y. and Hooper, P. A. and Arora, H. and Smith, D. and Pascoe, L. and Cormie, D. and Blackman B. R. K. and Dear, J. P. (2016). Determining Material Response for Polyvinyl Butyral (PVB) in Blast Loading Situations. *Experimental Mechanics, 56(9).*

Dhaliwal, A. K. and Hay, J. N. (2002). The characterization of polyvinyl butyral by thermal analysis. Thermochimica Acta, 91.

Farzana, R. and Rajarao, R. and Sahajwalla, V. (2016). Characteristics of waste automotive glasses as silica resource in ferrosilicon synthesis. *Waste management and research, 34 (2).*

Knapčíková, L. and Husár, J. and Fedák, M. (2016). Waste tires- the future material (Opotrebovaná pneumatika-materiál budúcnosti), 1. vyd., Brno: Tribun EU, pp. 90, 2016, [In Slovak].

Knapčíková, L. and Radchenko, S. and Husár, J. and Radič, P. and Bernát, A. (2016). Experimental study of thermoplastics material reinforced by various types of high-strength fibres. *MM Science Journal. No.October, 2016.*

Knapčíková, L. (2015). Life cycle assesment of composite materials on the thermoplastics base (Životný cyklus kompozitného materiálu s termoplastickou matricou). *Strojárstvo, 19(7-8).*

Knapčíková, L. and Herzog, M. and Oravec, P. (2010). Material characterization of composite materials from used tires. Manufacturing Technologies, 4.

Kotler, P. (2003). Marketing Management. New Jersey: Prentice-Hall. 11. vydanie. ISBN 978-01-303-3629-3.

Kulikov, A. and Fedák, M. and Abraham, M. and Vahovsky, J. (2018). Study of the gaseous fuel combustion respect to the O2 concentration and NOx formation. *Advance in Thermal Processes and Energy Transformation, I(1).*

Polyvinyl butyral-resin, Kuraray, from http://www.Kuraray.eu./, (accessed 20 January, 2019).

Lampel, J. and Mintzberg, H. (1996). Customizing Customization. In: Sloan Management Review.

Liu, B. H. and Sun, Y. and Li, Y. and Wang, Y. and Ge, D. and Xu, J. (2012). Systematic experimental study on mechanical behavior of PVB (polyvinyl butyral) material under various loading conditions. *Polymer Engineering and Science, 52(5).*

Mandičák, T. and Mesároš, P. and Tkáč, M. (2018). Impact of management decisions based on managerial competencies and skills developed trough BIM technology on performance of construction enterprises. *Pollack Periodica, 13(3).*

Mitaľová, Z. and Mitaľ, D. and Botko, F. (2016). Measuring of roughness and roundness parameters after turning of composite material with natural reinforcement. Science report: Project CIII - PL- 0007: Research on modern systems for manufacture and measurement of components of machines and devices, Kielce: Wydawnictwo Politechniki Świętokrzyskiej, Poland.

Mohammadian-Kohol, M. and Asgari, M. and Shakur, H. R. (2016). A detailed investigation of the gamma-ray radiation effects on the optical properties of polyvinyl butyral film. *Optik, 127(19).*

Patents and utility models, Industrial property office of the Czech Republic, from http://www.upv.cz/, (accessed on 10 January, 2019).

Sekisui chemical.com, from http://www. Sekisui chemical.com./,(accessed 20 December, 2018), 2018.

Botko, F. and Hatala, M. and Beraxa, P. and Duplak, J. and Zajac, J. (2018). Determination of CVD Coating Thickness for Shaped Surface Tool. *TEM Journal, 7(2).*

Schirmbeck GmbH, Recycled Polyvinyl butyral, from http://www.schirmbeck.com/(accessed 12 November , 2018).

Telišková, M. and Torok, J. and Dupláková, D. and Kaščák, J. and Mezencevová, V. and Birčák, J. (2018). Non-Destructive Diagnostics of Hard-to-Reach Places by Spatial Digitization. *TEM Journal, 7(3).*

Valášek, P. and Muller, M. and Ruggiero, A. (2016). Material utilization of waste originating during processing of plant jatropha curcas. Biocomposites – adhesive-cohesive characteristics and wear. *Technicky vjesnik 23(5).*

Výrobná stratégia podniku [online]. EuroEkonóm.sk, 2015. [cit. 2016-10-12]. Dostupné na internete: <http://www.euroekonom.sk/manazment/manazment-vyroby/vyrobna-strategia-podniku/>.

Zhang, H. and Healy, N. and Shen, L. and Huang, Ch. Ch. and Aspiotis, N. and Hewak, D. W. and Peacock, A. C. (2016). Graphene-Based Fiber Polarizer With PVB-Enhanced Light Interaction. *Journal of Lightwate technology, 34(15).*

Zhao, S.and Dharani, L.R. and Chai,L.and Barbat S.D.,(2006). Analysis of damage in laminated automotive glazing subjected to simulated head impact. *Engineering Failure Analysis, 13(4).*

Asik, M.Z.,(2003). Laminated glass plates:revealing of nonlinear behavior. Computers and Structures, (81).

Hidallana-Gamage,H.D.and Thambiratnam, D.P. and Perera N.J. (2014). Failure analysis of laminated glass panels subjected to blast loads. *Engineering Failure Analysis, (34).*

Fischer, K. and Häring, I. (2009). SDOF response model parameters from dynamic blast loading experiments. *Engineering Structures, (31).*

Sridhara, V. and Satapathy, L.N.(2015). Effect of Nanoparticles on Thermal Properties Enhancement in Different Oils -a Review, Critical reviews in solid state and materials sciences, (40).

Iwasaki, R. and Sato, C. and Latailladeand, J.L. and Viot, P.(2007). Experimental study on the interface fracture toughness of PVB (polyvinyl butyral)/glass at high strain rates. In. I*nternational Journal of Crashworthiness,(12).*

Sheng, J.L.and Zhang,M. et al.(2016). Thermally induced chemical cross-linking reinforced fluorinated polyurethane/polyacrylonitrile/polyvinyl butyral nanofibers for waterproof-breathable application. R*SC Advances, 6 (35).*

Cormie, D. and Mays, G. and Smith,P. (2009). Blast effects on buildings. 2nd ed. ICE Publishing.

Chen, S. and Zang,M. and Wang, D. and Zheng,Z. and Zhao, C. (2016). Finite element modelling of impact damage in polyvinyl butyral laminated glass. *Composites Structures,(138).*

Vasiliev,V.V. and Morozov, E.V. (2001). Mechanics and analysis of composite materials, Elsevier.

Saad, N. and Estevez, R. and Olagnon, C. and Séguéla, R.(2006). Cohesive zone description and quantitative analysis of glassy polymer fracture. *Oil &gas science and technology review. 61(6).*

Impact of land use changes on surface runoff in urban areas - Case study of Myslavsky Creek Basin in Slovakia

Martina Zeleňáková[1], Adam Repel[1], Zuzana Vranayová[2], Daniela Kaposztasová[2] *and* ***Hany F. Abd-Elhamid[3]***

The task of this work was to analyze the drainage conditions of the river basin Myslavsky Creek with the aim of proving the increasing flood risk in the area of Hornad River Basin as a result of newly constructed built areas. Drainage conditions of the reference area were compared on the basis of two time periods, for years 1980 and 2010. Two maps of land use were processed for two years. Total runoff coefficients were calculated based on the processed maps, which differed because in 1980 the territory was not so built up compared to now. The calculated results were also proved by using PCSWMM – Storm Water Management Model. The results prove that the maximum 2010 runoff at the area has increased by almost double from 1980. The increased discharge, therefore, requires flood protection measures in the area.

Keywords: *land use; runoff coefficient; urban areas, Myslavsky Creek*

Introduction

An accurate estimate of runoff from rain and snowmelt is one of the most important elements of the flood forecast process (Weng, 2001). It is important for flood control channel construction and possible flood zone hazard delineation (Bronstert, Niehoff, Bürger, 2002). A high runoff coefficient (*C*) value may indicate flash flooding areas during storms as water moves fast overland on its way to a river or a valley floor (Zeleňáková, 2018). Runoff coefficient is measured by determining the soil type, gradient, permeability and land use (Okkan, 2018). Hydrometeorological hazards, flood and drought especially, stand nowadays as some of the most frequent and disturbing danger phenomena (Mititelu-Ionuș, Licurici, 2018). Urbanization lowers maximum potential storage and increases runoff coefficient values (Wilby, 2007). As a consequence of increasing urbanization as well as rainfall totals and intensities over the second half of the 20th century, signs of increased flooding probability in many areas of the basins have been documented (Nirupama, Simonovic, 2007), (Kiss et al. 2014). These changes affecting rainfall characteristics are most evidently due to an increase in westerly atmospheric circulation types (Pfister et al., 2004). Land use changes, particularly urbanization, have significant effects in small basins (headwaters) with respect to flooding, especially during heavy local rainstorms (Vranayová et al., 2011) (Stec et al., 2017). The rainfall-runoff process depends not only on the space-time distribution of the rainfall but also on the kind and the state of the basin (Sivakumar et al., 2000), which in turn, depend on the climatic condition and vegetation states (Šlezingr, Fialová, 2012). Therefore, what is really important is a unified description of the complex behaviour of the dynamic system arising from the combination of all of its components (Zeleňáková et al., 2011) (Zeleňáková, Rejdovjanová, 2011), (Blišťanová and Blišťan, 2014), (Blišťanová, et al. 2016).

To model runoff from urbanized areas, the SWMM (Storm Water Management Model) is successfully used in different areas of the world. SWMM, a free-ride rainwater management model is a dynamic rainfall-drain simulation model used to simulate the quantity and quality of runoff from primary urbanized areas (Lewis, Rossman, 2015). Drainage modelling based on the principle of sub-basins that are exposed to precipitation create drains loaded with pollutants (Diaconu et al., 2017a). The SWMM model can be used in the following situations: drainage from the site, design and modelling of surface drainage, retention reservoir design, application of Low Impact Development (LID) to the area and their impact on runoff, drainage quality, design and modelling underground sewerage and drainage network, design and modelling of a single sewerage network, etc. (Gironás, Roesner, Davis, 2009; Diaconu et al., 2017b).

There were compared the results of the LID editor with those obtained by a detailed demand-driven tank model scheme used as a benchmark and developed using basic functions of SWMM. The comparison showed the LID Editor-based model generally overestimates the benchmark model in the evaluation of both volumetric and peak retention efficiency. The high variability of the results of the comparison suggested the use of the LID

[1] *Martina Zeleňáková, Adam Repel,* Department of Environmental Engineering, Faculty of Civil Engineering, Technical University of Košice, Košice 042 00, Slovakia, martina.zelenakova@tuke.sk

[2] *Zuzana Vranayová,* Department of Architectural Engineering, Faculty of Civil Engineering, Technical University of Košice, Košice 042 00, Slovakia

[3] *Hany F. Abd-Elhamid*, Department of Water and Water Structures Engineering, Faculty of Engineering, Zagazig University, Zagazig, 44519, Egypt, Civil Engineering Department, College of Engineering, Shaqra University, 11911, Duwadimi, Saudi Arabia.

editor rain barrel option for long-term simulation but not for single event analysis. A sensitivity analysis revealed that overestimation provided by the rain barrel option was significant for tanks smaller than 2 m^3 tank sizes for major collection of domestic rainwater (Campisano, Catania, Modica, 2017).

Long-term modelling of the green roof using SWMM presented the results of the monitoring of the extensive green roof in Bologna (Italy). The model simulated the hydrological behaviour of the green roof over one year and compared it with an adjacent impermeable roof of the same size. There was also a comparison of rainfall retention in the green and also in the classical impermeable roof. The total retention of the green roof was 48%, while the impermeable roof was only able to retain 11% of the precipitation (Cipolla et al., 2016).

In the study (Ouyang et al., 2012), runoff samples were collected and analyzed during rainy events in Beijing. Indicators such as chemical oxygen demand, total suspended solids, or total phosphorus were analyzed. In addition, the drainage water outflow from different substrates was analysed. The contribution expressed the relationship between the impermeability of the substrate and the total amount of effluent. It was clear from the results that in the sub-basin, which was made up of impermeable surfaces, the amount of runoff was almost equal to the amount of rainfall (Ouyang et al., 2012).

Palla and Gnecco (Palla, Gnecco, 2015) analyzed the implementation of LID systems as a solution to slow drainage during rainfall events. Their modelling explored the same territory with different scenarios of land use and hard surfaces, including the use of green roofs and permeable walkways. Modelling itself was done using SWMM. The authors stated that the suitability of the use of LID systems (green roofs, permeable walkways) in the management of precipitation-runoff processes in urbanized areas had been confirmed, as their use not only reduced the maximum runoff but also slowed down the overall runoff (Palla, Gnecco, 2015).

Rainwater system modelling is often used to manage rainfall-drainage processes in urbanized areas, in particular, to estimate rainfall drainage and the quality of drained and retained rainfall. These models are usually not adequately calibrated and verified due to limited availability of rainfall quantity and quality data (Sterren et al., 2014). They described the calibration and validation of the rainwater tank model using SWMM, which used data obtained from two systems of rainwater tanks in Sydney, Australia. The modelling takes into account the maximum inflow and volume of the rainwater reservoir, as well as water quality parameters (total phosphorus (P), total nitrogen (N) and insoluble matter). The authors suggested that the amount of P and N can be modelled more accurately than the amount of insoluble matter in the effluent. It has also been found that a drainage retention reservoir can significantly reduce the drainage of rainwater from the area (Sterren et al., 2014).

Tavakol-Davani et al. assessed the impact of climate change on single sewerage networks and the possibility of reducing these impacts in Toledo, Ohio. The aim of this study was to evaluate the effectiveness of rainwater retention in mitigating the potential impacts of climate change on sewer networks. For this purpose, Coupled Model Intercomparison Project Phase 5 (CMIP5) predicted future deductions based on historical records. Subsequently, SWMM runoff modelling was used to determine how the existing single sink system will respond to its expected impact in the future. The results of the study showed that 12% to 18% increase in the volume of water alone in the sewer system during intense rainfall might occur in future climate change developments. In order to mitigate these impacts, the study proposed a water retention plan in the country by using a tank of 0.76 m^3 (200 gallons) for half of the buildings from the whole area and modelling proved that such a measure is able to ensure the proper functioning of the single sewer system also in the future (Tavakol-Davani et al., 2016).

Application of permeable walkways and reinforced surfaces as systems to mitigate the negative impacts of urbanization on the outflow of water from the territory was a case study in Southern Spain (Rodriguer-Rojas et al., 2018). This was a project, where the hydrological performance of three types of permeable walkways had been analysed. Passable walkways were investigated directly in the field, but drains were also modelled using SWMM software. The pattern of such permeable walkways proved to be highly efficient, with up to 70% reduction in runoff compared to conventional reinforced surfaces. Permeable walkways appear to be a more appropriate alternative to green roofs from the results of this study since they are more effective, but also have a wider application (Rodriguer-Rojas et al., 2018).

From the above mentioned, it is obvious that SWMM has a very wide application and was also used in the current study. The aim of this paper is to evaluate the effects of surface condition and calculated runoff coefficient on the degree of flood protection in low lying areas and design potential measures to stabilize conditions in the drainage basin of Myslavsky Creek. The paper presents the current state of drainage situation in the study area – part of Kosice City in Slovakia – taking into account the existing outlets of rainwater drainage of the newly built constructions buildings, hypermarkets, etc.

Materials and methods

The methodology of the current research consists of the following steps:

1. Characteristics of the river basin of Myslavsky Creek.

2. Collecting the input data from the Chief Architect Department, Kosice (DCAK) and Slovak Water Management Enterprise, s.c. branch office Kosice (SWME), specifically:
   - Maps of land-use in the scale of 1:5 000 and 1:2 000; (*source: DCAK*),
   - Maps of land-use in digital form in .dwg (AutoCAD); (*source: DCAK*),
   - The situation of the basin in the scale of 1:50 000; (*source: SWME*).
3. Processing of input data:
   - Calculation of runoff coefficients,
   - Calculation of the total runoff.
4. Propose measures to stabilize the drainage conditions into the stream basin of Myslavsky Creek.

Study area

The study area is situated in the eastern part of Slovakia (Figure 1) near Kosice City.

Figure 1. Location map of the study area

Myslavsky Creek is the right-hand tributary of the Hornad River, which opens into the southern part of Kosice (Figure 2) (Hornad River basin).

Myslavsky creek is the right tributary of Hornad River (Figure 2). It opens into the Hornad in 135.70 river kilometre. Its catchment area is 59.67 km^2. From the west, it is defined by a sub-catchment of the Bodva River Basin. The highest point of the basin is at an altitude of 940 m above sea level; the lowest point is at an elevation of 188.90 m above sea level (Zeleňáková, 2014). Basic characteristics of the catchment are presented in Table 1.

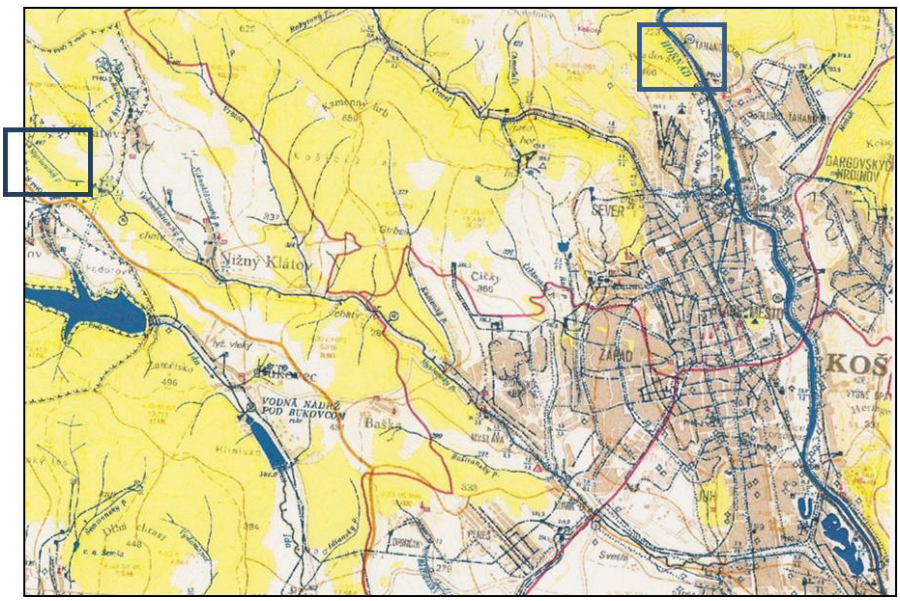

Figure 2. Myslavsky Creek, the right tributary of the Hornad River

Table 1. The basic characteristic of the catchment (Zeleňáková, 2014)

Basin area	The highest point	The lowest point	Runoff from the basin	Maximum flow stream
59.67 km^2	940 m asl.	188.90 m asl.	9.5 $l.s^{-1}.km^{-2}$	52 $m^3.s^{-1}$

Myslavsky Creek was regulated mainly within the boundaries of the city of Kosice and Myslava. A number of unilateral purpose-built bank reinforcements and many different types of bridges were constructed by landowners in the agricultural area. A large part of the basin is located in an urbanized area, which may significantly alter hydrological conditions.

The most frequent occurrence of floods is during the summer months, due to storms. The last major flood in the Myslavsky Creek occurred in May and June 2010 after long-term rains. The flood damages for Kosice city were enumerated at 11.935 € for Kosice and 69.566 € for a rural area.

Runoff calculations

The Rational method of runoff coefficient (*C*) calculation is a function of the soil type and drainage of the basin. The larger values correspond to higher runoff and lower filtration. The Rational equation is the simplest method to determine peak discharge from drainage basin runoff. A rational equation is as follows:

$$Q_{\max} = C \cdot i \cdot A \quad (l.s^{-1}) \tag{1}$$

Where: Qmax = peak discharge ($l.s^{-1}$),
C = rational method runoff coefficient (-),
i = rainfall intensity ($l.s^{-1}.ha^{-1}$) in time t (min),
A = drainage area (ha).

Runoff coefficient for the whole area was calculated as weighted average as follows:

$$C = \frac{\Sigma(C_i.A_i)}{\Sigma A_i} \quad (-) \tag{2}$$

The rainfall intensity (i) is typically found from Intensity Duration Frequency (IDF) curves for rainfall events in the geographical region of interest. The duration is usually equivalent to the time of concentration of the drainage area. The storm frequency is typically stated by local authorities depending on the impact of the development. A 10-yr, 25-yr, 50-yr, or even 100-yr storm frequency may be specified.

Runoff modelling

The PCSWMM modelling software, which is based on SWMM 5 model, was used for comparison of two different scenarios from the view of runoff from the area. SWMM (Storm Water Management Model), a free-ride rainwater management model is a dynamic rainfall-drain simulation model used to simulate the quantity and quality of runoff from primary urbanized areas. The SWMM monitors the amount and quality of runoff in each sub-basin, as well as the flow rate, water depth in pipelines and channels throughout the simulation time. The program itself is therefore used to plan, analyze, and design a drainage water system. It is also used to design uniform sewer systems and various rainwater management systems in the country (Cipolla et al., 2016).

In PCSWMM software, one sub-basin with the size of 431.961 ha was created. The runoff was modelled according to the values in Table 2. A difference between scenarios was presented by the percentage of impervious area.

Table 2. Basic characteristics of the catchment (Zeleňáková, 2014)

Ground cover	Area in 1980 A_i (m^2)	Partial runoff coefficient C_i (-)	Area in 2010 A_i (m^2)	Partial runoff coefficient C_i (-)
Roofs	139 978.60	0.8	473 427.26	0.8
Roads and streets	391 895.15	0.9	962 407.09	0.9
Cemeteries	140 911.91	0.15	174 441.46	0.15
Greenery	3 587 398.15	0.15	2 649 908.00	0.15
Un-built areas	59 425.98	0.3	59 425.98	0.3

Results and Discussion

Two maps were prepared for years, 1980 and 2010 for the whole catchment of the Myslavsky Creek. The maps of the selected area of the catchment, exactly the area of Košice city, where land use changed and human activities are manifested as presented in Figures 3 and 4.

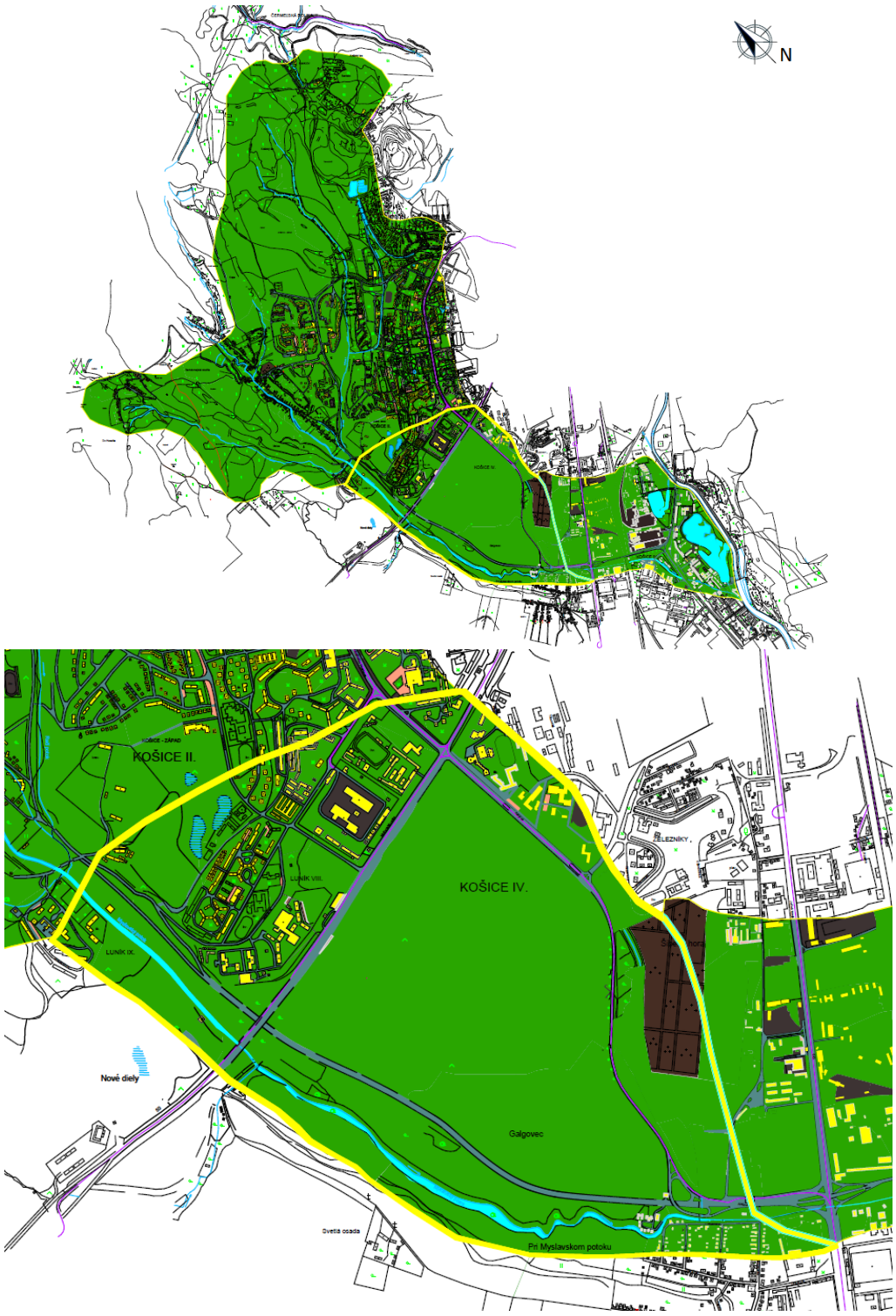

Figure 3. The selected area of Myslavsky Creek basin – land use in 1980

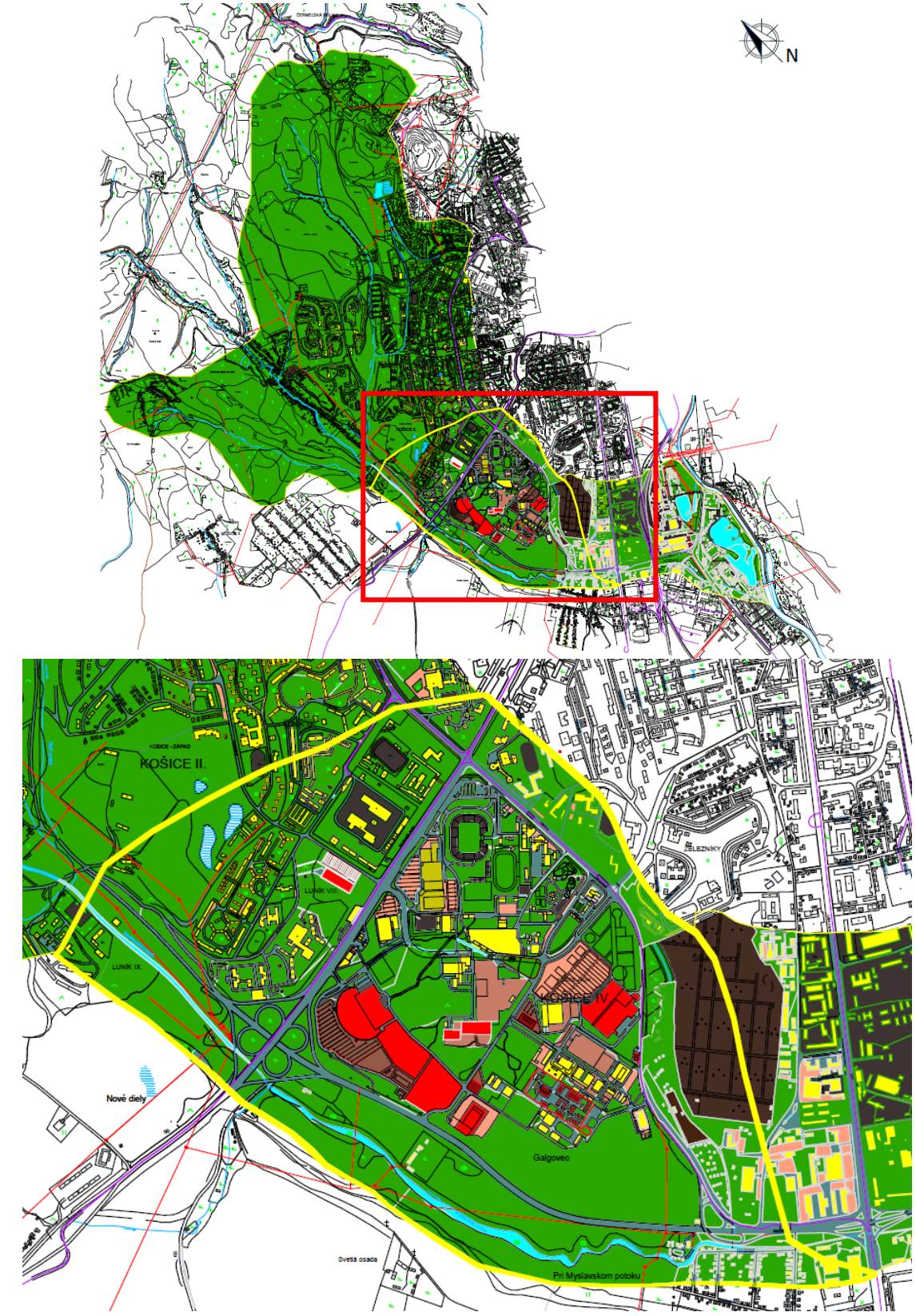

Figure 4. The selected area of Myslavsky Creek Basin – Land use in 2010

Legend:

- greenery
- roofs
- roads, and paved areas
- selected object
- un-built areas
- cemeteries
- parking
- border of the catchment

There were huge constructions in a given area during the period 1995-2005. The land use of the area is the same nowadays as is presented in Fig. 4.

According to equation (2) runoff coefficients were manually calculated for the two time periods for significantly influenced locality by human activities, with a different area of different land use of Myslavsky Creek Basin. The value of runoff coefficient is changed by 0.10 over the 30-years. Based on the calculated total runoff coefficients *C*, the drainage area of Myslavsky Creek and for a specific amount of rainfall was calculated maximum runoff for both time periods year 1980 and 2010 according to equation (1). The results are presented in Table 3.

Table 3. The maximum discharge Q for the year 1980 and 2010

Year	*C* (-)	*i* ($l.s^{-1}.ha^{-1}$)	*A* (ha)	*t* (min)	*Q* ($l.s^{-1}$)
1980	0.2412	139.8	431.9609	15	14 565.62
2010	0.3404	139.8	431.9609	15	20 556.12

For the selected part of Myslavsky Creek river basin in 2010, the above table of values indicates the maximum runoff *Q*, for 15 minute periods of rain was 20 556.12 $l.s^{-1}$. Compared to 1980, when the *Q* value was 14 565.62 $l.s^{-1}$, it represents an increase of 42% for the same drainage area.

The results from modelling by PCSWMM software are as follows.

It was determined that there was 12.31% of the impervious area on the modelled sub-basin in 1980, whereas in 2010, there was 33.24% of the impervious area. It is clear from this that the size of the impervious surfaces on the sub-basin has more than doubled. The period of 15 minutes' rainfall with a constant intensity of 50.328 mm/min was used to obtain the results of total runoff from the area with the same conditions as rainfall in the calculation method. Comparison of the total run-off from the model in 1980 (at 12.31% of impermeable areas) and in 2010 (at 33.24% of impermeable areas) during a 15-minute rain of constant intensity is presented in Figure 5 and Table 4.

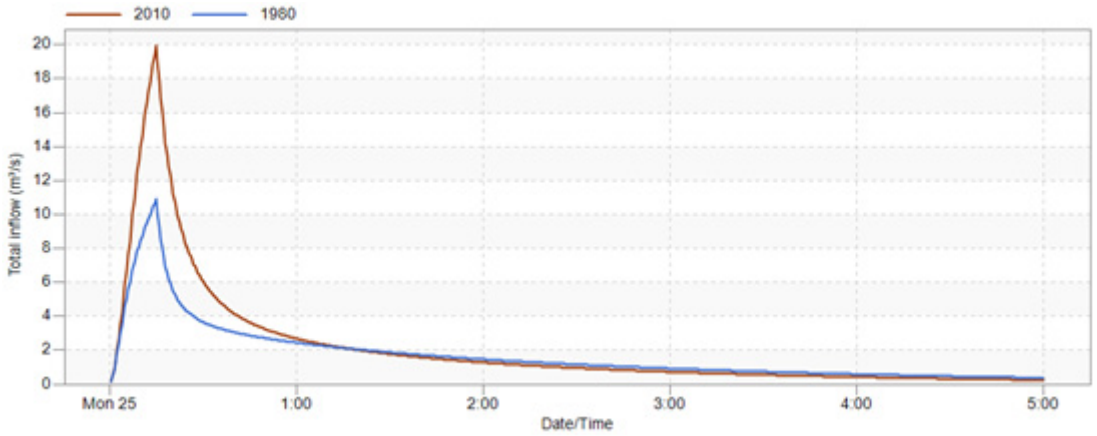

Figure 5. Run-off from the modelled area using PCSWMM

Table 4. Run-off in 1980 and 2010 using PCSWMM

	Outfall 1980	Outfall 2000
Maximum total inflow (m^3/sec)	10.9	19.93
Minimum total inflow (m^3/sec)	0.1859	0.1897
Mean total inflow (m^3/sec)	1.736	2.152
Duration of exceedances (h)	4.992	4.992
Duration of deficits (h)	0	0
Number of exceedances	1	1
Number of deficits	0	0
Volume of exceedances (m^3)	31190	38670
Volume of deficits (m^3)	0	0
Total inflow (m^3)	31200	38670

It is obvious that the maximum runoff at 2010 in the area has increased by almost double - as was the case with the rational method.

There are 10 objects which drained rainwater from the catchment of Myslavsky Creek to the water stream which are mainly business and shopping centres. From Figure 6, it is possible to see their location in the study area.

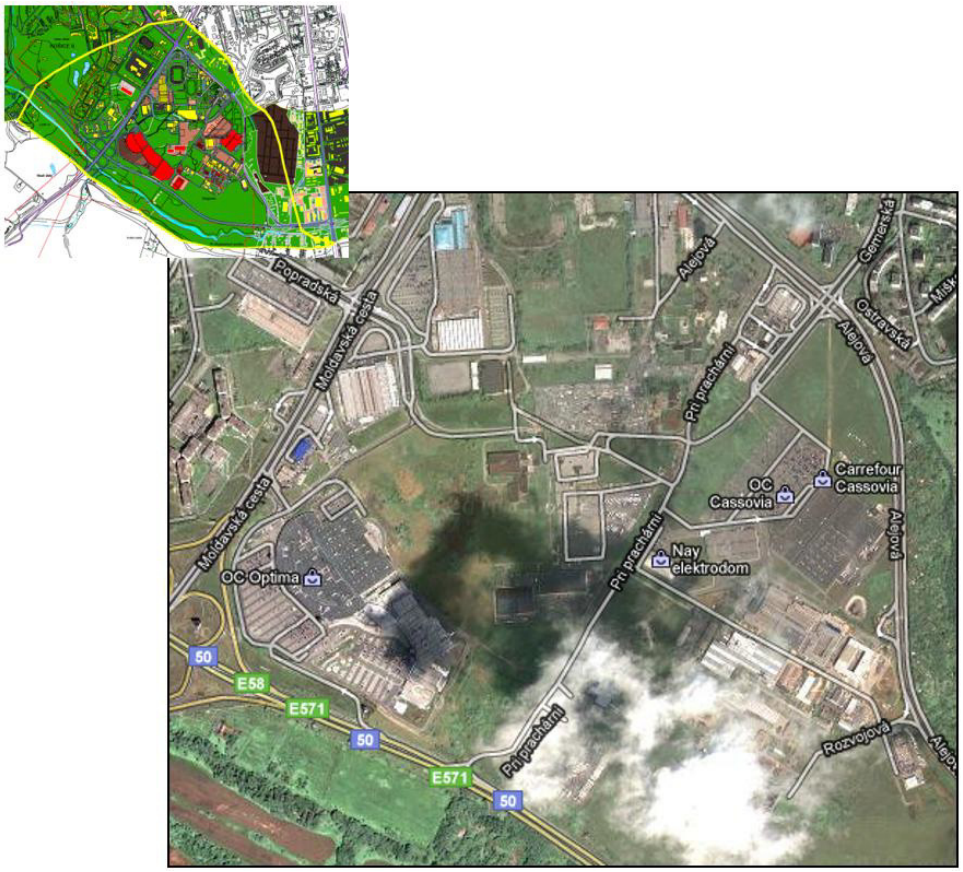

Figure 6. Business and shopping centres in the study area

Individual objects are equipped with different types of oil separators or grease traps, through which water from the surface runoff is purified before discharging into Myslavsky Creek. Some of the selected objects also have retention tanks. The drained water of the objects significantly increases the discharge in Myslavsky Creek, which resulted in the occurrence of the increased flow in the stream. Four drains were identified on the Myslavsky Creek by a survey of the area, which diverts the water from the surface runoff from selected objects, thus increasing the flow of the Myslavsky Creek Figure (Figure 7). Its level increases enormously and causes flooding of the surrounding area. This is due to the fact that in the past there were no so many built-up areas as today, and rainwater filtered into the soil, reducing the threat of a large flood.

Based on the changed outflows of the Myslavsky Creek, it is necessary to propose potential measures to stabilize the runoff in the catchment area, thus increasing the flood protection in the lowland areas. Protection measures may be environmental (removal of obstacles) as well as organizational (compliance with water management decisions, design of retention areas).

Proposal of protection measures for runoff condition stabilisation with the aim of flood protection of lower laying areas are the following:

a) non-structural flood mitigation measures- water management decision,
b) structural flood mitigation measures:
- directing the stream flow by removing sharp meanders
- removal of islands and random obstacles
- creation of longitudinal stream slopes, which creates a more steady-state of a river bed
- creation of a stream cross-section trough of a size and shape to harmlessly divert flow prior to such fortification, preventing the erosion and flush out of the banks.

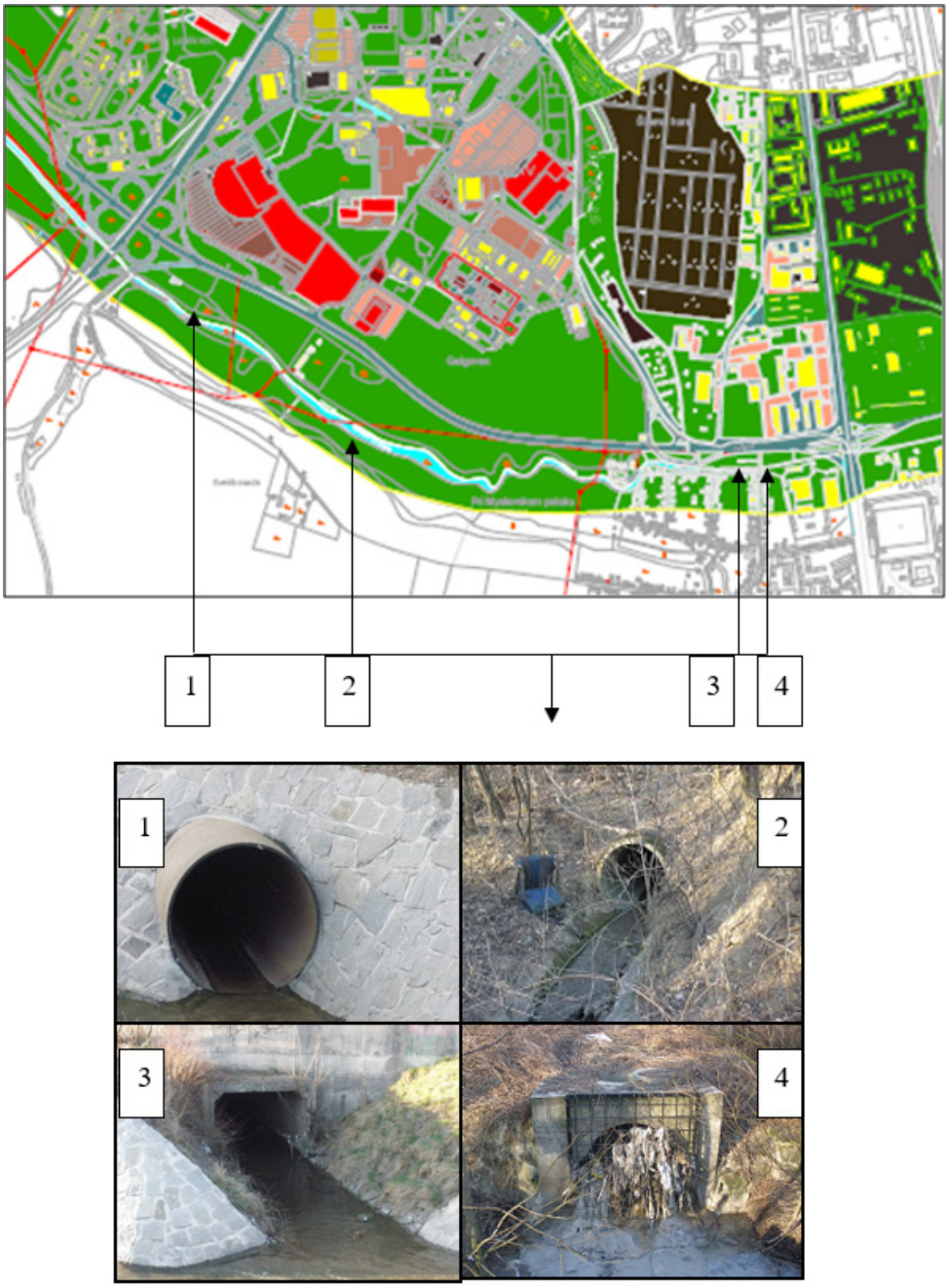

Figure 7. Drainage outlets to Myslavsky Creek

Conclusion

The world's population nowadays is concentrated in urban areas. This change in demography has brought land-use and land-cover changes that have a number of documented effects on streamflow. The most consistent effect is an increase in impervious surfaces within urban catchments, which alters the hydrology and geomorphology of streams. In addition to this, runoff from urbanized surfaces as well as municipal and industrial discharges result in increasing floods in urbanized areas as it decreases river bed capacity for flow. Nowadays, when the urbanization and expansion of urban settlements are at the forefront, much attention must be paid to water management, in particular, rainfall-drainage processes from the basin. One of the appropriate tools for managing these processes in a river basin is the SWMM precipitation-out model, which is widely used to model various situations that occur in urbanized locations. This model, as well as the rational method, was used in the current study. The SWMM can be used to model the amount of drainage from the basin from different underlying surfaces, and model design values for precipitation, sewerage and other phenomena associated with precipitation-drainage processes. The model can be used either in the scientific sphere or directly in designing rainfall-drainage processes in cities.

This paper presents the current state of runoff condition in the study area of Myslavsky Creek Basin, taking into account the urban development in the last 30 years, mainly of newly built hypermarkets. The goal of the study was an evaluation of the surface condition, calculation of the runoff coefficient and propose potential measures to stabilize conditions in the drainage basin of Myslavsky Creek located in the Eastern part of Slovakia.

The drainage ratios of the monitored area were compared based on two time periods, for 1980 and 2010, and two land use maps for both years were processed. From the processed land use map, total drainage factors were found, which varied considerably, because in 1980 the area was not as urbanized as it is today. The runoff coefficients for the different time periods 1980 and 2010 were compared. For 1980 the runoff coefficient was calculated of 0.2412, and for 2009, the runoff coefficient was calculated of 0.3404. Such a difference between the runoff coefficients results from the differences in the built-up area of the river basin in 1980 compared to 2010. The state of build-up area in the river basin at present is the same to 2010. In the past, rainwater has been filtered into the land surface directly into the soil, and so extensive flooded areas have not occurred. The situation is different nowadays because in 30 years the number of built-up and reinforced areas has increased enormously and all the rainwater is captured and discharged by rainwater drainage through the drains into the Myslavsky Creek. Due to the fact that almost all of the rainwater is diverted to Myslavsky Creek as well as the rainwater from selected objects in the monitored area, the flow of the Myslavsky Creek is increasing, and therefore its flow capacity for the corresponding amount of rainwater discharged is not satisfactory.

Based on the changed outflows of the Myslavsky Creek, it is necessary to propose potential measures to stabilize the runoff in the catchment area of the Myslavsky brook, thus increasing the flood protection in the lowland areas. Measures may be environmental (removal of obstacles) as well as organizational (compliance with water management decisions, design of retention areas). Such potential measures can help in saving money and the life of people.

Acknowledgements: *This work has been suported by project SKHU/1601/4.1/187. This work was supported by project 1/0217/19 of Ministry of the Education in the Slovak Republic: Research of Hybrid Blue and Green Infrastructure as Active Elements of a 'Sponge City'.*

References

Blišťanová, M., Blišťan, P. (2014): The GIS tools in the process of flood threat evalution. In: SGEM 2014: 14th International Multidisciplinary Scientific GeoConference (SGEM): Conference Proceedings :Volume III: 17-26 June, 2014, Bulgaria. Sofia : STEF92 Technology, 2014 P. 957-963.

Blišťanová, M., Zeleňáková, M., Blišťan, P., Ferencz, V. (2016).Assessment of flood vulnerability in Bodva river basin, Slovakia, *Acta Montanistica Slovaca, 21(1), 19-28.*

Bronstert, A., Niehoff, D., & Bürger, G. (2002). Effects of climate and land-use change on storm runoff generation: present knowledge and modelling capabilities. *Hydrological processes, 16(2), 509-529.*

Campisano A, Catania FV, Modica C (2017) Evaluating the SWMM LID Editor rain barrel option for the estimation of retention potential of rainwater harvesting systems, *Urban Water Journal, 14:8, 876-881.*

Cipolla SS, Maglionico M, Stojkov I (2016) A long-term hydrological modelling of an extensive green roof by means of SWMM. *Ecological Engineering 95: 876-887.*

Diaconu, D. C., Andronache, I., Ahammer, H., Ciobotaru, A. M., Zelenakova, M., Dinescu, R., Pozdnyakov, A. V. & Chupikova, S. A. (2017). Fractal drainage model--a new approach to determinate the complexity of watershed. *Acta Montanistica Slovaca, 22(1).*

Diaconu, D.C., Peptenatu, D., Simion, A.G., Pintilii, R.D., Draghici, C.C., Teodorescu, C., Grecu, A., Gruia, A.K., Ilie, A.M. (2017). The Restrictions Imposed Upon the Urban Development by the Piezometric Level. Case Study: Otopeni-Tunari-Corbeanca. *Urbanism Architecture Constructions, 8(1), 27-36.*

Gironás, J., Roesner, L. A., Davis, J., Rossman, L. A., & Supply, W. (2009). Storm water management model applications manual. Cincinnati, OH: National Risk Management Research Laboratory, Office of Research and Development, US Environmental Protection Agency.

Kiss, I., Wessely, E., Blistanova, M. (2014) Contribution to Logistics of Catastrophes in Consequence of Floods. Conference: 24th DAAAM International Symposium on Intelligent Manufacturing and Automation Location: Univ Zadar, Zadar, CROATIA Date: OCT 23-26, 2013. 24TH DAAAM INTERNATIONAL SYMPOSIUM ON INTELLIGENT MANUFACTURING AND AUTOMATION, 2013 Book Series: *Procedia Engineering Volume: 69 Pages: 1475-1480, 2014*

Lewis A, Rossman M (2015) Storm Water Management Model User´s Manual Version 5.1. U.S. Environmental Protection Agency, Water Supply and Water Resources Division: Washington D.C., USA.

Mititelu-Ionuş, O., Licurici, M., (2018), Flood risk management profile. A case-study of structural measures and communication tools development. pp. 285-296. In Gastescu, P., Bretcan, P. (edit, 2018), Water resources and wetlands, 4th International Conference Water resources and wetlands, 5-9 September 2018, Tulcea (Romania), p.312

Nirupama N, Simonovic SP (2007) Increase of Flood Risk due to Urbanisation: A Canadian Example. *Natural Hazards 40(1): 25-41.*

Okkan, U., Gedik, N. (2018), Evaluation of population based evolutionary optimization algorithms in the Conceptual Hydrological Model Calibration. pp. 130-136. In Gastescu, P., Bretcan, P. (edit, 2018), Water resources and wetlands, 4th International Conference Water resources and wetlands, 5-9 September 2018, Tulcea (Romania), p.312

Ouyang, W., Guo, B., Hao, F., Huang, H., Li, J., & Gong, Y. (2012). Modeling urban storm rainfall runoff from diverse underlying surfaces and application for control design in Beijing. *Journal of environmental management, 113, 467-473.*

Palla A, Gnecco I (2015) Hydrologic modelling of Low Impact Development systems at the urban catchment scale. *Journal of Hydrology 528:361-368.*

Pfister L, Kwadijk J, Musy A, Bronstert A, Hoffmann L (2004) Climate change, land use change and runoff prediction in the Rhine–Meuse basins. *River Research and Applications 20(3): 229–241.*

Rodriguer-Rojas MI, Huertas-Fernández F, Moreno B, Martínez G, Grindlay AL (2018) A study of the application of permeable pavements as a sustainable technique for the mitigation of soil sealing in cities: A case study in the south of Spain, *Journal of Environmental Management. 205: 151-162.*

Sivakumar B, Berndtsson R, Olsson J, Jinno K, Kawamura A (2000) Dynamics of monthly rainfall-runoff process at the Gota basin: A search for chaos. Hydrology and Earth System Sciences 4(3): 407-417.

Šlezingr M, Fialová J (2012) An examination of proposals for bank stabilization: the case of the Brno water reservoir (Czech Republic). *Moravian Geographical Reports 20(2): 47–57.*

Stec A, Kordana S, Słyś D (2017) Analysing the financial efficiency of use of water and energy saving systems in single-family homes *Journal Of Cleaner Production 151: 193-205.*

Sterren M, Rahman A, Ryan G (2014) Modelling of a lot scale rainwater tank system in XP-SWMM: A case study in Western Sydney, Australia. *Journal of Environmental Management 141:177-189.*

Tavakol-Davani H, Goharian E, Hansen CH, Tavakol-Davani H, Apul D, Burian SJ (2016) How does climate change affect combined sewer overflow in a system benefiting from rainwater harvesting systems? *Sustainable Cities and Society 27:430-438.*

Vranayová Z, Karelová Z, Očipová D (2011) Precipitation Monitoring Methodology at the Campus of Technical University of Košice. In: Selected Scientific Papers. *Journal of Civil Engineering 6(2).*

Weng Q (2001) Modelling Urban Growth Effects on Surface Runoff with the Integration of Remote Sensing and GIS. *Environmental Management 28(6): 737–748.*

Wilby RL (2007) Review of Climate Change Impacts on the Built Environment. *Built Environment 33(1): 31–45.*

Zeleňáková M (2014) Influence Of Urbanization For Runoff Conditions. In. Conference on Public Recreation and Landscape Protection - with Man Hand in Hand? Book Series: Public *Recreation and Landscape Protection, p: 149-153.*

Zeleňáková, M., Dobos, E., Kováčová, L., Vágo, J., Abu-Hashim, M., Fijko, R., & Purcz, P. (2018). Flood vulnerability assessment of Bodva cross-border river basin. *Acta Montanistica Slovaca, 23(1).*

Zeleňáková M, Rejdovjanová G (2011) Facilities for the percolation of precipitation water in the area of the Technical University in Košice. In: SGEM 2011: 11th international: conference proceedings: Volume 1: 20-25 June, 2011, Bulgaria, Albena. Sofia: STEF92 Technology Ltd., 2011. p. 451-457.

Zeleňáková M, Rejdovjanová G, Zvijáková L (2011) The concept of rainwater managment in Košice City. In: Environmental Engineering: 8th International Conference: proceedings: selected papers: May 19-20, 2011, Vilnius, Lithuania. Vilnius: *GTU. p. 723-726.*

The procedure of choosing an optimal offer for a conical pick as an element of realizing the sustainable development concept in mining enterprises

Łukasz Bołoz[1] *and* ***Katarzyna Midor***[2]

The contemporary market requires something more from the manufacturer than merely a good quality product. What matters nowadays for the consumer and co-operator is the fulfillment of certain ethical standards by an enterprise, such as, for example, the ones proposed by the sustainable development concept. This is particularly important for companies in the mining branch, which are frequently classified as "3D" - dirty, dangerous and difficult. Sustainable development should be realized in three areas: social, environmental, and economical. In the article, the authors present an engineering solution involving an optimal choice of conical picks, which realizes the sustainable development concept in the economic and social context. This allows saving the financial resources of a mining enterprise while choosing a high-quality product, which improves the working conditions. The article contains a description of a comprehensive procedure for selecting the most favorable offer of a conical pick, taking the geometry, material, durability, and the price into consideration. The procedure optimizes the choice of a conical pick while taking into account the technical requirements as well as allowing the price share to be tailored according to the current needs and financial possibilities of the user, which has been illustrated with an example of a mining plant where the procedure has been used.

Keywords: *conical pick, mine, procedure, choice of an offer, sustainable development.*

Introduction

In today's world, the sustainable development of enterprises has attracted the interest of managers and investors all over the world. The financial success of a company is no longer the only measure of economic activity; now, it is also viewed through the prism of high ethical standards. Contemporary Europe, in particular, the European Union, has decided that its strategic goal by the year 2020 will among others be intelligent development, which allows investing in the economy based on knowledge and innovation, therefore, an activity that enables increasing effectiveness while realizing the sustainable development concept in the mining branch. Realization of sustainable development in an enterprise is based on activities in three areas: social, ecological, and economical. Each of these areas needs the use of several tools. In this article, the authors present a tool that enables the most optimal choice of an offer of a conical pick, which, in line with the sustainable development idea, allows saving the company's resources and their rational managing in the future.

Conical picks, known in Poland as tangential-rotary picks, are typical tools used in underground mining. Depending on the working conditions, their consumption ranges from a few to several dozen a day for one mining shearer, and the unit cost of a pick ranges from PLN 60 to PLN 200. The mine's costs resulting from the purchase of conical picks are estimated to reach several million PLN annually, which for underground mining means a total of several dozen million. The users want to use the best accessible picks, but the choice of the most favorable offer is complicated, as many factors determine the quality of a pick. First of all, an important thing is resistance to abrasive wear as well as geometric and material parameters. Picks offered for coal mines vary considerably in their price, which is often not adequate to durability. For this reason, a parametric methodology for evaluating conical picks, allowing for the choice of an optimal offer, has been developed and implemented in three Polish coal mines. The procedure utilizes the method of measurements and laboratory tests. The methodology also involves control tests, which allow verifying the delivered picks' quality, and, in consequence, enable maintaining a good quality of deliveries. Conical picks are also used to mine rocks (underground mines of ores and salt as well as open-pit mines), concrete and asphalt (road building and maintenance, building works), so the procedure in question has a significant application potential.

Sustainable development of enterprises

At the turn of the 20th and 21st century, the notion of sustainable development grew in popularity. The concept began to be defined in the 1960s, when so-called Club of Rome, established in 1968, published four reports:" Limits of Growth", "Mankind at the Turning Point", "Future in Our Hands" and "The Barefooted Revolution", which was a pioneer attempt to forecast many global phenomena and problems as well as a serious warning. In the report-manifest entitled "Limits of Growth", a team of researchers headed by Dennis Meadows questioned the previous view that the development of humankind was not limited by anything, and the

[1] *Łukasz Bołoz,* AGH University of Science and Technology, Department of Mining, Dressing and Transport Machines, A. Mickiewicza Av. 30, 30-059 Krakow, Poland, boloz@agh.edu.pl

[2] *Katarzyna Midor,* Silesian University of Technology, Faculty of Management and Organization, Institute of Production Engineering, Roosevelta 26, 44-800 Zabrze, Poland, katarzyna.midor@polsl.pl

advancement of science and technology would break the environmental barrier. Further research conducted by independent institutions in subsequent years confirmed the mutual relationships between demographic phenomena, production, and natural environment. All that influenced the way of thinking and undertaken activities. The increasing knowledge of highly developed countries about the consequences of a continuing economy based solely on economic growth contributed to the concept of sustainable development. Global events which played the most significant role in propagating the sustainable development idea include UN Conference in Stockholm in 1972, UN Conference "Environment and Development" in Rio de Janeiro in 1992 and UN Conference in Johannesburg in 2002. These conferences caused that highly developed countries, in particular, UE states, started undertaking several activities to protect the environment and change the model of economic development (Midor and Tarasiński, 2010).

Initially, the sustainable development concept referred mainly to the development of the world and civilization. However, since Agenda 21 was published during the conference in Rio de Janeiro in 1992, sustainable development has been applied to towns, communes, and other local units as well as enterprises. Agenda 21 defines sustainable development as social and economic development which aims to meet the needs of contemporary societies without affecting the possibility of satisfying the needs by future generations (Midor, 2014). Since the time of Agenda publication, there have been many proposals specifying the way such development might be effected in the activity of companies. Currently sustainable development of enterprises is associated with such concepts as: social responsibility of business (Hąbek, 2015), business ethics (Hąbek and Brodny, 2017), triple bottom line or management of relationships with stakeholders (Zasadzień and Midor, 2015), design for manufacturing (DFM) strategies help companies to develop new products that are feasible to manufacture (Jakubowski, 2014) and (Božek, 2014).

On mature markets, the question about business style is asked more and more frequently. This question began to determine the choice of a particular brand, product, or even an institution. As a result, the focus has changed from moralizing arguments and social criticism of enterprise behavior to searches for the most effective instruments of management (Midor and Tarasiński, 2012), (Brodny and Tutak, 2016), (Biały, 2014). The most important challenge for creating a new way of enterprise management, based on the sustainable development concept is to introduce an appropriate channel for obtaining information about and from the environment. Organizations which want to increase their profitability in the future should focus their activities on four entities simultaneously: shareholders, society, natural environment, and finances. Devoting too much attention to one of the entities mentioned above at the cost of the remaining ones may prevent companies from achieving long-term success. The best method for implementing this multi-direction strategy is sustainable development. It allows introducing innovative solutions, making proper distinctions, and achieving long-term success.

In Poland, the necessity of undertaking innovative activity should be aimed first of all at mining enterprises, as hard coal mining is still a strategic branch of Polish industry. In coal mining, Poland has a 10th position in the world and ranks 1st in the European Union. For Poland, coal is a guarantee of energy security and is currently the primary source of electric energy production (Midor and Biały, 2016), (Biały, 2014). As the mining industry is often classified as "3D" – dirty, dangerous and challenging due to the difficulties and constant changes in the realization of the sustainable development idea (Gunarathe et al., 2016), solutions that will bring coal mines closer to the sustainable development concept have to be searched for on many levels. In the article the authors present a solution for an optimal choice of conical picks, which effects the idea of sustainable development in the economic and social aspect, allowing the financial resources of a mining company to be saved while choosing a high-quality product, thus improving the working conditions.

Conical picks

The exploitation of longwalls and galleries in global underground mining is mainly mechanical. Mechanical mining involves direct using an extraction tool on rock mass. The most common is rock mining by milling with a cutter loader and planning with cutting tools (Bołoz and Krauze, 2018), (Bołoz, 2018), (Krauze and Bołoz, 2018), (Bołoz, Krauze and Kubin, 2018). Currently, the global standard is to use conical picks in the mining elements of heading machines and longwall cutter-loaders. Milling elements are crucial parts of mining machines, and the durability of picks is essential from the point of view of operational costs, the time of machine work and the energy efficiency of the process. Users' expectations, as well as increasingly hard conditions, cause that mining machines have to meet increasingly strict requirements regarding their efficiency, safety reliability, and staff comfort. Fulfilling these requirements largely depends on the proper selection of cutting tools with handles and a mining element. This selection results from the milling process theoretical framework and is known from the literature (Bołoz and Kruze, 2018), (Krauze, Bołoz and Wydro, 2015), (Bołoz and Midor, 2018), (Bołoz and Leonel, 2018).

During exploitation, the conical pick contacts the excavated rock mass. It is the pick that is directly responsible for the mining process. The shape and appropriate manner of fixing the pick in the handle allows its free turn, which results in the blade's uniform wear. Due to the working conditions and the specific character of

the mining machine, picks can differ in geometry (shape, size, manner of mounting), materials and the way of protecting the body against abrasive wear. It is therefore crucial that the selected picks meet the requirements which guarantee a proper milling process for a particular machine and working conditions.

The problem of conical picks' durability is the subject of many investigations carried out in research centers around the world. Due to the construction of the pick, durability research is conducted in a few variants. The standard conical pick, presented in Fig. 1, is built of an operational part in a conical shape, a cylindrical pin, which is the holding part, and a blade in the form of an insert made of sintered carbide.

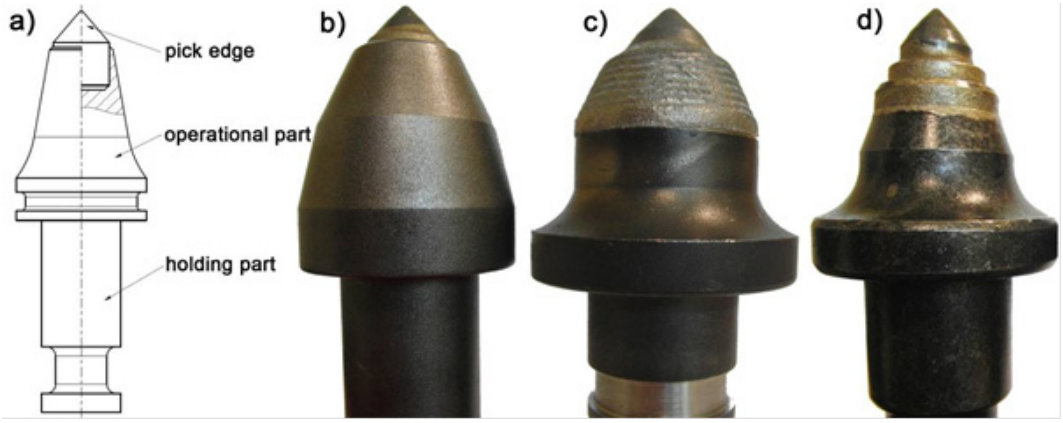

Fig. 1. Construction and example solutions for conical picks a. construction of pick, b. typical pick, c. pick with an abrasion-resistant coating,d. pick with a ring made of sintered carbide

The body can be additionally protected against abrasive wear with abrasion-resistant coatings, by weld surfacing or with rings made from sintered carbides (Krauze, Bołoz, Wydro and Mucha, 2017), (Chang et al., 2017). These investigations are aimed at finding a solution characterized by the highest abrasive resistance. Works are carried out to explore the mechanism of picks' abrasive wear (Dewangan et al., 2015), to predict the wear (Gajewski et al., 2013), or a possibility to support the mining process (Kotwica, 2011). Investigations are conducted for the material – sintered carbide (Nahak et al., 2015), (O'guigley et al., 1997), for a complete pick (Dewangan et al., 2015), (Songyong et al., 2017) or picks which form a mining element (Kotwica and Krauze, 2007). As a result, we obtain information about the mass loss in materials subjected to testing. Importantly, this research usually consists of searching for new solutions or are conducted for advertising purposes and are only marginally useful for picks users. The only way forward is the possibility of coating (Hornik, 2015).

Various producers can provide a particular selected pick. However, producers do not specify the quality or durability of picks in a way allowing their comparison before purchase.

A mining enterprise, which is obliged to follow the procedure of public tenders, use the prices as the only criterion when choosing an offer of picks. Therefore, bearing in mind the public procurement law that state-owned mining companies have to comply with, the testing of picks had to be developed in a way which would enable choosing the best offer while maintaining the lowest possible price. Therefore, the issue in question is essential from the point of view of sustainable development, as it allows saving the financial resources of an enterprise and improving the working conditions.

The methodology of the conducted investigations aimed at evaluating the quality of conical picks

Correct and extended operation of properly selected conical picks depends on the following elements:

- geometrical parameters of the whole pick and sintered carbide itself,
- material parameters of the body and blade,
- the hardness of the body and blade,
- the hardness of the pick.

The durability of picks is the most critical element of their quality description, but in practice checking the geometric and material parameters of the body and insert is also recommended and applied (Krauze, Bołoz and Wydro, 2015).

Determining the quality of picks requires measuring the above elements in a way that enables a comparison of their quality so that an optimal solution can be chosen. Moreover, the user must have the possibility of controlling the quality of picks provided by the producer.

Bearing the above in mind, investigations in three stages have been proposed (Krauze, Bołoz and Wydro, 2015) :

- measurement of conical picks' geometrical picks,

- testing of conical picks' material parameters,
- testing of conical picks' wear rate.

Measurement of geometric parameters

The testing of a conical pick is aimed at determining its selected linear and angular dimensions. The obtained results should be compared with the user's requirements and the producer's documentation. The pick must comply with both requirements.

Major linear and angular dimensions of the conical pick are (Fig. 2a):

- operational part length L_n,
- total length L_c,
- the diameter of diameters of the holding part d_u
- of the stopper ring collar d_k,
- the angle of the insert blade $2\beta_u$,
- height of sintered carbide insert h_w,
- the diameter of sintered carbide insert d_w,
- marking on the holding part z /d_w/$2\beta_u$ /L_n, where z is the producer's trademark

Measurement of shaped parts can be efficiently performed by 3D reverse engineering methods (Buransky and Peterka, 2013). Linear measurements were taken with an Insize altimeter (max. error ±30 μm), the angle measurement was taken with a Mitutoyo Digimatic protractor (max. error ±2'). The tests were conducted on a special measuring stand (Fig. 2b).

Material parameters testing

Determining the quality and properties of materials that the conical pick is made of requires separating the steel body from the blade, which is made of sintered carbide. Tests were carried out for the pick body material to determine the chemical composition of steel, the hardness of the holding and operational part as well as thermal treatment of the sintered carbide insert to determine the composition, density and hardness (Fig. 3).

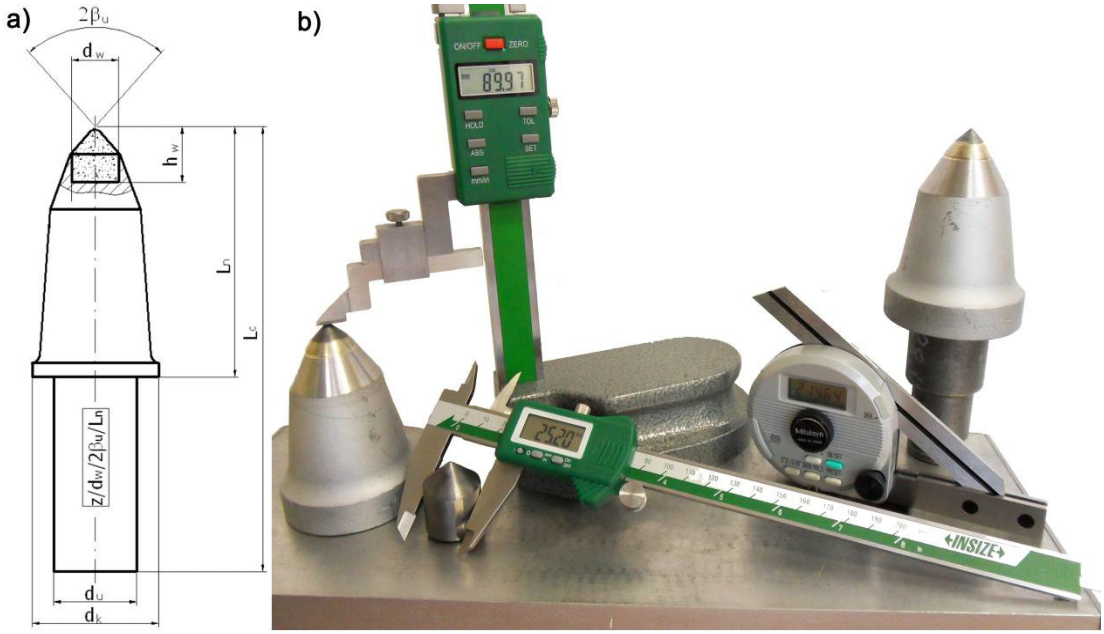

Fig. 2. Measurement of the pick's geometric values:
a. pick parameters subjected to measurement, b. measuring stand with measuring equipment

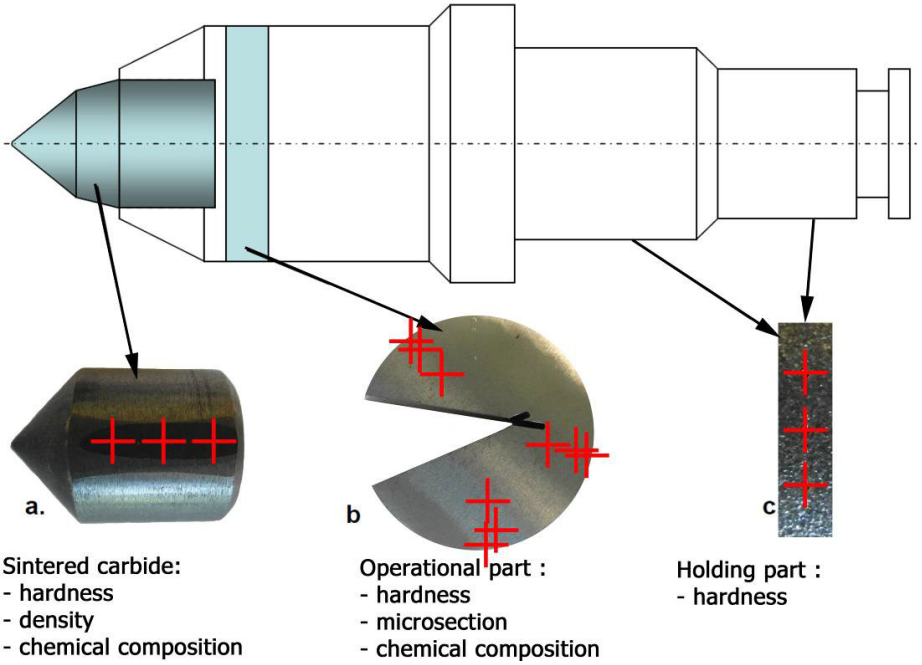

Fig. 3. Measurement of the pick's geometric values: a. pick parameters subjected to measurement, b. measuring stand with measuring equipment

The chemical composition of the pick body material was conducted by the spark testing method, with a Foundry Master device, whereas the hardness measurement was taken by the Rockwell method – it is carried out on a sample taken from the area near the insert in accordance with Polish standards. The composition, density and hardness of sintered carbide were proposed to be determined by the Vickers method in line with Polish standards.

Wear rate tests

In industrial conditions the hardness of cutting picks is usually determined as a ratio of the number of replaced (used) picks to the amount of material mined. Therefore, determining the hardness of picks required developing a plan and methodology of research, enabling determining their wear rate. A wear rate measurement must always be performed in the same controlled conditions so that the results can be reproducible and comparable. Such an approach allows indirectly determining the picks' durability, using a number index, and enables producers to compare various solutions and choose the best ones.

The methodology of conical picks' wear rate involves milling a rock sample with four picks of the same kind. To determine the wear rate, it is necessary to determine a mass loss of the examined picks as well as the volume of a sample mined by them. After testing the index characterizing, their wear rate can be calculated. The picks' wear rate, which describes durability, should be determined to utilize the following formula (Krauze, Bołoz and Wydro, 2015):

$$X1 = \frac{\Delta m}{m} \cdot \frac{V_w}{V_u}, \ [-] \tag{1}$$

where:

$X1$ – wear rate [-],
Δm - pick's mass loss during testing (body with the blade) [g],
m - pick's mass before test [g],
V_W – standard/reference volume of sample [m^3],
V_u – volume of sample mined by picks during testing [m^3].

Testing of all types of picks is performed in accordance with the prescribed methodology and research plan. Laboratory tests have to be carried out on a special stand (Fig. 4). Conical pick tests presented in the further part of the chapter were performed on a laboratory stand for testing the mining process by milling or rotary drilling with single cutting tools or elements, the description and possibilities of which have been quoted in literature (Krauze, Bołoz and Wydro, 2015), (Bołoz, 2018).

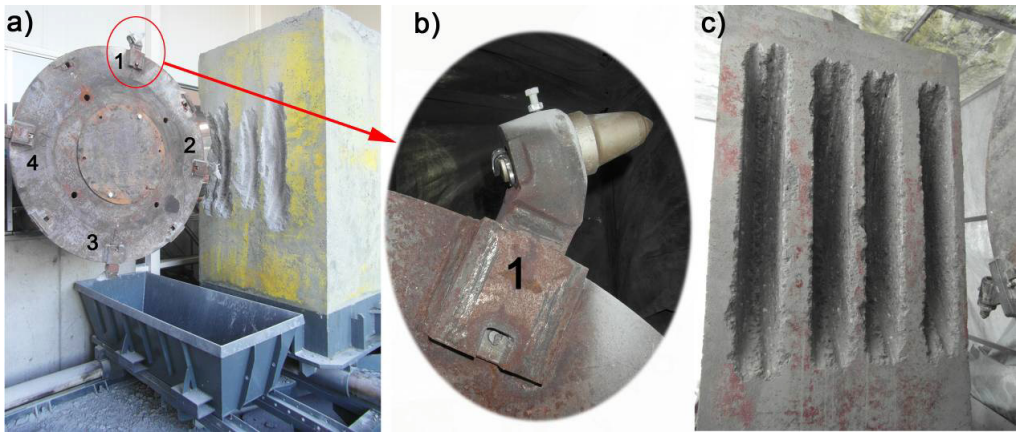

Fig. 4. Wear rate laboratory tests. a. stand with a testing disc, b. pick number 1 mounted on the disc, c. mined sample

Choosing an optimal offer of the conical pick

From the point of view of the user looking for the best pick characterized by good value for money, clear criteria which allow making an optimal choice are essential. When searching for the best offer, one should use multi-criteria optimization. An evaluation of the picks' quality must take into account two essential criteria – price and durability. The choice is made difficult by the mutual influence of criteria. i.e., the occurrence of Pareto optimality. Despite a lack of unambiguous correlation, in general, increasing the durability of picks involves the necessity of using more sophisticated technical means, which translates into an increased price. The weighed criteria method, which is a typical multi-criteria optimization method, was applied so that the user could decide about the influence of price and durability on the choice. Therefore, the procedure enables establishing the influence of the share of price criterion and durability criterion in the offer price. Knowing the pick's price K [PLN] and the determined wear rate $X1$ [-], the number of points P [-] is calculated according to formula 4.2. This formula provides the number of points P depending on the adopted weight W [-] of pick's quality within the range $W = 0 \div 100$. In practice, the quality criterion weight is in the range $W = 35 \div 70$. In the case of low-quality weight (for example, $W < 20$) there is a risk of choosing a pick characterized by a low price and, at the same time, low quality. In the case of high values (for example, $W > 80$), there is a risk of choosing the most expensive offer, in which the pick's durability can be slightly higher than in a much cheaper offer. Weight W can also be established by determining the maximum acceptable price of a single pick.

In results, a number value P, not higher than 100, is obtained. The higher the P-value, the more favorable the offer is.

$$P = \frac{\min\left(X1_n\right)}{X1_n} \cdot W + \frac{\min\left(K_n\right)}{K_n} \cdot \left(100 - W\right), \ [-] \tag{2}$$

where:
P – number of points awarded to a particular offer, $P \leq 100$ [-],
n – number of the subsequent offer [-],
W – quality weight in the final evaluation of the pick , $W = 0 \div 100$ [-],
$X1$ – wear rate of picks [-],
K – pick unit cost [PLN],
$X1_n$, K_n – index $X1$ and price K for offer i ,
$\min(X1_n)$, $\min(K_n)$ – minimum values of $X1$ and K among all the analyzed offers.

How to maintain a good quality of conical picks?

The proposed research methodology allows choosing picks of the best quality, but it is necessary to control deliveries to maintain the assumed quality. In the event, the user reports reservations regarding the quality of the picks, control testing is carried out. The control involves doing geometric and material tests of the picks delivered for checking. The results of tests can be quantitatively compared with the results of standard picks. To check the wear rate, comparative testing of the controlled and standard picks on the same rock sample must be conducted. Only then can one unequivocally determine whether the wear rate has changed.

This factor is comparable for various coal beds, and the bigger value it has, the more difficult is the bed mining capacity. In order to determine coal compactness (compact/weakly-cohesive), in parallel with the measurement of the mining capacity factor, the angle of side crushing is determined.

Example of applying the procedure of an optimal offer choice

The presented procedure was implemented in three Polish coal mining companies. The tendering procedure was applied for a total of ten underground mines. Each tender consisted of many tasks, and each task concerned one type of pick. The said procedure was used in four tenders:

- tender 1 – 5 mines, 9 types of picks, a total of 240 500 pcs, delivery time 2 years,
- tender 2 – 6 mines, 14 types of picks, a total of 371 640 pcs, delivery time 2 years,
- tender 3 – 2 mines, 12 types of picks, a total of 47 210 pcs, delivery time 1 year,
- tender 4 – 4 mines, 6 types of picks, a total of 66 677 pcs, delivery time 1 year.

Assuming the average value of a pick as PLN 110, we obtain big amounts (PLN 26.5 million, PLN 40.9 million, PLN 5.2 million, PLN 7.3 million, respectively). Due to their quantity, a minimal advantage in the price or durability of picks translates into considerable savings in the scale of the whole mine or company. In particular tenders, the ordering parties established a different weight W of the quality criterion. Subsequently, they used values W = {70, 40, 35, 40}.

In practice, each of the bidders in the tender for deliveries of picks of one particular type provided a representative sample consisting of 22 pcs of the product. In accordance with the procedure, 3 picks were sent for geometric tests, another 3 for material tests and 4 for wear rate tests. The remaining 12 picks were standards for quality control. In case of a complaint, the mine delivered 10 picks, which were checked for geometric parameters (4 pcs) by comparing them with standard picks (4 picks). Based on the test results, conclusions were formulated to confirm or reject the mine's claims. The complaint procedure was applied only eight times, which proves the fact that producers maintain the quality of picks.

Below have been presented the results of tests for one selected task, in which 5 producers, marked P1 to P5 respectively, took part. The subject or research was a pick for heading machine z/25/90/70 having the following dimensions (markings according to Fig. 2a):

- L_n,= 70 mm, admissible value range: 69.0 mm ÷ 71.0 mm,
- L_c, = 147 mm, admissible value range: 146.0 mm ÷ 148.0 mm,
- d_u = 38 mm, admissible value range: 37.8 mm ÷ 38.0 mm,
- d_k = 58 mm, admissible value range: 57.0 mm ÷ 59.0 mm,
- $2\beta_u$= 93°, admissible value range: 92.0° ÷ 93.0°,,
- h_w= 35 mm, admissible value range: 34 mm ÷ 36 mm,
- d_w = 25 mm, admissible value range: 24.5 mm ÷ 25.5 mm,

As a result of the conducted geometric parameters tests, check charts for 3 picks for each producer were obtained. The results for the first pick manufactured by each of the producers have been given in Table 1. Despite a wide tolerance field, the required dimensions were not fulfilled by all the producers (item 5). As a result, producer P5 was rejected; the remaining offered picks complied with the requirements. Values given in red font mean failure to meet the user's requirements or the manufacturer's declaration.

Tab. 1. Results of geometric parameters' measurements

No.	Pick No.	Geometrical parameters of the pick								
		L_c [mm]	L_n [mm]	L_u [mm]	h_k [mm]	$2\beta_u$ [°]	d_k [mm]	d_u [mm]	d_w [mm]	h_w [mm]
1.	P1/1	147.12	70.11	77.01	15.98	92.87	58.16	38.00	24.85	35.08
2.	P2/1	146.73	69.76	76.97	15.54	93.00	58.07	37.98	25.00	35.06
3.	P3/1	146.66	69.62	77.04	16.22	93.00	57.88	38.00	24.75	35.11
4.	P4/1	146.95	69.98	76.97	16.22	93.00	58.09	37.95	25.48	34.89
5.	P5/1	148.31	71.40	76.91	16.20	93.68	58.04	37.97	24.96	34.55

Metallographic tests consist of many elements. The results of tests for the pick produced by each manufacturer have been presented in example tables. The hardness of the body operational part is quoted in Tab.

2, the hardness of the body holding part – in Tab. 3, the chemical composition of the body steel – in Tab. 4, sintered carbide hardness – in Tab. 5, density and chemical composition of sintered carbide – in Tab. 6.

Tab. 2. Results of HRC hardness tests for the pick operational part

No.	Pick No.	HRC 1mm	HRC 3 mm	HRC 10 mm	Requirements
1.	P1/1	53	53	52	≥ 45
2.	P2/1	51	53	52	
3.	P3/1	54	55	53	
4.	P4/1	52	52	52	
5.	P5/1	35	41	40	

Tab. 3. Results of HRC hardness of the pick holding part (for 3 picks)

No.	Pick No.	pick 1	pick 2	pick 3	Requirements
1.	P1	32	31	33	25 ÷ 35
2.	P2	32	32	34	
3.	P3	35	37	34	
4.	P4	33	36	34	
5.	P5	48	47	47	

Tab. 4. Results of chemical composition analysis for the body material

No.	Pick No.	C %	Mn %	Si %	S %	P %	Cr %	Ni %	Mo %	V %	Grade
1.	P1	0.336	0.899	1.18	0.009	0.009	1.13	0.077	0.005	0.002	35HGS
2.	P2	0.326	0.901	1.33	0.021	0.009	1.10	0.08	0.016	0.002	35HGS
3.	P3	0.372	0.667	0.294	0.020	0.012	0.98	0.227	0.140	0.010	42CrMo4
4.	P4	0.343	0.840	1.24	0.006	0.010	1.12	0.056	0.008	0.002	35HGS
5.	P5	0.444	0.719	0.272	0.006	0.005	1.14	0.128	0.170	0.007	42CrMo4

Tab. 5. Results of sintered carbide HV30 hardness (for 3 picks)

No.	Pick No.	pick 1	pick 1	pick 1	Requirements
1.	P1	1171	1160	1156	≥ 1050
2.	P2	1141	1129	1136	
3.	P3	1306	1294	1274	
4.	P4	1163	1153	1176	
5.	P5	1148	1158	1151	

Tab. 6. Results of sintered carbide density and composition analysis

No.	Pick No.	Density g/cm^3	Co %	W %	Grade
1.	P1	14.634	7.9	92.1	B2
2.	P2	14.549	9.6	90.4	B23
3.	P3	14.665	7.5	92.5	B2
4.	P4	14.560	9.4	90.6	B23
5.	P5	14.423	10.8	89.2	B40

The last element of testing was determining the wear rate. Tests for all the picks were conducted on a sand-cement sample with basalt aggregate characterized by the grain size 2 mm ÷ 8 mm, resistance to single-axis compression R_c = 11.49 MPa and density ρ = 2.095 kg/m^3. The results of tests were juxtaposed – selected picks produced by all the manufacturers after testing have been presented in Fig. 5.
The lower the value of the calculated *XI* index, the better the durability of the pick. In the presented table the best pick is P2, whereas the least durable one is P5. Selected picks of all the producers after testing have been presented in Fig. 4.

Tab. 7. Results of pick wear rate tests (average value for 4 picks)

No.	Producer	Mass before g	Mass after g	Loss G	Volume mined m^3	Index X1 -
1.	P1	157.,30	1568.66	8.64	0.0260	1.055
2.	P2	1579.24	1572.63	6.61	0.0261	0.801
3.	P3	1581.78	1574.04	7.74	0.0267	0.916
4.	P4	1590.69	1583.59	7.10	0.0245	0.910
5.	P5	1497.03	1488.81	8.22	0.0255	1.076

The values of index *XI*, after taking the picks' price into account, allow choosing an optimal offer. The results of geometric and material parameters measurements enable excluding the offers which do not fulfill the requirements. Table 8 contains the results of score evaluation *P* of the offers, taking into account the producers' average prices and various levels of weight *W*. the influence of weight *W* on offer evaluation is clearly visible, hence, its value should be determined with caution. The optimal values for a given level of significance of quality have been marked in green. It is worth noting that there are disproportions in prices and durability; the durability of picks P3 and P4 is similar despite a considerable difference in the price. Determining weight *W* at the stage of issuing a call for tenders allows an objective, unambiguous, and indisputable choice of an optimal offer.

Tab. 8. The juxtaposition of an optimal choice results for three values of weight W

No.	Producer	X1 -	price PLN	P - W = 90	P - W = 70	P - W = 40	P - W = 35	P - W = 10
1.	P1	1.055	90	77.78	81.48	87.04	87.96	92.59
2.	P2	0.801	100	**98.50**	**95.50**	**91.00**	90.25	86.50
3.	P3	0.916	160	84.01	77.15	66.85	65.14	56.56
4.	P4	0.910	130	85.76	81.23	74.44	73.31	67.65
5.	P5	1.076	85	77.00	82.11	89.78	**91.05**	**97.44**

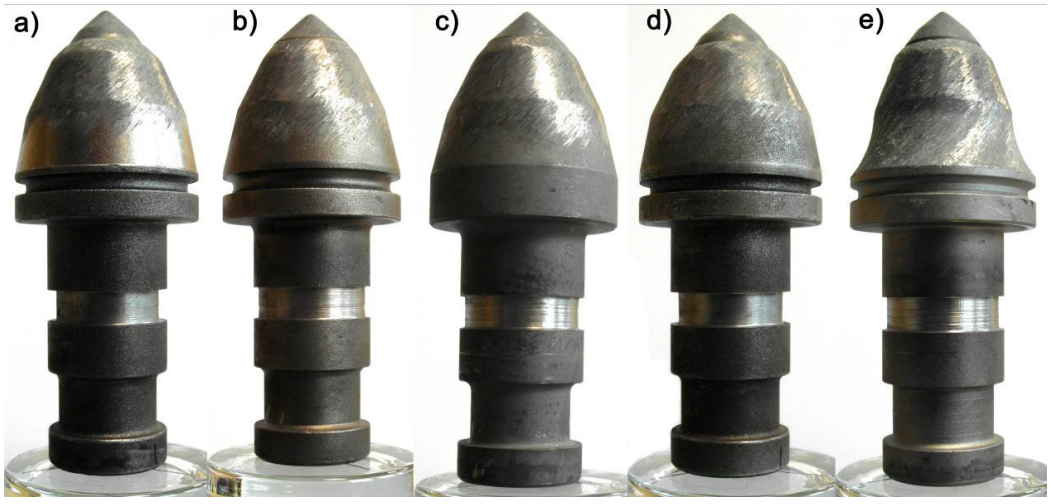

Fig. 5. Conical picks number 1 after tests (number according to Fig. 3) a. P1, b. P2, c. P3, d. P4, e. P5

Conclusions

Contemporary enterprises in the mining branch are facing the necessity of improving their image in society. They can do this by implementing the idea of sustainable development, which is based on ethical behavior. In the issue presented in this article, the ethical behavior consists in applying an engineering solution aimed at eliminating waste in an enterprise as well as improving the working conditions by using a high-quality product.

The correct operation of conical picks guarantees high durability of tools and milling elements as well as the low energy efficiency of the process, low level of dust and sparking. Achieving such a result depends on a proper selection of kinematic and geometric parameters of the element with the whole mining machine as well as geometric and material parameters of picks with handles. To achieve the set goal, it is necessary to ensure compliance of the above-mentioned parameters with the ones assumed at the stage of design, i.e., the highest possible quality and durability of the product must be achieved. Technically, the producer has no possibility to specify the durability of his product in a way enabling a comparison of offers. Therefore, an appropriate research methodology for the needs of Polish mining companies has been developed. Based on a three-stage analysis of research results, it is possible to choose an optimal offer while taking the price into account. However, it should be noted that despite the significance of the research in question, in the future testing should also include the milling elements and pick handles to maintain the highest possible durability of machine operational parts.

Acknowledgements*: Bołoz Ł. - Work financed from the Dean's Grant at the Faculty of Mechanical Engineering and Robotics at AGH University of Science and Technology in 2019.*

References

Biały, W. (2014). Coal cutting force measurement systems - (CCFM). 14th SGEM GeoConference on Science and Technologies In Geology. Exploration and Mining. SGEM2014 Conference Proceedings, Vol. III, pp. 91-98.

Biały, W. (2015). Innovative solutions applied in tools for determining coal mechanical properties. *Management Systems in Production Engineering, 4(20), pp. 202-209.*

Bołoz, Ł. and Krauze, K. (2018). Ability to mill rocks in open-pit mining. In: 18th International Multidisciplinary Scientific GeoConference SGEM 2018. SGEM2018 Conference Proceedings, 18(1.3), pp. 41-48.

Bołoz, Ł., Krauze, K. and Kubin, T. (2018). Mechanisation of longwall extraction of hard and abrasive rocks. Multidisciplinary Aspects of Production Engineering. MAPE.

Bołoz, Ł., Leonel, F. and Castañeda, (2018). Computer-aided support for the rapid creation of parametric models of milling units for longwall shearers. *Management Systems in Production Engineering, 4/2018.*

Boloz, £. and Midor, K. (2018). Process innovations in mining industry and effects of their implementation presented on example of longwall milling heads. *Acta Montanistica Slovaca, 3/2018.*

Bołoz, Ł. (2018). Model tests of longwall shearer with string feed system. *Archives of Mining Sciences, 63(1), pp. 61-74.*

Bołoz, Ł. (2018). Results of a study on the quality of conical picks for public procurement purposes, Ochrona człowieka w miejscu pracy. Obsługiwanie maszyn i urządzeń. Zintegrowane systemy zarządzania: jakość-środowisko-bezpieczeństwo-technologia.

Božek, P. and Pokorný, P. (2014). Analysis and evaluation of differences dimensional products of production system. *Applied Mechanics and Materials. Vol. 611, pp. 339-345.*

Brodny, J. and Tutak, M. (2016). Determination of the zone endangered by methane explosion In goaf with caving of longwalls ventilated on „Y" system. Management Systems in Production Engineering, 4(24), pp. 247-251.

Buransky, I., Morovic, L. and Peterka, J. (2013). Application of Reverse Engineering for Redesigning and Manufacturing of a Printer Spare part. In: *Advanced Materials Research. Vol 690-693.*

Chang, S., Lee, Chulho and Kang. (2017). Tae-HoEffect of hardfacing on wear reduction of pick cutters under mixed rock conditions*. Geomechanics and engineering, 13(1), pp 141-159.*

Dewangan, Saurabh, Chattopadhyaya, and Somnath. (2015). Critical Analysis of Wear Mechanisms in Cemented Carbide. Jorunal of materials engineering and performance, 24(7), pp. 2628-2636.

Dewangan, S., Chattopadhyaya, S. and Hloch, S. (2015). Wear Assessment of Conical Pick used in Coal Cutting Operation. Rock mechanics and rock engineering, 48(5), pp. 2129-2139.

Gajewski, J., Jedlinski, L. and Jonak J. (2013). Classification of wear level of mining tools with the use of fuzzy neural Network. *Tunnelling and underground space technology, 35, pp. 30-36.*

Gunarathne, N., Gunarathne, N., Samudrage, D., Samudrage, D., Wijesinghe, D.N., Wijesinghe, D.N. and Lee, K.H., (2016). Fostering social sustainability management through safety controls and accounting: A stakeholder approach in the mining sector. *Accounting Research Journal, 29(2), pp.179-197.*

Hąbek, P. (2014). Evaluation of sustainability reporting practices in Poland. Quality & Quantity, 48 (3), pp.1739–1752.

Hąbek, P. and Brodny J. (2017). Corporate Social Responsibility Report – An Important Tool to Communicate with Stakeholders. Proceedings of "4th International Multidisciplinary Scientific Conference on Social Sciences & Arts SGEM 2017. *Business and Management", pp. 241-248.*

Hornik, J., Krum, S., Tondl, D., Puchnin, M., Sachr, P., and Cvrcek, L. (2015). Multilayer coatings ti/tin, cr/crn and w/wn deposited by magnetron sputtering for improvement of adhesion to base materials. In *Acta Polytechnica. Vol 55, Issue 6, pp.388-392.*

Jakubowski, J and Peterka, J. (2014). Design for manufactrurin in virtual environment using knowledge engineering. In *Management and Production Engineering Rewiew. Vol 5, Numb 1, pp. 3-10.*

Kotwica, K. (2011). The influence of water assistance on the character and degree of wear of cutting tools applied in roadheaders. *Archives of Mining Sciences, 5(3), pp. 353-374.*

Krauze, K. and Bołoz, Ł. (2018). Disc unit dedicated to mine abrasive rocks and in particular copper ores. In: 18th International Multidisciplinary Scientific GeoConference SGEM2018, 18(1.3), pp. 311-318.

Krauze, K., Bołoz, Ł. and Wydro T. (2015). Parametric factors for the tangential – rotary picks quality assessment. *Archives of Mining Sciences, 60(1).*

Krauze, K., Bołoz, Ł., Wydro, T. and Mucha, K. (2017). Durability testing of tangential-rotary picks made of different materials. *Mining – Informatics, Automation and Electrical Engineering, 1/2017.*

Krauze, K. and Kotwica, K. (2007). Selection and underground tests of the rotary tangential cutting picks used in cutting heads of the longwall and roadway miners. *Archives of mining science, 52(2), pp. 195-217.*

Midor, K. (2014). Innovations in the field of enterprise quality management as an element of sustainable development implementation. In: GeoConference on Ecology, Economics, Education and Legislation. 14th International Multidisciplinary Scientific GeoConference SGEM2014, 3, pp. 215-222.

Midor, K. and Biały, W. (2016). Wyzwania stojące przed górnictwem węgla kamiennego. In: Mechanizacja, automatyzacja i robotyzacja w górnictwie. T. 1, Wybrane problemy górnictwa podziemnego. Red. Krzysztof Kotwica. Lędziny : Centrum Badań i Dozoru Górnictwa Podziemnego, pp. 164-170.

Midor, K. and Tarasiński, L. (2012). Sustained development in economy as a direction of enterprise development w Innovations in management and production engineering. Monografia. Red. R. Knosala. Oficyna Wydawnicza Polskiego Towarzystwa Zarządzania Produkcją, Opole, pp 175-183.

Midor, K. and Tarasiński, L. (2010). Zrównoważone oddziaływanie przedsiębiorstw na środowisko. *Ekonomika i Organizacja Przedsiębiorstwa, 4, pp. 74.*

Nahak, S., Dewangan, S. and Chattopadhyaya, S. (2015). Discussion on Wear Phenomena in Cemented Carbide, Conference. Global Challenges, Policy Framework & Sustainable Development for Mining of Mineral and Fossil Energy Resources (GCPF). *Procedia Earth and Planetary Science, 11, pp. 284-293.*

O'quigley, D.G.F., Luyckx, S. and James, M.N. (1997). An empirical ranking of a wide range of WC–Co grades in terms of their abrasion resistance measured by the ASTM standard B 611-85 test. Int J. Refract. Met. Hard Mater, 15, pp. 73-79.

Peterka, J., Morovic, L., Pokorny, P., Kováč, M. and Hornák, F. (2013). Optical 3D scaning of cutting tools. *Applied Mechanics and Materials 421, pp. 663-667.*

Prokopenko, S., Vorobiev, A., Andreeva; L. and Janocko J. (2018). Waste Cutters Utilization in Underground Coal Mining. *Acta Montanistica Slovaca, 1/2018.*

Songyong, L., Huifu, J. and Xiaohui, L. (2017). Experimental research on wear of conical pick interacting with coal-rock. *Engineering failure analysis, 74, pp. 172-187.*

Zasadzień, M. and Midor, K. (2015). Innovative application of quality management tools in a hard coal mine. In: 15th International Multidisciplinary Scientific GeoConference SGEM 2015. Science and technologies in geology, exploration and mining. Vol. 3, Exploration and mining, applied and environmental geophysics. Sofia : STEF92 Technology, 415-421.

Impacts of noise and technical seismicity from blasting works during tunnel construction on the surrounding environment

Ján Fehér[1], Jozef Čambál[1], Martin Cvoliga[2], Ladislav Kačmár[3], Vladimír Sulovec[4], Martin Šuver[4] *and* ***Ján Beca[4]***

The paper is focused on the measurement of adverse effects caused by blasting works in tunnels on the environment. The disintegration of the rock massif during tunnel construction is performed in most cases by explosions due to the release of the explosion energy, which is transformed into the energy of the seismic waves and causes disruption of the massif balance. Blasting works generate noise and seismic waves with different maximum vibration velocities and a wide range of frequencies. The intensity of the seismic waves is proportional to the massif of the explosives used. If the vibration has sufficient energy, the surrounding buildings may be damaged or destroyed. Assessing the negative effects of blasting and quantifying seismic security is currently a very challenging issue. However, based on periodic measurements, prediction of these effects is possible. The paper presents the results of monitoring of blasting works in tunnels in the Slovak Republic. The evaluation of noise and seismic effects of blasting works verified that in tunnels is a methodological basis for noise and seismic effects of blasting works not only on surrounding buildings but also on the surrounding environment.

Keywords*: tunnel, blasting works, technical seismicity, noise*

Introduction

Tunnel excavation affects the surrounding environment (Mishra and Mallick, 2012). Adverse effects include mainly noise and seismic effects (Jonson, 2012). The systematic measurement of noise and seismic effects in blasting operations is an essential part of determining the adverse effects on the environment (Fei et al., 2018). Based on the measured values, we are able, if necessary, to operatively carry out measures to optimize the performance of blasting operations (Mihalik and Pandula, 2008; Pandula and Kondela, 2010; Kalab et al., 2013). Based on the research activities, noise measurement and technical seismicity measurements were carried out in the construction of the tunnel, in the implementation of tunnel blasting (Murayama et al., 2014). Measurements were made in the residential area near the tunnel based on residents' complaints. The importance of the measurements has resulted from the need to detect adverse effects on the environment (Müncner, 2011; Kondela and Pandula, 2012; Lesso et al., 2013; Shin at al., 2018; Blistan, 2007; Kalab, 2018; Kalab and Štemon, 2017). Noise and seismic instruments were calibrated and sensitized prior to measurement (Nistov et al., 2012). The graphs of the individual components of seismic waves (França et al., 2011) were recorded in the measurement positions. Seismic apparatuses have been placed on the measuring positions to assess the impact of the seized technical seismicity on the objects under assessment (Pandula et al., 2012).

Measuring position and apparatus used for measurement

The measuring position or noise measurement was carried out about 200 m from the blasting works, which were carried out in the tunnel of residential buildings. A special instrument from SVANTEK - SVAN 958A was used to measure noise. SVAN 958A Class 1 Four-Channel Sound and Vibration Analyzer is designed for all applications requiring simultaneous Class 1 audio and vibration assessment. Each of the four input channels can be independently configured to detect sound or vibration with different filters and RMS detector time constants that give users great flexibility in measurement. The real advantage of the SVAN 958A is the ability to perform advanced analysis simultaneously with a level meter. In practice, this allows the user to obtain broadband results, such as L_{eq}, RMS, L_{Max}, L_{Min}, L_{Peak}, along with a four-channel analysis such as FFT or octave band analysis (Raisian et al., 2016).

[1] *Ján Fehér, Jozef Čambál,* Faculty of Mining, Ecology, Process Control and Geotechnologies, Technical University of Kosice, Department of Montaneous Sciences, Letná 9, 042 00 Košice, Slovak Republic, jan.feher@tuke.sk, jozef.cambal@tuke.sk
[2] *Martin Cvoliga,* NDS a.s., Dúbravská cesta 14, 841 04 Bratislava, Slovak Republic, martin.cvoliga@ndsas.sk
[3] *Ladislav Kačmár,* TUBAU, a.s., Pribylinská 12, 831 04 Bratislava, Slovak Republic, kacmar@tubau.sk
[4] *Vladimír Sulovec, Ján Beca,* EUROVIA - Kameňolomy, s.r.o. Osloboditeľov 66, 040 17 Košice, Slovak Republic, vladimir.sulovec@eurovia.sk, martin.suver@eurovia.sk, jan.beca@eurovia.sk

Fig. 1. Device SVAN 958A (Fehér et al., 2019)

Measured value

From the outputs of the special SVAN 958A instrument in case of noise measurement of blasting operations, it is necessary to use the permissible values of the maximum sound level A in the monitored time interval using the time weight function F. Value LAF_{max} (dB).

Time 16:28:24, LAF_{max} 66.7 dB

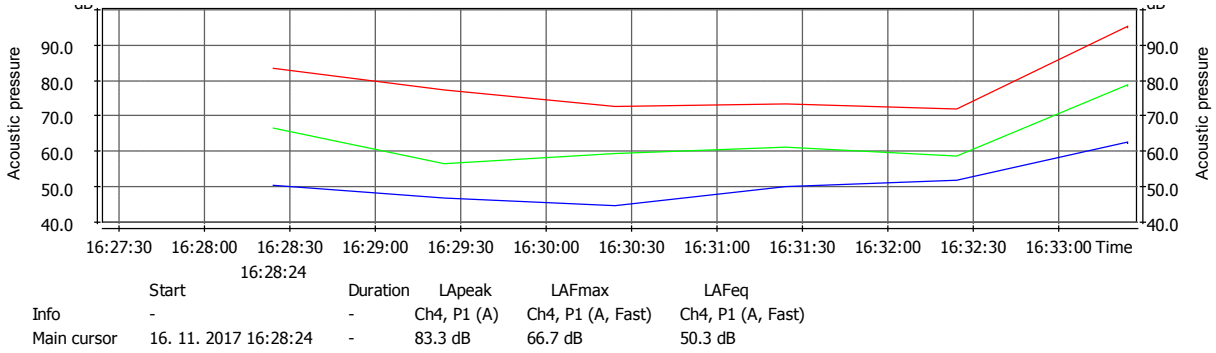

Fig. 2. Measured value, time 16:28:24 (Fehér et al., 2019)

Time 16:29:24 LAF_{max} 56.6 dB

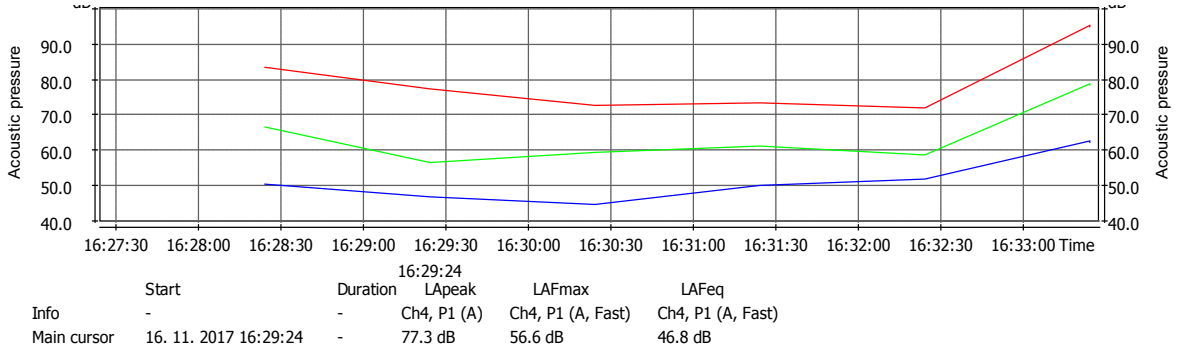

Fig. 3. Measured value, time 16:29:24 (Fehér et al., 2019)

Time 16:30:24 LAF_{max} 59.4 dB

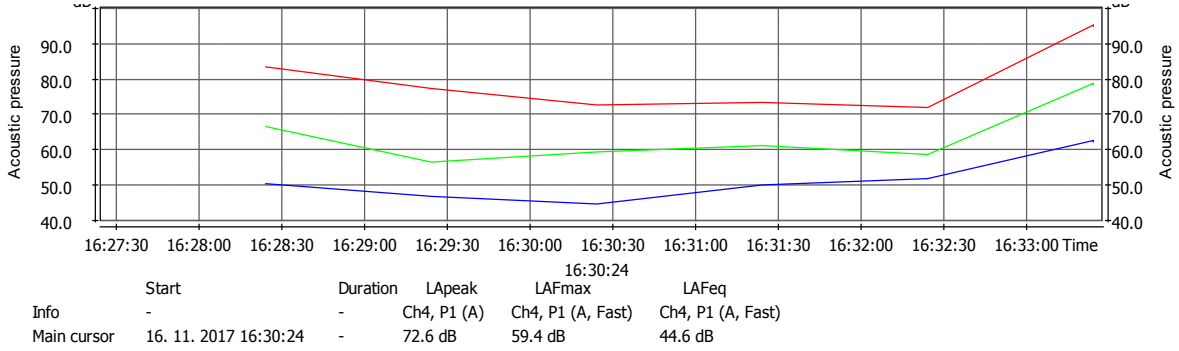

Fig. 4. Measured value, time 16:30:24 (Fehér et al., 2019)

Time 16:31:24 LAF_{max} 61.1 dB

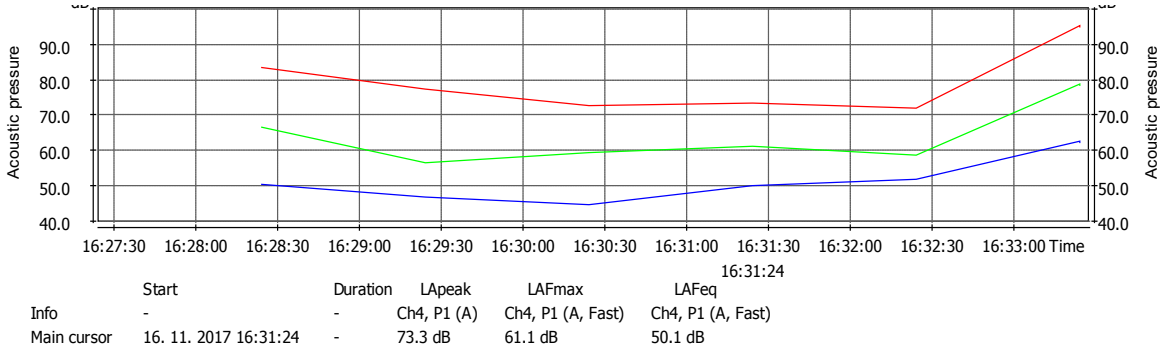

Fig. 5. Measured value, time 16:31:24 (Fehér et al., 2019)

Time 16:32:24 LAFmax 58.8 dB

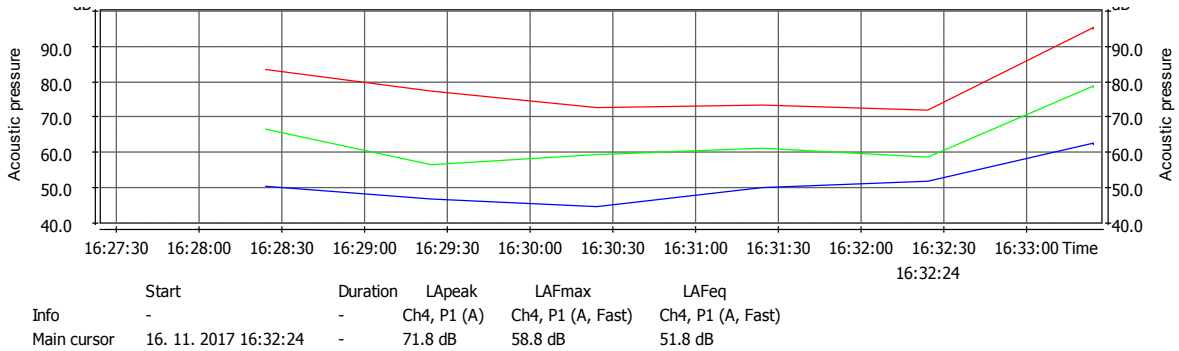

Fig. 6. Measured value, time 16:32:24 (Fehér et al., 2019)

Time 16:33:24 LAF_{max} 78.8 dB

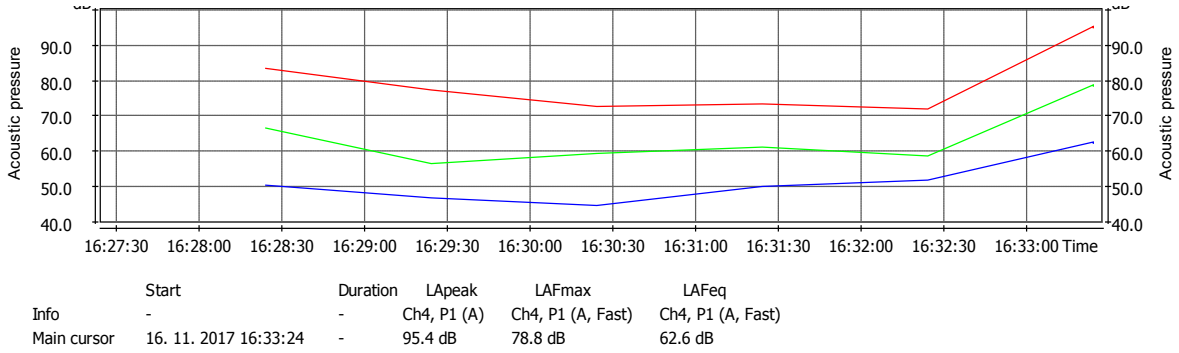

Fig. 7. Measured value, time 16:33:24 (Fehér et al., 2019)

Tab. 1. Measured value from blasting in the tunnel

Measurement time	Measured value LAF_{max} (dB)	Allowable value (dB)
16:28:24	66.7	118
16:29:24	56.6	118
16:30:24	59.4	118
16:31:24	61.1	118
16:32:24	58.8	118
16:33:24	78.8	118

Fig. 8. SVAN 958A installed near a residential building in Nimnica (Fehér et al., 2019)

Analysis and evaluation of noise measurements

Impulsive noise is the most subjective perceived by the population when measuring the noise level from blasting operations or the tunnel shot. Blasting works are, however, sporadic in time, and therefore these noise levels are not subject to permissible values according to the Ministry of Health Decree no. 549/2007. According to the decree, we use the maximum sound level A in the monitored time interval when using the time weight function F. LAF_{max} (dB) value according to MZSR no. 549/2007. The maximum A-level sound at a single occurrence may not exceed 118 dB in places and people's possible residence. From the above graphs, or the outputs from the measuring instrument SVAN 958A, it can be stated that the noise level generated by the blasting operations in the tunnel did not exceed the maximum value of LAF_{max} 118 dB.

Measuring position and devices used to measure seismic effects of blasting operations in Diel tunnel

The measuring position, or the measurement of technical seismicity, was carried out in residential buildings approximately 200 m from the blast. A special instrument from INSTANTEL - MINIMATE PRO 6 was used for seismic measurement. The MINIMATE PRO 6 offers 64 MB of memory, improved durability, metal housing, connectors and water resistance. It is possible to connect two standard ISEE or DIN triaxial geophones to monitor vibration sources from two different locations. Another option is to connect one ISEE or DIN triaxial geophone and one ISEE linear microphone, as well as the possibility to connect an audio microphone if air overpressure measurement is required.

Fig. 9. Device MINIMATE PRO 6 (Geonor, Inc., 2018)

The MINIMATE PRO 6 situated in the measured position was calibrated before the measurement, and its sensitivity was also checked. The graphs of the individual components of the seismic wave were recorded in the positions of measurement. Seismic apparatuses have been placed on the measuring positions so that the impact of technical seismicity on the objects under consideration can be assessed. On the basis of measured values of velocities and frequencies of individual components of the wave at the shot, we were able to evaluate according to STN EN 1998-1 / NA / Z1 seismic load of building constructions or effects on a housing development near the tunnel (Pandula and Kondela, 2010).

Criterion seismic effects

Effects of the technical seismicity induced by blasting are measured and assessed by the velocity of the environmental particles (particle velocity) "*v*" according to the maximum value of one of its three components *x*, *y*, *z*. The principle of seismic protection of seismic safety of building objects against technical seismicity can be expressed by the relationship

$$v \leq v_d \tag{1}$$

where *v* is the maximum value of the particle velocity component caused by the vibration source, measured at the so-called vibration rate. The reference position of the protected (assessed) object; the reference opinion is the ground floor of the building; the value of "*v*" depends mainly on the maximum mass of the explosive charge fired at one time point Q_{eq} [kg], further from the minimum source distance from the shock vibration receptor *L* [m] and the properties of the geological transfer environment between the source and the shock receptor. At the current knowledge level, the value of "*v*" cannot be calculated in advance either analytically or empirically; the most reliable is determined by a specific measurement, as in our case, v_d is the maximum allowable (limiting) particle velocity for the object (s) under consideration; there is no damage to the object at this vibration speed - the degree of damage is 0; this value is determined independently of the blast (before blast) based on practical experience. Different standards or on the basis of expert assessments by specialists. STN 73 0036: 1973-11 / STN EN 1998-1: 2005/NA shows the relationship between the vibration intensity expressed by the particle velocity of the individual components and the possibility of damage to the building. In accordance with the standard, the following criteria may be adopted for masonry civil buildings in an average building condition:

At particle velocity:

- v = 0 – 10 mm.s^{-1} – there is no damage to the building,
- v = 10 – 30 mm.s^{-1} - possibility of first signs of damage,
- v = 30 – 60 mm/s^{-1} – the possibility of minor damage.

Tab. 2 Dependence of the degree of damage from maximum particle velocity, type of object and ground soil according to STN EN 1998-1 / NA / Z1 (Pandula et al., 2010)

Maximum vibration rate for frequency range			Damage degree	Class of resistance	Type of soil
fk < 10 Hz	10 Hz<fk< 50 Hz	fk> 50 Hz			
less than 3	3 to 6	6 to 5	0	A	a
3 to 6	6 to 12	12 to 20	0	A	b,c
				B	a
6 to 10	10 to 20	15 to 30	0	B	b,c
				C	a
			1	A	a
8 to 15	15 to 30	20 to 30	0	C	b
				B	c
			1	A	b,c
				B	a
10 to 20	20 to 30	30 to 50	0	C	c
				D	a
			1	B	b
				C	a
			2	A	a
15 to 25	25 to 40	40 to 70	0	D	b,c
				E	a
			1	C	b
				B	c
			2	A	b,c
				B	a
20 to 40	40 to 60	60 to 100	0	E	b,c
				F	a
			1	C	c
				D	a
			2	B	b,c
				C	a
30 to 50	50 to 100	100 to 150	0	F	b,c
			1	D	b,c
				E	a
			2	C	b

Tab. 3. Seismic effects depending on vibration velocity (Pandula et al., 2010)

Velocity of vibration ($mm.s^{-1}$)	Characteristics of vibration and their effects
< 2	man does not perceive vibration, vibration can only be detected by devices
2 - 5	sensitive people perceive vibration
5 - 10	vibration is already a human perception
10 - 15	vibration is perceived by most people, the window pan shakes
15 - 30	first signs of very slight damage
30 - 75	light damage to buildings
75 - 100	possible damage to damaged buildings
100 - 200	serious damage to buildings, cracks in concrete
200 - 400	building disintegration, serious damage in reinforced concrete
> 400	possible demolition of buildings

In these blasting works in the Diel tunnel, explosives of the type AUSTROGEL and EMULEX 1 were used. The total weight of the blast in the tunnel was 110 kg per blast.

The pressure force generated at the point of the explosion causes a pressure wave in the surrounding environment. Waves spread to the environment and transmit part of the blast energy to a greater distance. The pressure wave propagates increased tension and rock movement. Near the centre of the blast and at a distance of a few meters, the induced tension is a compression wave. The pressure tension rapidly rises to a certain maximum and then slowly decreases to zero so that damped environmental vibration occurs. As the distance from the center of the explosion increases, the shape of the tension and the resulting movement of the transmission environment change so that after a sudden rise in pressure, its drop does not stop at zero, but the first portion of the overpressure is followed by the second portion of the vacuum propagating wave. Environmental distortions take on the character of vibration. In any flexible solid state, the formation of a longitudinal wave P is accompanied by a transverse wave S, which arises from the passage and reflection of the longitudinal wave at the interface of different environments (Pandula and Kondela, 2010).

Especially the graphical dependence of the maximum particle velocity components on the reduced distance in the tunnel, which depends on the amount and type of explosive used and the timing stages of the detonators used in the blast or timing of the blast itself (Pandula et al., 2012; Kondela and Pandula, 2012), is important when evaluating the results.

Tab. 4. The measured values of seismic effects caused by blasting works in tunnel (Fehér et al., 2019)

Date of measurement	Y $mm.s^{-1}$	Z $mm.s^{-1}$	X $mm.s^{-1}$
16.11.2017	0.268	0.686	0.252
16.11.2017	0.260	0.946	0.418
14.12.2017	0.126	0.985	0.260
14.12.2017	0.260	0.796	0.213
16.05.2018	0,283	0,178	0,127

Based on the measured values of the seismic effects at the blast in the Diel tunnel, the graphical dependence of the maximum particle velocity components on the reduced distance was sharpened - the red line represents the maximum permissible values of the particle velocity for the primary tunnel lining, the residential buildings in the village of Nimnica and the water sources in the Nimnica (Pandula et al., 2012).

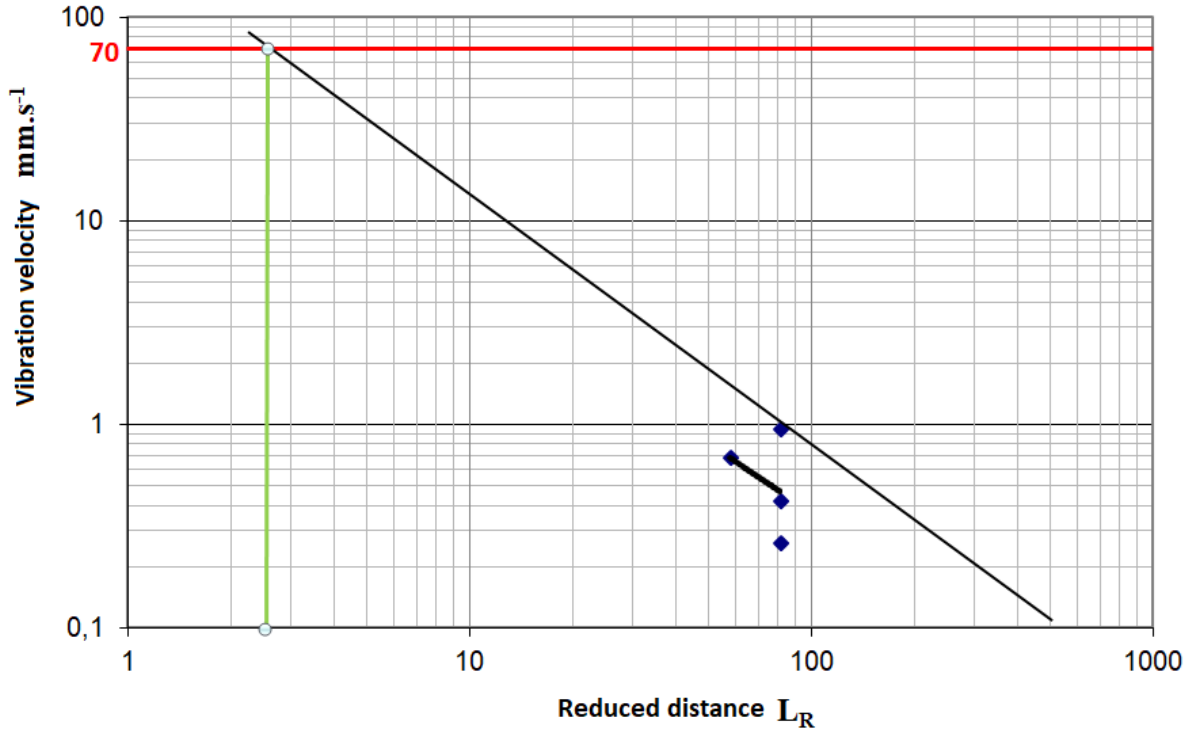

Fig. 10. Graphical dependence of particle velocity at the reduced distance on primary tunnel lining. The red line represents the maximum allowable particle velocity values for the primary tunnel lining (Fehér et al., 2019)

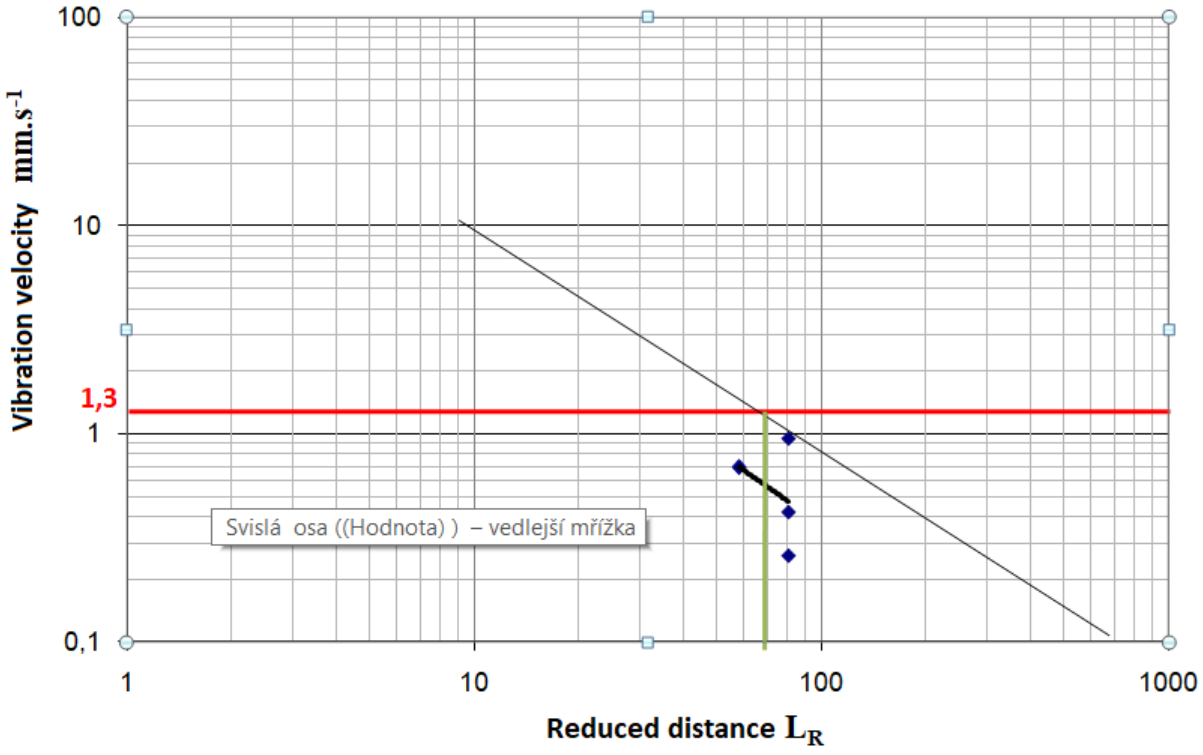

Fig. 11. Graphical dependence of particle velocity on reduced distance acting on Nimnica spa. The red line represents the maximum permissible particle velocity values for water sources at Nimnica Spa (Fehér et al., 2019)

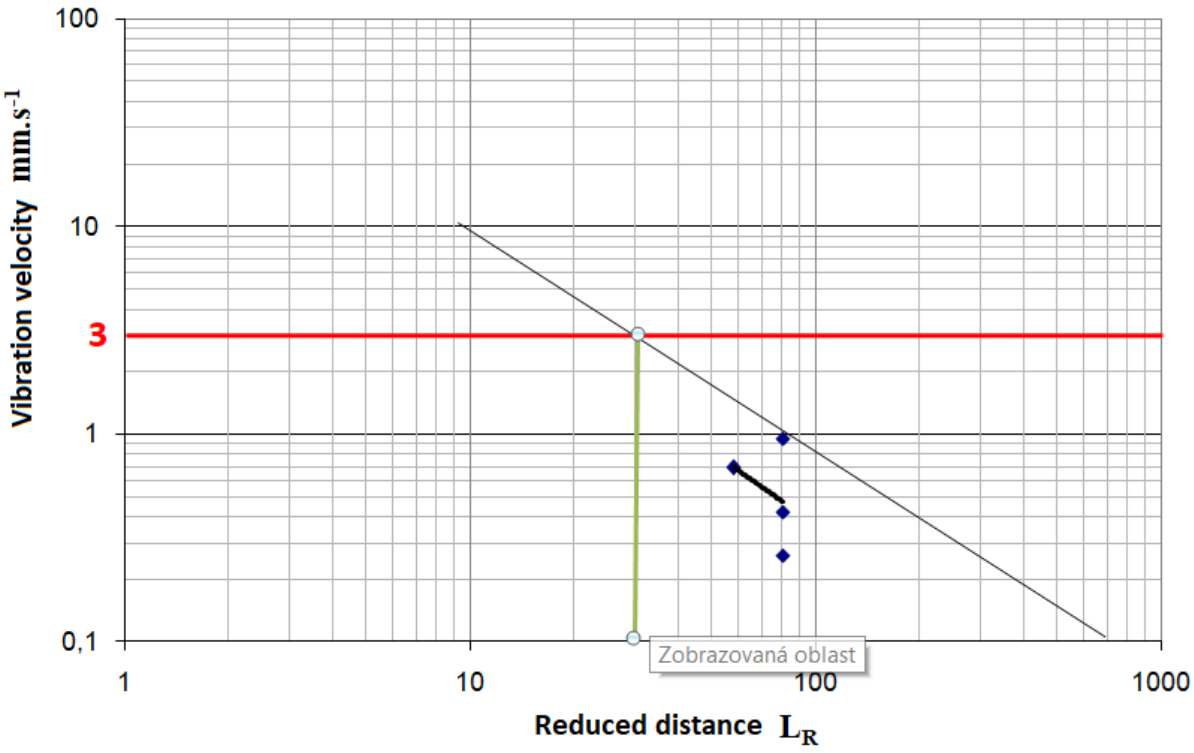

Fig. 12. The graphical dependence of the particle velocity at a reduced distance on residential buildings near the Diel Tunnel. The red line represents the maximum permissible particle velocity values for residential buildings in Nimnica (Fehér et al., 2019)

Fig. 13. Location of MINIMATE PRO 6 on the foundations of a residential building (Fehér et al., 2019)

Analysis and evaluation of seismic measurements

In the measurement of technical seismicity caused by blasting from tunnel blasts, vibrations were applied to residential buildings in accordance with Slovak technical standard STN EN 1998-1: 2005/NA (Fig. 10). Depending on the outputs of the MINIMATE PRO 6, the highest value measured (0.946 mm.s^{-1}) did not exceed 1 mm.s^{-1}, which is a non-perceptible figure (Fig. 11). Residents most perceive impulsive noise rather than shocks or vibrations caused by blasting. Measurements have confirmed that vibrations do not adversely affect residential buildings near the Diel Tunnel and citizens:

- v_d = 0 – 3 mm.s^{-1} – there is no damage to the building, nor do the inhabitants feel the vibration negative.

Conclusion

Noise levels from tunnel blasting do not exceed the maximum allowable noise for the reference time interval - a rare occurrence per day. The results show that blasting in the tunnel will not affect the current acoustic parameters in the nearest residential zone and will not endanger the environmental parameters in terms of noise.

From the seismic measurements and the graphical dependence of the vibration velocity on the reduced distance, or from the outputs of the MINIMATE PRO 6, we can conclude that the blasting works carried out at the tunnel excavation do not exceed the values that would lead to damage to the environment around the tunnel. The measured values did not exceed the values stipulated by the valid Slovak technical standard STN EN 1998-1 / NA/Z1 Seismic load of buildings.

As a result of the continuous tunnelling process, the distance between blasting operations and the residential area increases every day, which will only reduce the noise level and the effects of the season, which has a positive impact on the residential area and the surroundings of the tunnel.

The law of attenuation for the surrounding tunnel implies that the seismic effects caused by the blasting work will not cause such voltage changes that would break the bedrock in the living area and the nearby spa.

References

Blistan, P (2007). Presentation of geological date in geographic information systems. *Acta Montanistica Slovaca, Vol. 12, no. 3, (2007), pp. 329–334.*

Fei H., Liu M., Qu G., Gao Y. (2018) A method for blasting vibration signal denoising based on ensemble empirical mode decomposition-wavelet threshold, Baozha Yu Chongji/Explosion and Shock Waves, Volume 38, Issue 1, January 2018, pp. 112-118.

França G.S., Vasconcelos M.A.R., Chimpliganond C.N., Tomás, S.S. (*2012)* Study of vibrations generated by explosions made in the work of civil Tucuru? Locks 2 (PA), Revista Brasileira de GeofisicaVolume 29, Issue 1, January 2011, pp. 57-70.

Jonson D. (2012) Controlling shock waves and vibrations during large and intensive *blasting* operations under Stockholm City, Tunnelling in Rock by Drilling and Blasting: Workshop Hosted by FRAGBLAST 10 - The 10th International Symposium on Rock Fragmentation by Blasting2013, November 2012, pp. 49-58.

Kalab Z. (2018) Influence of vibrations on structures. *Acta Montanistica Slovaca, Volume 23, Issue 3, 2018, Pages 293-311.*

Kalab, Z., Štemon, P. (2017) Influence of seismic events on shallow geotechnical structures. *Acta Montanistica Slovaca Volume 22 (2017), number 4, 412-421*

Kalab Z., Pandula B., Stolárik M., Kondela J. (2013) Examples of law of seismic wave attenuation. Metalurgija Vol. 52, no. 3 (2013), pp. 387-390.

Kondela, J., Pandula, B. (2012) Timing of quarry blasts and its impact on seismic effects. Acta Geodynamica and geomaterialia Vol. 9, no. 2. (2012), pp. 155 – 163.

Leššo I., Flegner P., Pandula B., Horovčak P. (2007) New principles of process control in geotechnics by acoustic methods. *Metalurgija Vol. 46, no. 3 (2007), pp. 165-168.*

Mihalik R., Pandula B. (2008) The influances undesirable seismic effct of blasting by driving of Borik tunnel. In: Sborník vědeckých prací Vysoké školy báňské - Technické univerzity Ostrava. Vol. 8, no. 2 (2008), pp. 135-149.

Mishra A.K., Mallick, D.K. (2012) Analysis of blasting related accidents with emphasis on flyrock and its mitigation in surface mine, Rock Fragmentation by Blasting, FRAGBLAST 10 - Proceedings of the 10th International Symposium on Rock Fragmentation by Blasting 2013, November 2012, pp. 555-561.

Murayama H., Niwa H., Shimizu N., Higashinaka M., Noda K. (2014) Use of seismic interferometry for geological surveying ahead of the tunnel face, ISRM International Symposium - 8th Asian Rock Mechanics Symposium, October 2014, pp. 1353-1361.

Müncner E. (2011) Príručka pre strelmajstrov a technických vedúcich odstrelov. Banská Bystrica : SSTVP, 2011. ISBN 80-968748-4-5.

Nistov A., Klovning R., Lemstad F., Risberg J., Ognedal T.A., Haver P.A. Skogesal A.J. (2012) Noise reduction interventions in the Norwegian Petroleum Industry, Society of Petroleum Engineers - SPE/APPEA Int. Conference on Health, Safety and Environment in Oil and Gas Exploration and Production 2012: Protecting People and the Environment - Evolving ChallengesVolume 2, 2012, pp. 1278-1285.

Pandula B., Kondela J. (2010) Metodológia seizmiky trhacích prác, SSTVP Banská Bystrica, 2010, p. 156. ISBN 978-80-970265-0-9.

Pandula B., Kondela J., Pachocka K. (2012) Attenuation law of seismic waves. Metalurgija Vol. 51, no. 2 (2012), pp. 249-252.

Geonor, Inc. (2018): Minimate Pro6, http://geonor.com/live/products/vibration-monitors/minimate-pro6/

Raisian K., Yahaya J., Deraman A., Hamdan A.R., Rais I.A.I, Yahaya N.Z. (2016) A model for environmental quarry system based on particles, vibration and *noise* components, Journal of Environmental Management and Tourism, Volume 7, Issue 2, 2016, pp. 186-194.

Shin E.C., Park J.J., Kang J.K. (2018) Stability Analysis of Underground Tunnel for 2nd Perimeter Highway Construction *Work* in Incheon, *Indian Geotechnical Journal, Volume 48, Issue 2, 1 June 2018, pp. 235-250.*

Zákon Národnej rady Slovenskej republiky č. 355 z 21. júna 2007 o ochrane, podpore a rozvoji verejného zdravia a o zmene a doplnení niektorých zákonov

Vyhláška Ministerstva zdravotníctva Slovenskej republiky č. 549 z 16. augusta 2007, ktorou sa ustanovujú podrobnosti o prípustných hodnotách hluku, infrazvuku a vibrácií a o požiadavkách na objektivizáciu hluku, infrazvuku a vibrácií v životnom prostredí

Vyhláška Ministerstva zdravotníctva Slovenskej republiky č. 237 z 15. januára 2009, ktorou sa mení a dopĺňa vyhláška Ministerstva zdravotníctva Slovenskej republiky č. 549/2007 Z. z., ktorou sa ustanovujú podrobnosti o prípustných hodnotách hluku, infrazvuku a vibrácií a o požiadavkách na objektivizáciu hluku, infrazvuku a vibrácií v životnom prostredí

STN Eurokód 8, Navrhovanie konštrukcií na seizmickú odolnosť. Časť 1, Národná príloha, zmena 1 (STN EN 1998-1/NA/Z1).

Mining coal production in Slovakia

Eva Manová[1], Jozef Lukáč[1], Slavomíra Stašková[1], Roman Kozel[2], Jana Simonidesová[1] *and* ***Marek Meheš[1]***

The paper aims to describe the development of mining and utilization of black coal in the territory of the Slovak Republic. The authors also try to analyse the state of the financial health of black coal mining companies in our territory. The result of the paper is to provide a compact view of the development of coal mining in the context of the financial health of enterprises in this sector. We compare the development of coal production in Slovakia with the development of coal production in the Czech Republic, Hungary, Poland, Austria and Ukraine. We analyse the development of coal production within the Visegrad group along with the neighbouring state - Ukraine. Mining production in Slovakia decreased 15.70 per cent in November of 2018 over the same month in the previous year. Mining Production in Slovakia averaged -1.08 per cent from 2001 until 2018, reaching an all-time high of 135.30 per cent in July of 2007 and a record low of – 57 per cent in July of 2008.

Keywords: *coal, mining production, financial health, Slovakia, Ukraine, Austria, Czech Republic, Poland.*

Introduction

In 2010, more than 20 countries in the world had already reached maximum capacity in their coal production (peak coal production) such as Japan, the United Kingdom and Germany (Lin, 2010). An estimate for world coal production, in the long run, would be helpful for developing policies for alternative energy sources and climate change. This production has often been estimated from reserves that are calculated from measurements of coal seams. We show that where the estimates based on reserves can be tested in mature coal regions, they have been too high and that more accurate estimates can be made by a curve that fits the production history (Rutledge, 2011). After 2011, the production rates of coal and CO2 decline, reaching 1990 levels by the year 2037, and reaching 50 % of the peak value in the year 2047 (Patzek, 2010). The model of Mohr (2009) indicates that worldwide coal production can peak between 2010 and 2048 on a mass basis and between 2011 and 2047 on an energy basis. The Best Guess scenario assumed a URR of 1144 Gt and peaks in 2034 on a mass basis, and in 2026 on an energy basis.

Although coal may be viewed as a dirty fuel due to its high greenhouse emissions when combusted, a strong case can be made for coal to be a primary world source of clean H2 energy. Apart from the fact that resources of coal can outlast oil and natural gas by centuries, there is a shift towards developing environmentally benign coal technologies, which can lead to high energy conversion efficiencies and low air pollution emissions as compared to conventional coal-fired power generation plant (Shoko, 2006). A global peak in coal production can be expected between 2020 and 2050, depending on estimates of recoverable volumes. This is also compared with other forecasts. The overall conclusion is that global coal production could reach a maximum level much sooner than most observers expect (Hook, 2010). Coal and natural gas, the other fossil fuels, have played and will continue to play important roles as the United States works towards a comprehensive sustainable energy policy. That being said, coal will continue to be replaced by natural gas, and natural gas in the long-term will be replaced by wind and solar energy sources (Kuhns, 2018).

State of the problems

The research of coal production in individual countries is dealt with by several authors. India's coal demand is expected to grow at a rapid pace in the future due to the country's economic and population growth. According to Wang (2018), predicted demand shows that domestic production of coal will be insufficient to meet the country's rising coal demand, with the gap between demand and production rising from its current value of about 268 $\overline{Mt}$, it will reach 300 $\overline{Mt}$ in 2035, and 700 $\overline{Mt}$ by 2050. This increasing gap will be challenging for the energy security of India.

China has the largest coal production in the world due to abundant resource requirements for economic development. In recent years, the proportion of opencast coal mine production has increased significantly in

[1] *Eva Manová, Jozef Lukáč*, *Slavomíra Stašková*, *Jana Simonidesová*, *Marek Meheš*, Faculty of Business Economics of the University of Economics in Bratislava with seat in Košice, Tajovského 13, 040 01 Košice, Slovakia, eva.manova@euke.sk, jozef.lukac@student.euke.sk, slavomira.staskova@euke.sk, jana.simonidesova@euke.sk, marek.mehes@euke.sk

[2] *Roman Kozel,* VŠB – Technical University of Ostrava, Faculty of Mining and Geology Department of Economics and System Control, 17. Listopadu 15, Ostrava – Poruba, roman.kozel@vsb.cz

China. Opencast coal mining can lead to many environmental problems, including air pollution, water pollution, and solid waste occupation (Zhang, 2018). As the most significant material flow in China, coal resource flow has many problems, including unnecessary CO2 emission and energy waste (Liu, 2018). Liu (2015) find that total energy consumption in China was 10 % higher in 2000–2012 than the value reported by China's national statistics that emission factors for Chinese coal are on average 40 % lower than the default values recommended by the Intergovernmental Panel on Climate Change, and that emissions from China's cement production are 45 % less than recent estimates. China is facing the problem of a decline in coal demand in recent years. Traditional coal production has suffered from excess capacity and higher inventory in China since 2012. The development of the coal industry in China will change to rely more on quality and efficiency, developing scientific capacity, and achieving clean utilization (Bai, 2018).

Even in China and the USA, countries that have or had temporary bans on new coal mines, climate considerations played second fiddle, and there is little to no evidence that normative ideas regarding coal extraction have shifted, assisting in the emergence of a global anti-coal mining norm. Instead, the current Chinese and US coal extraction policies can best be explained as strategic moves to protect the industry from the headwinds it is facing. The Chinese moratorium's main purpose was to serve as an industrial policy to combat growing overcapacity, and it might be easily overturned (Blondeel, 2018).

According to Ozonoh (2018), South Africa has a large deposit of coal that supports about 95 % of electric power generation in the country. The fuel is fast depleting, though the current reserve may serve for the next century. However, the emissions from the coal project massive threat to the environment.

Russian coal industry possesses all capabilities to become an advanced branch of economy with high-quality products. Russian coal mining companies have many competitive advantages in the framework of the domestic fuel and power sector: tremendous coal reserves; significant experience in utilisation of this type of energy resources, especially in crisis situations; opportunity to come into the world market; high potential to enhance efficiency; diversity of coal products; adaptability to varying market environment; tight integration into priority lines of innovative economic development; essential contribution to the regional energy security. Russia is according to Zhaglovskaya (2017) one of the world leaders in coal production.

According to Litvin (2017), there is no method of coal losses regulation under challenging conditions, in particular in mining coal seams in tectonically disturbed zones. For deposits having hard conditions of stratification, the creation of this technique is a very urgent task. The author proves the necessity for the creation of this document.

On December 2015, more than 190 countries adopted the Paris Agreement, the most ambitious climate change pact to date. The document lays out a plan to curb greenhouse gas emissions, among other climate-related initiatives. Participating countries must now find ways to translate those ambitions into policy, and answer important questions about financing, transparency and accountability, national implementation, and accelerated emissions reduction goals, to name but a few. However, one issue looms large – coal (Boersma, 2016).

In 2011 (Germany) the conservative government announced the Energiewende - energy transformation and decided to reduce the number of fossil fuels from 80 % of the energy supply to 20 % by 2050. However, while the verdict on nuclear was unequivocal with a final phase-out date of 2022, the share of coal in the electricity market did not decrease, and the amount of carbon dioxide released into the air slightly increased from 2011 to 2013 (Renn, 2016). According to Vogele (2018) reasonable management in Germany of the niche technology "coal-fired power plants" could include protection of space for ensuring a smooth removal of the links between the regime and the technology with respect to, for example, social and environmental aspects. The phase-out pathways for the coal-fired power plants elaborated on in this paper help to better inform policy-makers to design transformation processes not only for coal-fired power but also for other declining technologies. The analysis of Stojiljkovič (2014) of the measurement data allows us to improve control of existing and newly opened coal mines, as well as their ancillary products that act as polluters. Emil (2000) dealt with the problems of liquidating buildings of former underground mining, especially of shafts of closed and damped mines. It is stated that strict maintaining the Decree of the Czech Bureau of Mines (ÈBÚ) No. 52/1997, Collection of Laws, has its justification for deep and gassy hard coal mines, but it cannot be absolutely valid in the full extent for shallow ore, and mainly brown coal mines. Soong (1998) described some technical aspects of triboelectrostatic separation and the results of the application of this process in the treatment of three types of coal, namely Cígeľ, Handlová and Nováky. It has been found that the separation efficiency is very closely related to the second part of the coal. The first results demonstrated the correlation between the efficiency of ash separation in coal. Cehlár (2019) describes a new tool, the brownfields methodology, which can help revitalize old mining areas as part of their technological modernization and underground full extraction with environmental damage reduction.

Several authors have dealt with the issue of the financial performance of enterprises that make up the mineral resource. Peng (2018) analysed the scale efficiency, efficiency and projection value of 17 coal enterprises, meanwhile, make a horizontal comparison of the environmental performance level among coal enterprises. Gonenc (2017) investigated the relationship between environmental and financial performance of

fossil fuel firms. To this extent, we analyse a large international sample of firms in chemicals, oil, gas, and coal with respect to several environmental indicators in relation to financial performance. Strouhal (2015) determined the linkage between CSR and financial performance within two countries in the CEE region – Czech and Estonia – using data from 2012 – 2013. We compare the return on assets and normalised market value added of listed companies. Based on the results, we can state that the implementation of a standalone CSR report does not have any direct linkage with the financial performance of the tested companies. Manová (2018) researched of the evaluation in the contribution presents cluster analysis, through which we determine companies' clusters from chosen sectors according to chosen financial indexes. The results confirm that the position of the analysed companies in the frame of the sector is satisfactory. Improvement of the economic activity of industrial companies determines conditions for the possible improvement of mining and metallurgical business activity and finds the sources of companies' growth. Tworek (2018) analysed to give an overview of the risk management problems experienced by coal mines, with the focus on the integrated enterprise risk management (IERM) concept, as well as proposing that the concept should be implemented in coal mines operating in Poland and the Czech Republic. In particular, it proposes that the traditional approach to the risk management process, i.e. Enterprise Risk Management (ERM), should be modified and transformed into an integrated process. Cehlár (2011) gave some information about risk management and its significance for financing project in the mining industry. The projects in the mining industry are very exacting for financial sources. Vaněk et al. (2017) benchmarked the mining companies in a 5-year period: from 2009 to 2014. Six financial indicators were used to achieve the ROE, ROS, ROA, Debt to Equity Ratio, Asset, and Cash Flow Liquidity Ratio of four coal mining companies in the Upper Silesian Coal Basin located on the border of the Czech Republic and Poland: OKD a.s. operating in the Czech Republic and three Polish entities, Jastrzebska Spolka Weglowa S.A. (JSW), Katowicki Holding Weglowy S.A., and Kompania Weglowa S.A.

The finding of the significant positive effect of CO2e intensity on firm financial performance contrasts with the findings of previous studies carried out in several developed countries. The finding of the research is that the mediating variable of customers' responses strengthens the effect of CO2e intensity on ROS (Rokhmawati, 2017). Vilamová (2016) analysed an economic evaluation of using a geopolymer from coal combustion as a possible alternative raw material. The results of the analysis show possible reducing of cost, which is possible through the replacement of cement by fly ash more than 18 % of the material.

Methodology and data

The aim of the paper is to describe the state of coal production in Slovakia and neighbouring countries (Czech Republic, Poland, Hungary, Austria and Ukraine). We focus on the development of production in countries through different trends analysis. We also focus on the financial situation of the selected company Hornonitrianske bane Prievidza from the perspective of the financial health of the year 2017. In the first place, we focus on the comparison of the financial indicators with the average values of financial indicators of economic activities in the Slovak Republic. We analyse the indicators of liquidity, activity, profitability and company indebtedness.

The data comes from the sources of the Statistical Office of the Slovak Republic, Eurostat, the World Bank or other annual reports of the organizations, ministries and multinational companies engaged in coal mining or trade with this commodity.

In the present case study, we use several specific methods of financial analysis (Zalai, 2016). Among the most represented methods, we consider the methods of financial ratios. The construction of these indicators consists of several items of assets and liabilities, costs and revenues. The system of financial ratios itself has a low informative value. It would only be a group of numbers that didn't tell us anything. Therefore, it is important to compare the individual indicators with other companies, in our case with the whole industry. Based on this, we find out how the company has stood the competition and find its location in space. As a result, the company may be worse off than the industry average. If it is better, it needs to be compared with the upper quartile - with a better quarter of the industry. In addition to the methods of financial analysis, we also use methods of graphical representation of development trends.

Results

According to the data of Statistics office, mining represents one per cent of total industrial production in Slovakia, which also includes mining of coal and lignite. The trend of this mining has a declining tendency in Slovakia. The largest coal producer in Slovakia is Hornonitrianske bane Prievidza. Hornonitrianske bane Prievidza in 2018 delivered to customers over 1.5 million tonnes of brown coal. Coal is mined by the deep-mined method in three mining areas (Handlová, Nováky and Čáry.) The entire mining production consists of dust coal for energy purposes.

Coal and lignite generated 11.8 % of electric energy in the Slovak Republic in 2015. The others are nuclear energy (57.6 %), gas (5.9 %), oil (1.0 %) and waste and renewable energy sources (7.6 %). Overall, the energy mix within the national energy policy is balanced with the support of domestic brown coal and renewable energy sources. Considering the high share of nuclear energy in electricity production, Slovakia's dependence on imported energy sources (60.9 %) is only slightly above the EU average, despite almost 100 % dependence on imported oil and natural gas. For example, in the Eastern of Slovakia, there is the Vojany Power Station, where boilers (4 x 110 MW) are located for the use of imported semi-anthracitic hard coal from Ukraine. In the years 2014-2015, due to the conflict in Ukraine, there were problems with this supply of this coal.

Lignite sources are estimated at over 400 million tonnes, and another 500 million tonnes should be available in the future. Usable reserves of lignite, including brown coal, are estimated at 100 million tonnes. In 2015, 1.8 million tonnes of lignite were produced. Lignite is mined by two companies in four underground mines, located in the central and western part of Slovakia. More than 90 % of total lignite production is used for generating electricity and heating.

In the following chart, we may notice the development of the production of mining companies in Slovakia during the reference period from January 2018 to November 2018. The graph reflects the development in this area – a decrease, which is expressed as a percentage. We see a decline in January of 23.3 %, while the only increase of 0.7 % is in April, then again the decrease was recorded.

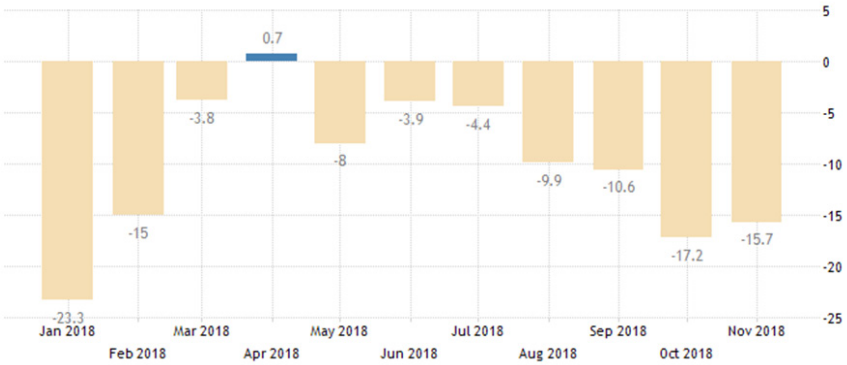

Graph. 1: Mining production in Slovakia
Source: Trading Economics

In the following graph, we can monitor the final consumption of coal in the Slovak Republic from 1990 to 2015. In the 1990s, almost the whole part of coal consumption creates brown coal, predominantly for heating and electricity production. Small consumption represented the production of coke, attraction and bituminous coal.

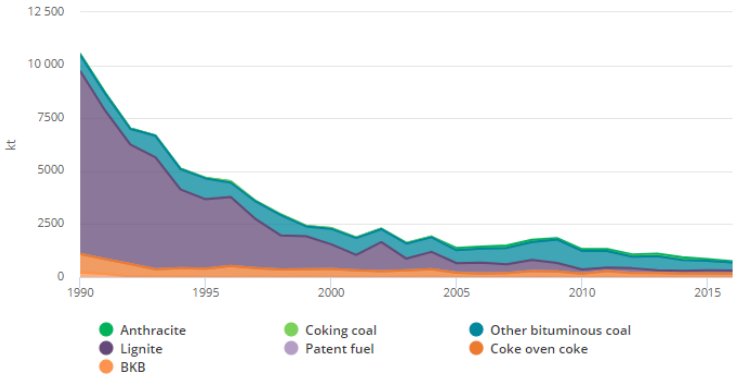

Graph. 2: Coal total final consumption by type (Slovak Republic)
Source: International Energy Agency

The production of coal in Slovakia from 1990 to 2016 is shown in graph no. 3. We can say that there has been an overall decline in production and also in brown coal. The level of coke over coke is the same. Since 2004, there has been a noticeable increase in the production of coal tar.

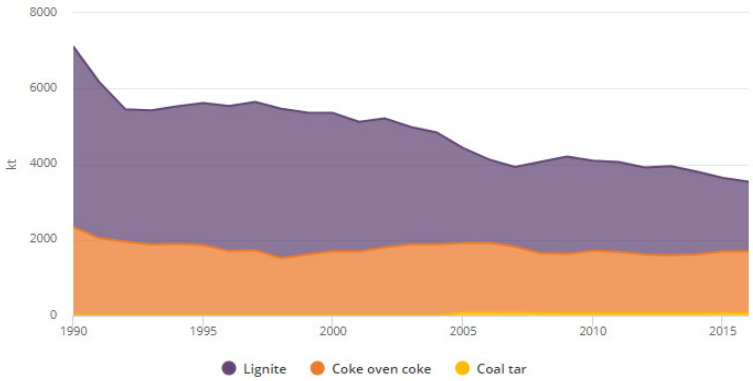

Graph. 3: Coal production (Slovak Republic)
Source: International Energy Agency

In the following section, we compare the production of coal between the Slovak Republic and the neighbouring countries. Differences that occur between countries can be caused by many factors that can arise from multiple areas. First of all, there are the conditions of distribution of natural resources – coal fields in the analysed countries. The second area is the policy, which is conducted in the field of coal mining, also through the influence of the EU, which does not affect Ukraine. Another important factor is the need for coal mining for the country's economy – the question is how to use coal (energy, trade, sales), with which imports and exports are related.

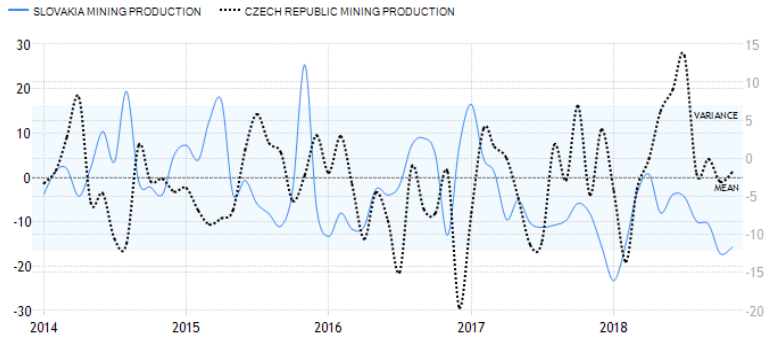

Graph. 4: Comparison of coal production between Slovakia and the Czech Republic in %
Source: Trading Economics

Production of coal compared to production in the Czech Republic in the years 2014 and 2015 resembled and fluctuated at approximately the same intervals. More significant changes can be observed in the last two analysed years when production in the Czech Republic increased significantly compared to the production of the Slovak Republic.

In the decision from October 2015, the Government of the Czech Republic corrected its raw material and energy policies by modifying the scope of the territorial ecological limits placed on the mining of lignite. Such action is impacting the energy sector operating in the North Bohemian Basin, the largest region for lignite production in the Czech Republic (Sivek, 2017).

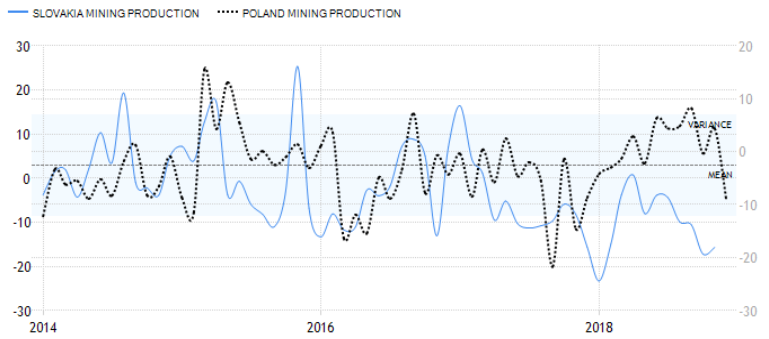

Graph. 5: Comparison of coal production between Slovakia and Poland in %
Source: Trading Economics

By comparing production with Poland, we can also say that compared to Slovakia, coal production is higher in 2018, 2017 and 2016. Lower production of coal compared to Slovakia is recorded in 2014.

In Poland, contemporary policymakers mobilise a national imaginary inherited from communist times – encapsulated in the slogan 'Poland stands on coal' – that fuses infrastructures of coal extraction and combustion with the fate of the nation. This socio-technical imaginary provides support for coal futures, even in the face of contradictory evidence for domestic resource depletion, poor regional air quality, and global climate change (Kuchler, 2018).

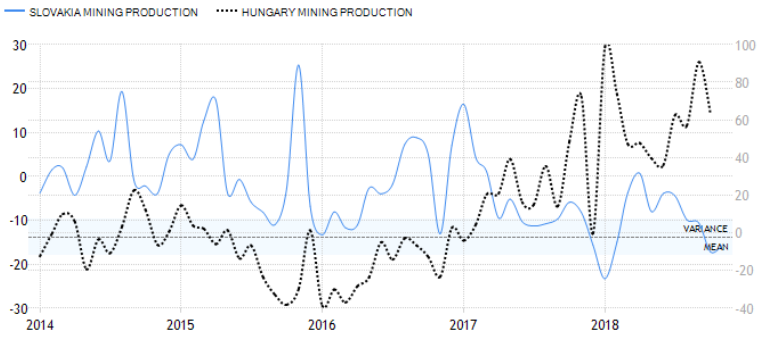

Graph. 6: Comparison of coal production between Slovakia and Hungary in %
Source: Trading Economics

The Slovak Republic, compared with the production in Hungary, achieve higher production of coal from 2014 to half of 2016, which is replaced by a reduction in coal production in Slovakia.

In Hungary, there is great uncertainty about Hungary's energy policies and security of supply, with the role of coal, gas and renewables in the energy/electricity mix still not settled. Their future is expected to be heavily dependent on political decisions rather than energy market factors, though energy market uncertainties are also high (Weiner, 2017).

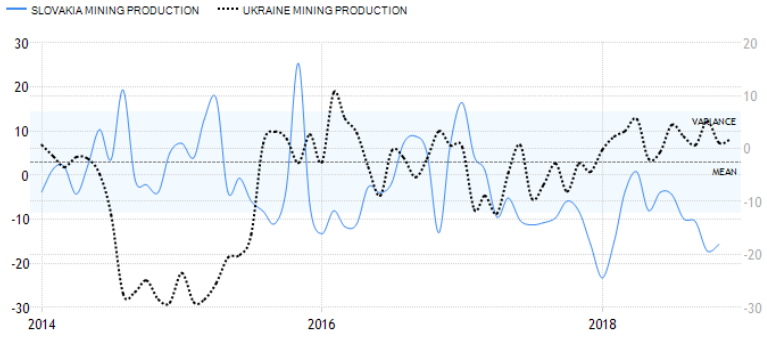

Graph. 7: Comparison of coal production between Slovakia and Ukraine in %
Source: Trading Economics

By comparing the production of Slovakia with Ukraine, we can say that production is also affected by ongoing conflicts in Eastern Ukraine, which leads to a decrease in production in 2014 and 2015. However, in the last two years, Ukraine has achieved higher production than Slovakia.

According to Snihur (2016), the current state of Ukraine coal mining industry and prospects of its development for the period until 2020 are considered. The analysis of Ukraine mine fund conditions is carried out. Statistical data of gross coal production at state-maintained and private mines are given. The reasons for low profitability and coal production decline in the country are considered.

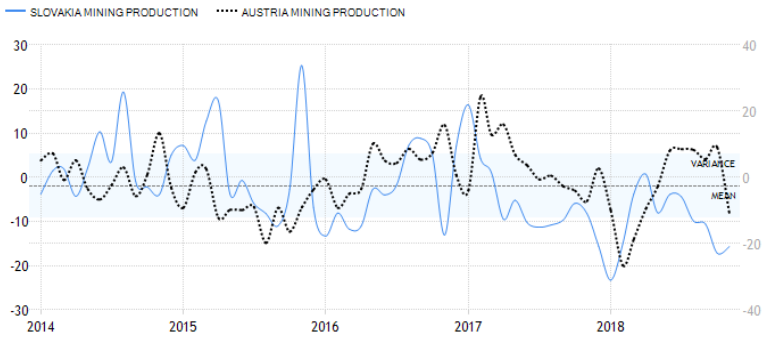

Graph. 8: Comparison of coal production between Slovakia and Austria in %
Source: Trading Economics

Austria's production is quite similar to the Slovak production in recent years (2017 and 2018). However, production is still higher in our neighbours, but we achieved better results from 2014 until the beginning of 2016.

The next part is devoted to the financial health of the most important employer and producer of coal in Slovakia – Hornonitrianske bane Prievidza. The most important coal buyer is Slovenské elektrárne, Elektráreň Nováky. In the position of the leading domestic coal producer and the guarantor of the supply of brown coal for combined heat and power, Hornonitrianske bane Prievidza supplied 1 507 193 tonnes to the Elektráreň Nováky. Hornonitrianske bane Prievidza supplied it smoothly, in the required daily quantity and quality. Out of the Elektráreň Nováky the company dispatched 29 855 tons of energetic coal.

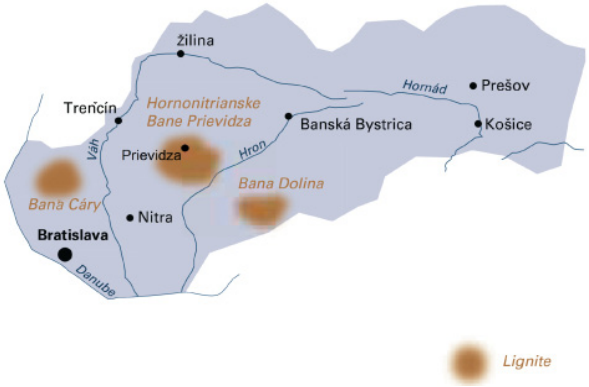

Graph. 9: The occurrence of lignite in Slovakia
Source: Trading Economics

The year 2018 was a breakthrough in the sale of coal in the history of the company. After the end of coal mining in mine Cigeľ, at the end of 2017, Hornonitrianske bane Prievidza finished the production and sale of sorted coal for small consumers and households. The quality and heat value of domestic brown coal (9 to 14 MJ / kg) used for energy purposes is standard, comparable to coal from other European Union countries. In the neighbouring countries, brown coal and lignite are mined with significantly lower heating capacity (Greece – about 4 to 9 MJ / kg, Romania – 7 to 8 MJ / kg, Germany – 8 to 11 MJ / kg, Poland – 8 to 11 MJ / kg) and significantly higher annual mining than in Slovakia (Hornonitrianske bane Prievidza, 2019).

Within the analyses of the financial health of the selected company, we focus on several financial indicators of the company, and we compare them with the average values of the financial indicators in the Slovak Republic. We have calculated the financial indicators from the company's publicly available financial statements, which are in the database of Slovak accounting records. The analysed indicators can be found in the following table, and because our company ranks among companies with assets exceeding of 5 million Euro and with turnover over 3,3 million Euro, we use the relevant indicators taking these criteria.

From the results of the previous table, we can say that the majority of the financial indicators of the enterprise achieved worse results than those in sector B: Mining. In particular, these indicators are indicators of profitability, inventory turnover time, debit collection and other activity indicators. Compared to the industry, the company is financially well in the area of debt and liquidity. The decline in the mining industry, as well as the low demand for coal may in the future lead to worse business results, which can also be reflected in financial indicators.

Table. 1: Comparison of the mean values of indicators in the mining sector

Financial indicator – values of 2017	statistical characteristics	unit of measure	Recommended values	
			property over 5,0	turn over 3,3
	Lower Quarter		1.17	1.19
Liquidity of 2. degree	Median	coefficient	1.67	1.26
1,65	Higher Quarter		5.28	1.91
	Lower Quarter		1.48	1.26
Liquidity of 3. degree	Median	coefficient	1.95	1.77
1,83	Higher Quarter		7.20	2.36
	Lower Quarter		11.97	8.74
Inventory turnover time	Median	day	25.50	24.77
9,87	Higher Quarter		34.06	34.06
	Lower Quarter		51.73	50.69
Receivables turnover time	Median	day	71.88	66.76
119,82	Higher Quarter		87.89	75.33
	Lower Quarter		51.25	48.26
Short-term receivables turnover time	Median	day	60.04	57.14
75,24	Higher Quarter		71.26	70.07
	Lower Quarter		52.93	47.49
Liabilities turnover time	Median	day	71.59	63.32
121,46	Higher Quarter		199.08	105.92
	Lower Quarter		27.81	27.81
Short-term liabilities turnover time	Median	day	39.72	43.70
41,11	Higher Quarter		56.25	62.39
	Lower Quarter		0.46	0.70
Turnover of assets	Median	coefficient	0.59	0.95
0,82	Higher Quarter		0.75	1.73
	Lower Quarter		11.42	20.65
The total indebtedness of assets	Median	%	29.06	42.43
38,8	Higher Quarter		48.59	57.00
	Lower Quarter		1.06	0.76
Long-term indebtedness of assets	Median	%	8.89	6.73
13,5	Higher Quarter		23.67	22.01
	Lower Quarter		5.83	5.06
Return of assets	Median	%	7.43	7.96
1,8	Higher Quarter		12.55	11.58

Source: own processing according to accounting information and database of mean values of indicators 2017

Discussion

In relation to coal mining, total CO2 emissions in the energy sector decreased by five per cent in 2018. This process has driven the gradual downsizing of coal production, primarily in Germany and the United Kingdom. In Britain, the share of electricity produced from coal has fallen from 40 % in 2012 to 5 % in 2018. In Germany, it fell from 19 % to 13 % in the same period. In the European Union in 2018, coal production fell by 6 % year-on-year, compared to 30 % in 2012. The analysis thus confirmed the rapid decline of coal in electricity production across European countries. The study noted that countries that are planning to eliminate black coal have usually plans to expand their electricity production from renewable sources. An example may be Austria. Last year, solar energy accounted for only four per cent of the European Union's total energy mix. However, according to the study, the newly built solar infrastructure has increased the solar electricity production capacity by more than 60 % to almost 10 gigawatts. The study assumes that by 2022, this number can be multiplied by three times. We have experienced a decline in coal production in the Slovak Republic, but in Hungary and Ukraine, for example, the coal production trend has a growing tendency.

Summary

The result of the paper is the clarification of the issue of coal production in Slovakia. We have presented the results of the comparison of coal production in Slovakia with individual countries – Czech Republic, Poland, Hungary, Ukraine and Austria. We have found that the Slovak Republic has experienced a decline in production over the last two years. On the other hand, countries such as Ukraine and Hungary are increasing coal production in 2017 and 2018. We also analysed the largest enterprise dedicated to coal mining in Slovakia. We have assessed the financial health of the company, with the result that the company achieved good result in the area of solvency and liquidity, as well as its indebtedness. However, the company has achieved worse results in indicators of profitability and activity. Excessive inventory turnover time and receivables collection represent a risk for the future, and the analysed company should consider the change of its receivables policy.

Acknowledgement: *This paper is a partial output of the Project of Young Researchers and PhD Students, number I-19-110-00, 2019: Aspects of Financial Management of Towns and Municipalities in Slovakia in the Context of Financial Health.*

References

Bai, Xiangfei, et al. Coal production in China: past, present, and future projections. International Geology Review, 2018, 60.5-6: 535-547.

Blondeel, Mathieu; Van DE Graaf, Thijs. Toward a global coal mining moratorium? A comparative analysis of coal mining policies in the USA, China, India and Australia. Climatic Change, 2018, 1-13.

Boersma, Tim; Vandeveer, Stacy D. Coal after the Paris agreement. Foreign Affairs, 2016.

Bureau, Slovak Credit. Stredné hodnoty finančných ukazovateľov ekonomických činností v Slovenskej republike za rok 2017. Bratislava, SCB, 2017.

Cehlár, Michal, et al. Mine Sited after Mine Activity: The Brownfields Methodology and Kuzbass Coal Mining Case. Resources, 2019, 8.1: 21.

Cehlár, Michal; Teplická, K.; Seňová, Andrea. Risk management as instrument for financing projects in mining industry. In: SGEM 2011: 11th International Multidisciplinary Scientific GeoConference: conference proceedings. 2011. p. 913-920.

Coal (2019) online at https://tradingeconomics.com/commodity/coal

Fröhlich, Emil; Hudeček, Vlastimil; Kryl, Václav. The problem of liquidating the buildings of former underground brown coal mines in the Podkru nohoøí area in connection with the decree of the czech bureau of mines no. 52/1997, collection of laws, and problems of open cast mines in places of their occurrences. Acta Montanistica Slovaca, 2000, 5.4: 377-382.

Gonenc, Halit; Scholtens, Bert. Environmental and financial performance of fossil fuel firms: A closer inspection of their interaction. Ecological Economics, 2017, 132: 307-328.

Höök, Mikael, et al. Global coal production outlooks based on a logistic model. Fuel, 2010, 89.11: 3546-3558.

Hornonitrianske bane Prievidza a. s. Company. 2019. Online: http://www.hbp.sk/index.php/en/coal

Hornonitrianske bane Prievidza, a. s. – Účtovné závierky (2019) online at https://www.finstat.sk/36005622/zavierka

Kuhns, Roger James; Shaw, George H. Coal and Natural Gas. In: Navigating the Energy Maze. Springer, Cham, 2018. p. 65-69.

Kuchler, Magdalena; BRIDGE, Gavin. Down the black hole: sustaining national socio-technical imaginaries of coal in Poland. Energy Research & Social Science, 2018, 41: 136-147.

Lin, Bo-qiang; LIU, Jiang-hua. Estimating coal production peak and trends of coal imports in China. Energy Policy, 2010, 38.1: 512-519.

Litvin, Oleg, et al. Methodology of coal losses calculation at open pit mining for complex geological conditions-review. Acta Montanistica Slovaca, 2017, 22.2.

Liu, Feng, et al. Optimization for China's coal flow based on matching supply and demand sides. Resources, Conservation and Recycling, 2018, 129: 345-354.

Liu, Zhu, et al. Reduced carbon emission estimates from fossil fuel combustion and cement production in China. Nature, 2015, 524.7565: 335.

Manová, Eva, et al. Position of the chosen industrial companies in connection to the mining. Acta Montanistica Slovaca, 2018, 23.2.

Mohr, Steve H.; Evans, Geoffrey M. Forecasting coal production until 2100. Fuel, 2009, 88.11: 2059-2067.

Ozonoh, M., et al. Techno-economic analysis of electricity and heat production by co-gasification of coal, biomass and waste tyre in South Africa. Journal of Cleaner Production, 2018, 201: 192-206.

Patzek, Tadeusz W.; Croft, Gregory D. A global coal production forecast with multi-Hubbert cycle analysis. Energy, 2010, 35.8: 3109-3122.

Peng, Ruohong; Pang, Lei. Comparison and analysis of the coal enterprises environmental performance in our country based on the DEA. In: 2018 International Conference on Smart Grid and Electrical Automation (ICSGEA). IEEE, 2018. p. 206-212.

Renn, Ortwin; Marshall, Jonathan Paul. Coal, nuclear and renewable energy policies in Germany: From the 1950s to the "Energiewende". Energy Policy, 2016, 99: 224-232.

Rokhmawati, Andewi; Gunardi, Ardi; Rossi, Matteo. How powerful is your customers' reaction to carbon performance? Linking carbon and firm financial performance. International Journal of Energy Economics and Policy, 2017, 7.6: 85-95.

Rutledge, David. Estimating long-term world coal production with logit and probit transforms. International Journal of Coal Geology, 2011, 85.1: 23-33.

Shoko, E., et al. Hydrogen from coal: production and utilisation technologies. International Journal of Coal Geology, 2006, 65.3-4: 213-222.

Sivek, Martin, et al. Lifting lignite mining limits–correction of the Czech Republic energy policy. Energy Sources, Part B: Economics, Planning, and Policy, 2017, 12.6: 519-525.

Snihur, V.; Malashkevych, D.; Vvedenska, T. Tendencies of coal industry development in Ukraine. Mining of mineral deposits, 2016.

Soong, Y., et al. Triboelectrostatic separation of mineral matter from Slovakian coals. Acta Montanistica Slovaca, 1998, 3: 393-400.

Stojiljkovic, Evica; Grozdanovic, Miroljub; Marjanovic, Dobrivoje. Impact of the undergroud coal mining on the environment. Acta Montanistica Slovaca, 2014, 19.1.

Strouhal, Jiri, et al. Finding the link between CSR reporting and corporate financial performance: Evidence on Czech and Estonian listed companies. Central European Business Review, 2015, 4.3: 48.

Total Primary Energy Supply (TPES) by source. World 1990 – 2016 (2016) online at https://www.iea.org/statistics/?country=WORLD&year=2016&category=Energy%20supply&indicator=TPESbySource&mode=chart&dataTable=BALANCES

Tworek, Piotr; Tchórzewski, Seweryn; Valouch, Petr. Risk Management in Coal-Mines-Methodical Proposal for Polish and Czech Hard Coal Mining Industry. Acta Montanistica Slovaca, 2018, 23.1.

Vaněk, Michal, et al. Benchmarking of mining companies extracting hard coal in the Upper Silesian Coal Basin. Resources Policy, 2017, 53: 378-383.

Vilamová, Šárka; Piecha, Marian. Economic evaluation of using of geopolymer from coal fly ash in the industry. Acta Montanistica Slovaca, 2016, 21.2.

Wang, Jianliang; Bentley, Yongmei; Bentley, Roger. Modeling India's Coal Production with a Negatively Skewed Curve-Fitting Model. Natural Resources Research, 2018, 27.3: 365-378.

Weiner, Csaba. Managing energy supply security and gas diversification in Hungary. 2017.

Zalai, Karol et al. Finančno-ekonomická analýza podniku. Bratislava: Sprint, 2016. 487 p.

Zhaglovskaya, A., et al. Production activity analysis Methodology for open pit coal mines (in terms of Shestaki open pit mine). Eurasian mining, 2017, 1: 27.

Zhang, Li; Wang, Jinman; Feng, Yu. Life cycle assessment of opencast coal mine production: a case study in Yimin mining area in China. Environmental Science and Pollution Research, 2018, 25.9: 8475-8486.